Thermodynamic Modeling of the Mg-Cu-Y System

MD. MEZBAHUL ISLAM

A Thesis
in

The Department
of
Mechanical and Industrial Engineering

Presented in Partial Fulfillment of the Requirements
for the Degree of Master of Applied Science (Mechanical Engineering) at
Concordia University
Montreal, Quebec, Canada

September 2007

Abstract

Thermodynamic Modeling of the Mg-Cu-Y System

Md. Mezbahul Islam

Thermodynamic modeling of the Mg-Cu-Y system is carried out as a part of thermodynamic database construction for Mg alloys. This system is being modeled for the first time using the Modified Quasichemical model which considers the presence of short range ordering in the liquid.

A self-consistent thermodynamic data base for the Mg-Cu-Y system is constructed by combining the thermodynamic descriptions of the constituent binaries, Mg-Cu, Cu-Y, and Mg-Y using a suitable ternary extrapolation technique. All the three binaries have been re-optimized based on the experimental phase equilibrium and thermodynamic data available in the literature.

The constructed database is used to calculate and predict the thermodynamic properties, binary phase diagrams and liquidus projections of the ternary Mg-Cu-Y system. Calculated phase diagrams and the thermodynamic properties such as activity, enthalpy of mixing and partial Gibbs energy of the binary liquid alloys are found to be in good agreement with the experimental data reported in the literature. Moreover, for the Mg-Cu-Y ternary system, isothermal sections, vertical sections and polythermal sections are calculated, and the invariant reaction points are predicted for the first time.

Acknowledgements

First of all, I would like to express my sincere appreciation, gratitude and thanks to my thesis supervisor Dr. Mamoun Medraj for his constant guidance, invaluable and constructive suggestions throughout the period of this work. Without his support it would not be possible to complete this work.

I would like to thank my family members for their endless love and support. Especially my parents, who always contacted me and encouraged me to finish my research work.

I thank the members of Dr. Medraj's research group especially, Dmytro Keverkov, Mohammad Al jarrah and Muhammad Ashraf -ul- Arafin for their help and support during my research.

I thank all the staff members of our department for their kind help in solving my academic and technical problems.

Finally, I would like to thank Drs. Patrice Chartrand and Christian Robelin for their support and valuable suggestions which helped me a lot in understanding the FactSage software.

Table of Contents

List of Figures

List of Tables

CHAPTER 1

Introduction

1.1 Thermodynamics of Phase Diagrams

Phase diagrams are visual representations of the state of materials as a function of temperature, pressure and composition of the constituent components [1]. It can be considered as a graph that is used to understand the equilibrium conditions between the thermodynamically distinct phases. The information obtained from phase diagrams can be utilized for alloy design, development and processing.

Experimental determination of phase diagrams is a time-consuming and expensive task. Sometimes it becomes extremely difficult to achieve the equilibrium conditions. This is even more complicated for a multicomponent system. The calculation of phase diagram reduces the effort and time required to determine the equilibrium phase diagram.

The CALPHAD method gives the most scientific way of calculation of phase diagram. It is based on minimization of the Gibbs free energy of the system and is thus, not only completely general and extensible, but also theoretically meaningful. A preliminary phase diagram can be obtained by calculation of the thermodynamic functions of constituent subsystems. This preliminary diagram can then be used to

accumulate information in terms of temperature and composition. In this way maximum information can be obtained with minimum experimental effort [1].

The calculation of phase equilibrium provides information not only about the phases present and their compositions, but also provides numerical values for different thermodynamic properties i.e. enthalpy, entropy, activity etc. This is very important for a multi component system especially for systems having more than three constituent elements, where the graphical representation of the phase diagram becomes complicated. The lack of sufficient experimental information makes the situation worse. Thus the calculation of phase diagram is significant in developing new alloys. Also, the introduction of computer programs made the calculation much easier and reliable which eventually helped the rapid progress in this field.

1.2 Motivation

In the last decade a new class of wonder materials called ‘metallic glasses’ have begun to emerge from materials labs around the world. They exhibit properties of incredible strength and elasticity and are promoted as a true wonder material [2].

Most metals have a crystalline structure in which the atoms are arranged in neat, orderly arrays; these typically consist of small regions of aligned atoms, called grains, and the boundaries between them. But for metallic glasses atoms are packed together in a somewhat random fashion, similar to that of a liquid.

Unlike conventional metals, which are usually cooled slowly until they fully solidify, metallic glasses must be cooled very rapidly and very uniformly to freeze their random atomic pattern in place before crystallization occurs due to the nucleation and growth of crystal grains. Until the middle of last decade only thin films of metallic glass could be produced at that high speed cooling rate. However the high cost involved in this process makes it unfeasible for any commercial application.

Scientists were trying to find a way to prepare metallic glass in bulk form. The only way to get it in bulk form is to reduce the cooling rate. Recently it was possible to produce metallic glasses in bulk form on mixes of zirconium, magnesium, aluminum, and iron. The cooling rate was reduced to 100 K/Sec down to 1 K/Sec or even less [2]. These slower cooling rates mean that large parts can be fabricated. Furthermore, many of these metallic glasses remain stable against crystallization even when heated to temperatures slightly higher than their glass-transition temperatures.

The availability of metallic glasses in relatively large samples allows the measurement of some relevant physical properties, particularly mechanical properties. They are very promising for industrial applications because of their high strength to weight ratios, high hardness, good elasticity and rebound characteristics, corrosion resistance, good forming and shaping qualities and good magnetic properties. They are being considered for a range of applications including golf-club heads, high performance diaphragms for pressure sensors, precision micro gear, surgical prosthetics etc [2]. Some of these products are shown in Figures 1.1 to 1.3.

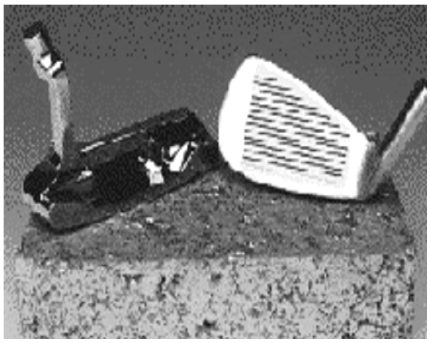

Figure 1.1: Golf Club heads [3].

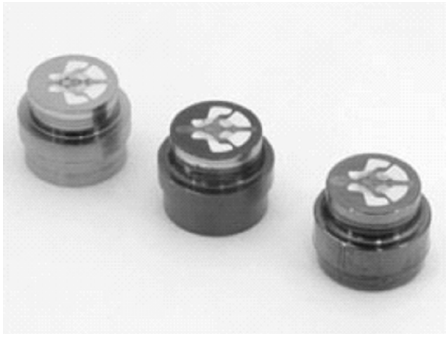

Figure 1.2: High performance Diaphragms for Pressure Sensors [4].

Figure 1.3: Very small micro geared motor [4].

Mg-based alloys are very attractive as BMG (Bulk Metallic Glass) formers because of their high strength- to- weight ratio. Among the Mg alloys, Mg-Cu-Y has the largest supercooled liquid region [5]. Inoue *et al.* [5] produced Mg-Cu-Y metallic glass by mold casting method into a copper mould. They obtained glasses of the $Mg_{80}Cu_{10}Y_{10}$

alloy as cylindrical specimens with diameters 1 mm and 1.5 mm. They got even better result for $Mg_{65}Cu_{25}Y_{10}$ composition with a diameter upto 7 mm.

Despite the high potential of Mg-Cu-Y system, a complete thermodynamic analysis of this system is scarcely known. Palumbo *et al.* [6] made an effort to calculate the ternary phase diagram but their calculation was based on glass transition of the liquid. Also, very few experimental data is available on this system, probably due to the high cost and extremely active yttrium metal. Thus a computational modeling and creation of a multicomponent database for the Mg-Cu-Y system will be useful for the researchers who are working on the field of the metallic glass.

1.3 Aim of this Work

Mg alloys are becoming a major industrial material due to their potential weight saving characteristics and hence constructing a reliable thermodynamic database for these alloys is very essential. As a part of this effort, the thermodynamic optimization of the ternary Mg-Cu-Y system is carried out in this work and a database is created as well. This is achieved by:

- Evaluation of all the available data on Mg-Cu, Cu-Y and Mg-Y binary and Mg-Cu-Y ternary system.
- Thermodynamic modeling of all the phases present in the three binary systems.

- Calculation of the phase diagrams and the thermodynamic properties of Mg-Cu, Cu-Y and Mg-Y systems and comparing the results with the experimental data reported in the literature.
- Construction of a database for the Mg-Cu-Y ternary system by combining the thermodynamic descriptions of the constituent binaries using a suitable extrapolation technique.
- Calculating the Mg-Cu-Y ternary phase diagram from the constructed database for this system.
- Identification of the invariant points and the primary crystallization field of each phase in the Mg-Cu-Y ternary system.
- Calculation of the thermodynamic properties of the Mg-Cu-Y system from the constructed data base and comparing the results with the experimental data reported in the literature.

CHAPTER 2

Literature Review

A brief description of different works on the Mg-Cu-Y ternary system and its subbinaries Mg-Cu, Cu-Y and Mg-Y are given here. Emphasis is given on the critical evaluation of the phase diagram, thermodynamic properties and crystallographic data of these systems.

2.1 Mg-Cu Binary System

2.1.1 Phase Diagram

The first work on Mg-Cu system was carried out by Boudouard [7] who used metallography and thermal analysis to determine the existence of three congruently melting compounds $CuMg_2$, CuMg and Cu_2Mg and their corresponding melting points 823 K, 858 K and 1213 K. His thermal analysis also showed the presence of four minima that belongs to the eutectic reactions. However, it is confirmed by different experimental analysis [8-11] that there are only three eutectics and two congruently melting compounds in this system.

Sahmen [8] investigated the Mg-Cu system by thermal and microscopic examination. He determined the liquidus line, three eutectic points and two intermetallic compounds; Cu_2Mg and $CuMg_2$, which melt congruently at 1070 K and 841 K,

respectively. These values are clearly inconsistent with those of Boudouard [7]. Also, the thermal and microscopic analysis by Urazov [9] showed the melting temperature of Cu_2Mg and $CuMg_2$ to be 1072 and 843 K, respectively which are relatively in close agreement with those of Jones [10] who reported the values to be 1092 K and 841 K. Jones [10] did not consider the homogeneity range of Cu_2Mg, hence his reported value for the melting temperature of Cu_2Mg was not used in this work.

According to Sahmen [8], one of the eutectics was located near Cu rich region at 78 at.% Cu and at a temperature of 1001 K, the eutectic near Mg rich region was placed at 13.6 at.% Cu and at a temperature of 758 K. Another eutectic was placed between the two intermetallic compounds at 44 at.% Cu and at 828 K. These values agree well with those of Urazov [9] and Jones [10].

The most extensive work on Mg-Cu system was done by Jones [10] using both thermal and microscopic analysis. He prepared more than one hundred alloys to investigate this system. Most of his reported data, especially for the liquidus curve, were used in this work.

Hansen [12] determined the solubility of Cu in Mg by metallographic analysis. His experiments showed that the solubility increases from about 0.1 at.% Cu at room temperature to about 0.4-0.5 at.% Cu at 758 K. However, Jenkin [13] was doubtful about the accuracy of the above solubility limit and reported that the limit should be very much less. The metallography of the high-purity alloys prepared by Jenkin [13] clearly indicates that the solubility of Cu in Mg is less than 0.02 at.% Cu at 723 K. Besides the metallographic analysis of Jones [10] showed that the solubility of Cu in Mg is only 0.007 at.% Cu at room temperature, increasing to about 0.012 at.% Cu near the eutectic

temperature. These values are contradictory to those given by Hansen [12]. On his discussion of Jones [10] work, Ageew [14] did not mention any evidence of the presence of solid solubility of Cu in Mg. Also the analysis of Grime and Morris-Jones [15] did not show any solid solubility. Latter Stepanov and Kornilov [16] revealed that the solubility is 0.2 at.% Cu at 573 K, 0.3 at.% Cu at 673 K and 0.55 at.% Cu at 753 K. This is in considerable agreement with the metallographic work of Hansen [12]. However considering the accuracy of the analysis and vast amount of samples prepared by Jones [10] it appears that the solubility limits given by [12] and [16] are quite high. Hence the solubility range reported by Jones [10] was used in this work.

The solubility of Mg in Cu was determined by Grime and Morris-Jones [15]. According to their X-ray powder diffraction results, the maximum solubility is approximately 7.5 at.% Mg. According to Jones [10] the solubility is about 5.3 at.% Mg at 773 K, increasing to about 6.3 at.% Mg at 1003 K. Stepanov [11] showed the presence of solid solution with maximum solid solubility of 10.4 at.% Mg using an electrical resistance method. The published data by Bagnoud and Feschotte [17] placed the maximum solubility at 6.94 at.% Mg. Except Stepanov [11] most of the data [10, 15, 17] are in close agreement with each other. For this work, the data of Jones [10] has been considered for its consistency in representing the entire phase diagram.

No homogeneity range is mentioned for the intermediate phase Mg_2Cu, whereas $MgCu_2$ was reported with a narrow homogeneity range that extends on both sides of the stoichiometric composition. According to Grime and Morris-Jones [15], the solubility was 2 to 3 at.% on both sides of the stoichiometric compound $MgCu_2$. Also, XRD (X-ray diffraction) analysis from Sederman [18] disclosed that the extend of this solubility at

773 K does not exceed 2.55 at.% (from 64.55 to 67.20 at.% Cu) and considerably less at lower temperature. However X-ray diffraction, microscopic and differential thermal analysis (DTA) by Bagnoud and Feschotte [17] confirmed that the maximum solid solubility at the eutectic temperatures on both sides of $MgCu_2$ are 64.7 and 69 at.% Cu. The solubility range data reported by Bagnoud and Feschotte [17] is more reliable because they used different techniques to confirm the range of solubility and their results were used in this work.

Mg_2Cu was mentioned to have hexagonal structure [15] whereas Runqvist *et al.* [19] had found that the crystal structure was orthorhombic with lattice parameters a = 0.9070 nm, b = 1.8247 nm and c = 0.5284 nm. The orthorhombic crystal structure for Mg_2Cu was confirmed by Ekwald and Westgren [20]. Thus it appears that the structure determined by [15] is incorrect and was not used in this work.

Fcc Crystal structure for $MgCu_2$ phase was reported by Friauf [21] by X-ray powder diffraction. The structure was found to be C15 type, with lattice parameter a = 0.699 nm for an alloy of 69.28 at.% Cu. Runqvist *et al.* [19] reported the lattice parameter of $MgCu_2$ in the range of 0.70354 to 0.7050 nm. Chatterjee and Mukherjee [22] reported the lattice parameter to be 0.7064 nm at 773 K. However, Bagnoud and Feschotte [17] determined this to be 0.735 nm at 573 K which belongs to the stoichiometric $MgCu_2$ phase and was used for this work. The difference in the reported lattice parameters is due to the presence of nonstoichiometric phase and the dependence of the lattice parameter on the composition of this phase.

Nayeb-Hashemi and Clark [23] assessed Mg-Cu system based on the experimental data provided by Jones [10], Bagnoud and Feschotte [17] and Sederman

[18]. They made an excellent work by summarizing all the experimental data prior to their work. But they did not mention what kind of thermodynamic modeling they used in their calculation. Actually, their work is more a review work rather than an optimization.

Coughanowr *et al.* [24] reviewed the experimental work of Mg-Cu system and carried out a thermodynamic assessment for this system. Their calculated phase diagram with experimental data is shown in Figure 2.1. They considered random mixing in the liquid phase and used Redlich-Kister polynomial [25] to describe it. They made two different calculations to describe Cu_2Mg phase; as a stoichiometric phase and as a solid solution. In the case of solid solution, they modeled the homogeneity range using a Wagner-Schottky type model [26].

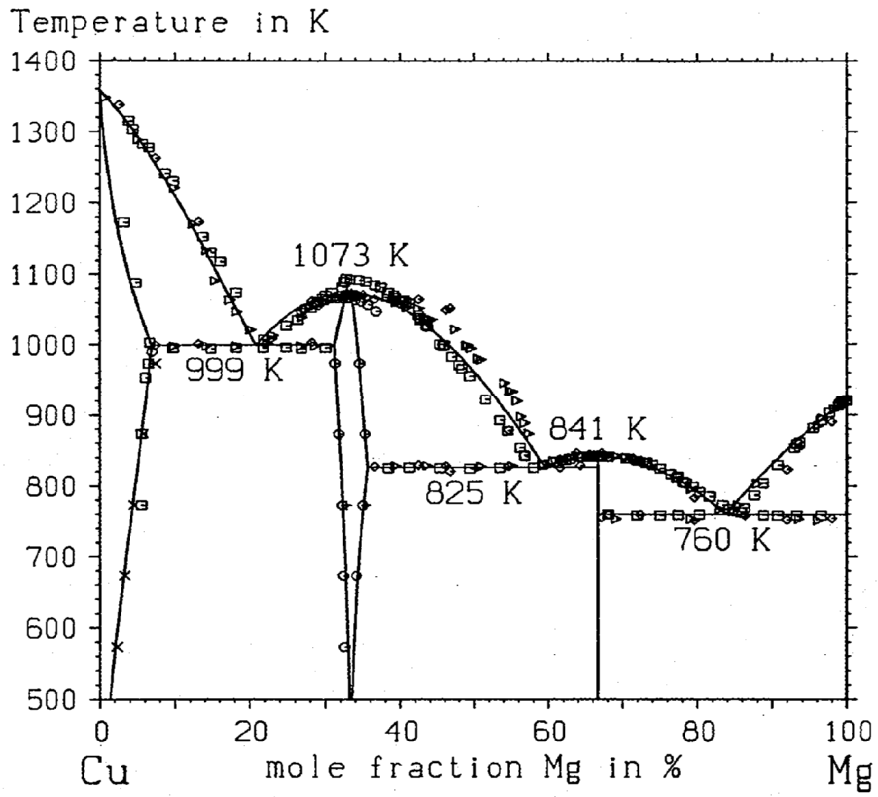

Figure 2.1: Calculated Mg-Cu phase diagram [24].

The calculated phase diagram by Coughanowr *et al.* [24] in Figure 2.1 shows good agreement with the experimental data. But they used a six-term Gibbs energy equation to describe the stoichiometric $MgCu_2$ phase. Usually a model with fewer parameters is preferred.

Later Zuo and Chang [27] evaluated the Mg-Cu binary system by thermodynamic modeling. Their calculated phase diagram is shown in Figure 2.2. The data for pure elements, Mg and Cu were taken from Dinsdale [28]. Similar to Coughanowr *et al.* [24], they also reported two thermodynamic descriptions for the Mg-Cu binary system and treated $MgCu_2$ phase as stoichiometric compound as well as an ordered phase with appreciable range of homogeneity. They used less number of parameters than [24] to reproduce the system.

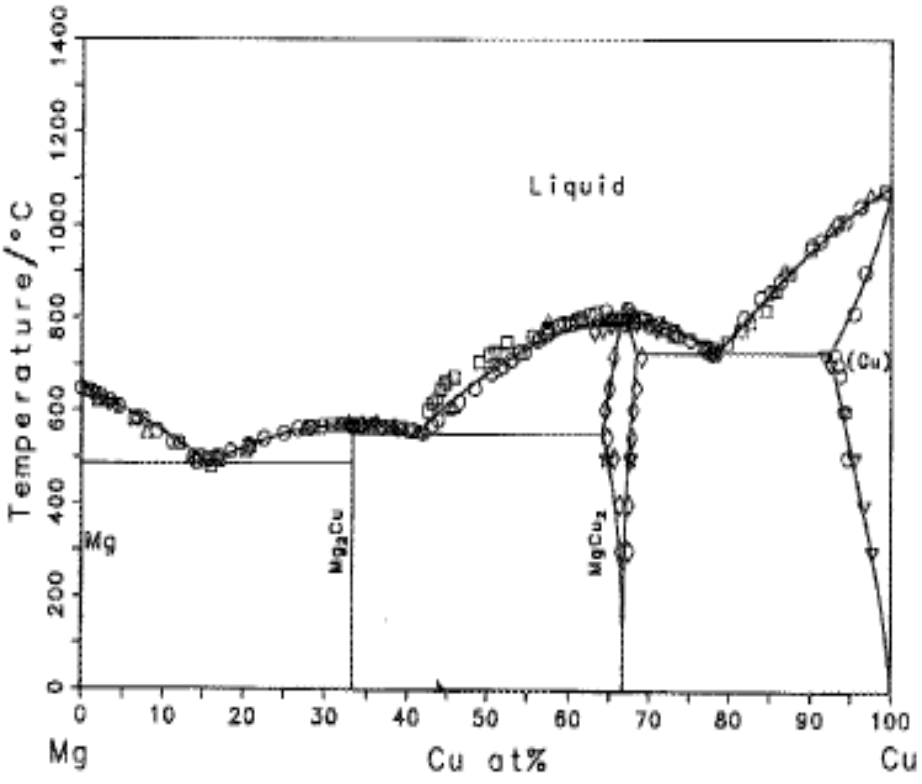

Figure 2.2: Calculated Mg-Cu phase diagram [27].

2.1.2 Thermodynamic Properties

Garg *et al.* [29] and Schmahl and Sieben [30] measured the vapor pressure of Mg over Mg-Cu alloys. These authors calculated the Mg activity in the alloys as a function of temperature, based on the partial pressure measurement. The activity values of Mg at 1000 and 1200 K calculated by Garg *et al.* [29] are shown in Figure 2.3 where dotted lines for 1000 K corresponds to the two phase region (Cu_2Mg and liquid) in the composition range 22 to 44 at.% Mg, and the broken lines in the composition range 0 to 22 at.% Mg, show the activities for the supercooled liquid alloys. The values for Cu were calculated by Gibbs-Duhem equation.

Juneja *et al.* [31] measured the vapor pressure of Mg using boiling temperature method and estimated different thermodynamic properties. Errors can be involved in this type of measurement due to uncertainly in the sample temperature, uncertainty in the reproducibility and measurement of pressures and also from compositional variations of the alloy due to preferential vaporization of Mg. Juneja *et al.* [31] tried to minimize the errors and was able to confine the total error to ± 1.46 $kJ.mol^{-1}$ of the chemical potential of Mg in the alloys. Also, Hino *et al.* [32] measured the activity of liquid Mg whose results are in good agreement with the measured values of [29]. Activity measured by four different groups [29-32] using different techniques are more or less in good agreement.

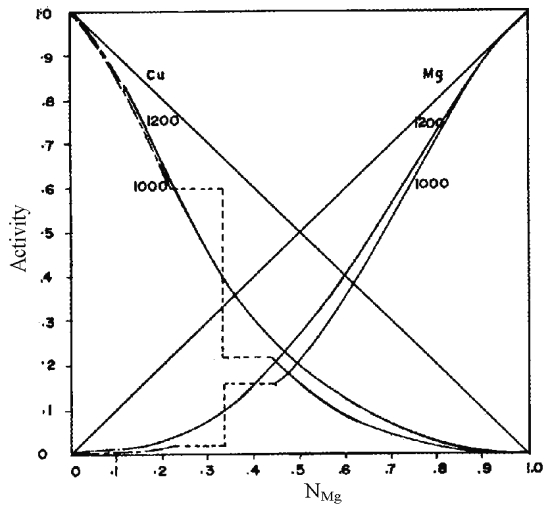

Figure 2.3: Activity of Copper and Magnesium in liquid Cu-Mg alloy at 1000 and 1200K [29].

Enthalpy of mixing of the Mg-Cu liquid was measured by Sommer *et al.* [33] and Batalin *et al.* [34] by calorimetric method. Figure 2.4 shows the calculated enthalpy of mixing by Coughanowr *et al.* [24] which is in good agreement with the measured values. However, between 20 to 60 at.% Mg, the data of [34] are more positive than those of [33] as well as the calculated values by [24].

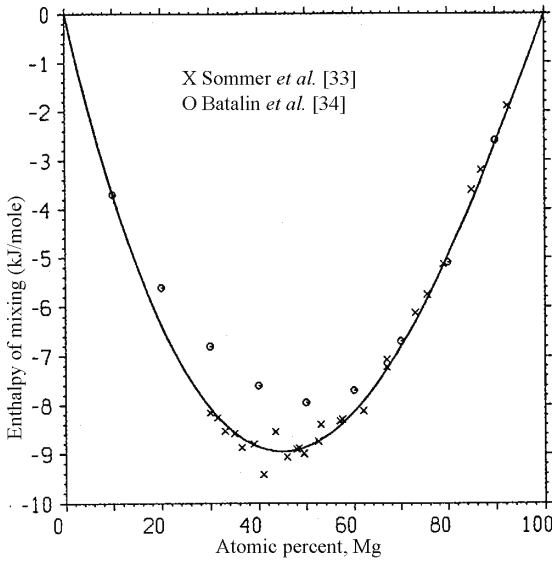

Figure 2.4: Calculated liquid phase enthalpy of mixing for Mg-Cu system at 1100Kwith the experimental data [24].

King and Kleppa [35] determined the enthalpies of formation for $MgCu_2$ and Mg_2Cu by calorimetric method. Similar values have been determined by Eremenko *et al.* [36] using EMF measurement. Their measured enthalpies, along with published data from vapor pressure measurements by Smith *et al.* [37] are given in Table 2.1. Due to different measurement techniques these values are contradictory to one another. Since vapor pressure measurements usually do not provide highly reliable data the values of [35] would be more acceptable. Entropies of formation for the two compounds published by [36] are higher than those obtained by [37]. However the values from [36] seem to be more reliable than those from [37] due to the use of more acceptable experimental technique.

Table 2.1: Enthalpy and entropy of formation of Mg_2Cu and $MgCu_2$ compounds.

Phase	**$-\Delta H^o_{298}$ (kJ/mol)**	**ΔS^o_{298} (J/mol.K)**	**Ref.**
$MgCu_2$	33.54±1.26	-	[35]
	38.59±2.09	11.72±6.28	[36]
	22.61±5.02	1.26±2.51	[37]
Mg_2Cu	28.64±1.26	-	[35]
	31.94±3.35	28.39±15.07	[36]
	16.71±7.54	- 4.48±4.14	[37]

2.2 Cu-Y Binary System

2.2.1 Phase diagram

The first experimental investigation of Cu-Y system was performed by Domagala *et al.* [38] applying metallography, X-ray and incipient fusion techniques on arc melted alloys of 99.99% Cu and 99% Y. They reported the composition and temperature of four eutectic points, one peritectic point and three intermediate compounds CuY, Cu_2Y and Cu_6Y which melt at 1208, 1208 and 1203 K, respectively. Cu_4Y was predicted as a solid solution which melts at 1258 K. But they did not mention any definite homogeneity range. The maximum solid solubility of copper in yttrium as well as yttrium in copper was found to be less than 1 wt.%. The accuracy of the experimental temperature is within ± 15 K. It is worth noting that they [38] missed the presence of Cu_7Y_2 compound.

Buschow and Goot [39] investigated Cu-Y system by X-ray diffraction and metallography in the concentration range 80-90 at.% Cu. They obtained evidence for the existence of two hexagonal Cu-rich phases. They defined the composition as CuY_5, having a hexagonal $CaCu_5$ type structure and CuY_7, having hexagonal $TbCu_7$ type structure. The lattice constants of CuY_7 were determined as a = 4.940 Å and c = 4.157 Å with 0.843 c/a ratio.

Chakrabarti and Laughlin [40] proposed Cu-Y phase diagram using the experimental data from Domagala *et al.* [38] and Sudavtsova *et al.* [41]. The information on the system was incomplete especially with regard to the entire liquidus region. Different transition temperatures were also not accurately determined. Their reported phase diagram is shown in Figure 2.5. The main features of their phase diagram are: Cu

(fcc) terminal solid solution with negligible (<0.04 at.%) solubility of Y; Y (hcp) terminal solid solution with marginal solubility of Cu (maximum between 0.07 to 0.14 at.%) and is stable upto 1751 K; β-Y terminal solid solution with (αY) ⇆ (βY) transition temperature at 1743 K; four intermediate compounds Cu_6Y, Cu_4Y, Cu_7Y_2, Cu_2Y which melt at temperatures of 1183 K±5, 1248 K±5, 1193 K±5 and 1208 K±15 respectively and four eutectic reactions. They [40] did not report any thermodynamic data for the Cu-Y system.

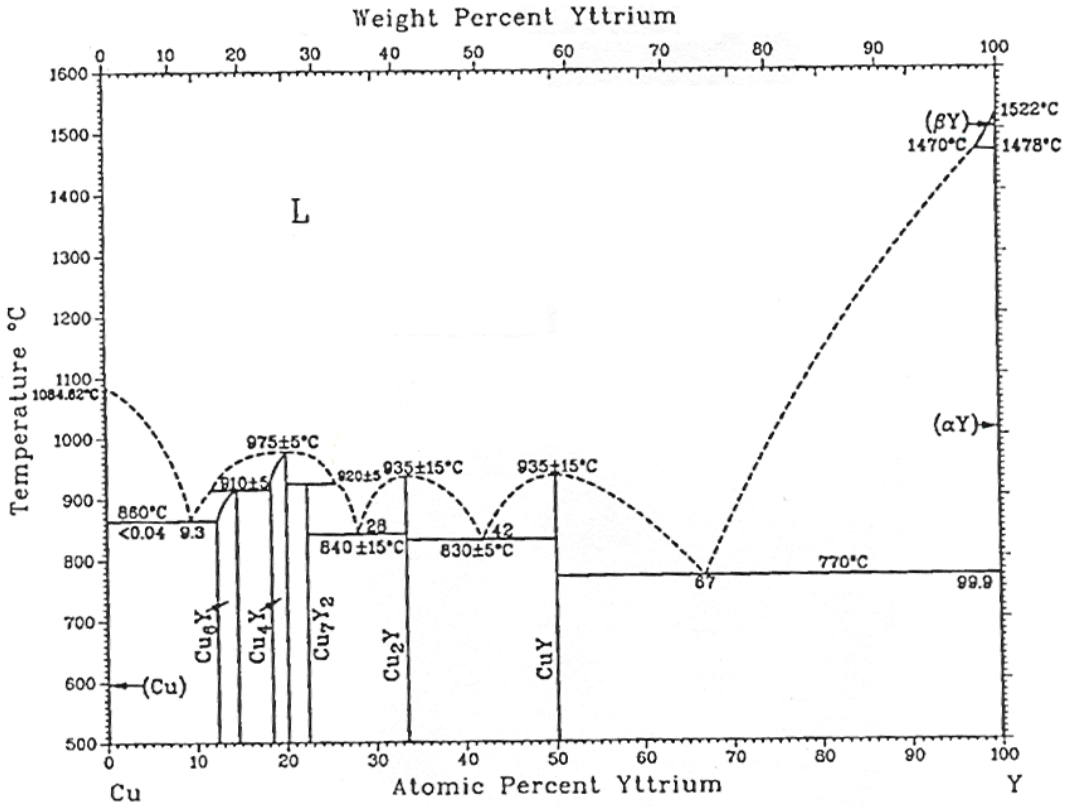

Figure 2.5: Calculated Cu-Y phase diagram [40].

Guojun *et al.* [42], measured the heat contents of Cu-Y binary alloys using drop calorimetery in a temperature range of 850-1300 K. The congruent melting temperatures and heats of fusion of the intermetallic compounds CuY, Cu_2Y, and Cu_4Y, as well as

temperatures of other phase transformations were derived from the heat content data. Their experimental results are contradictory with those of [38] where the melting temperatures of the compounds deviate up to 38 K. However the experimental procedure and the purity of the elements used by [42] are more reliable than those of [38].

Itagaki *et al.* [43] optimized the Cu-Y system using the experimental data reported by Guojun *et al.* [42]. Their calculated phase diagram is shown in Figure 2.6. Unlike Chakrabarti and Laughlin.[40], they considered Cu_4Y as a stoichiometric compound. The temperature and composition of the eutectic points show discrepancy with the data of [38] and [42]. The reported data of Massalski *et al.* [44] show deviation from those of Guojun *et al.* [42] as well as the calculated values of Itagaki *et al.* [43].

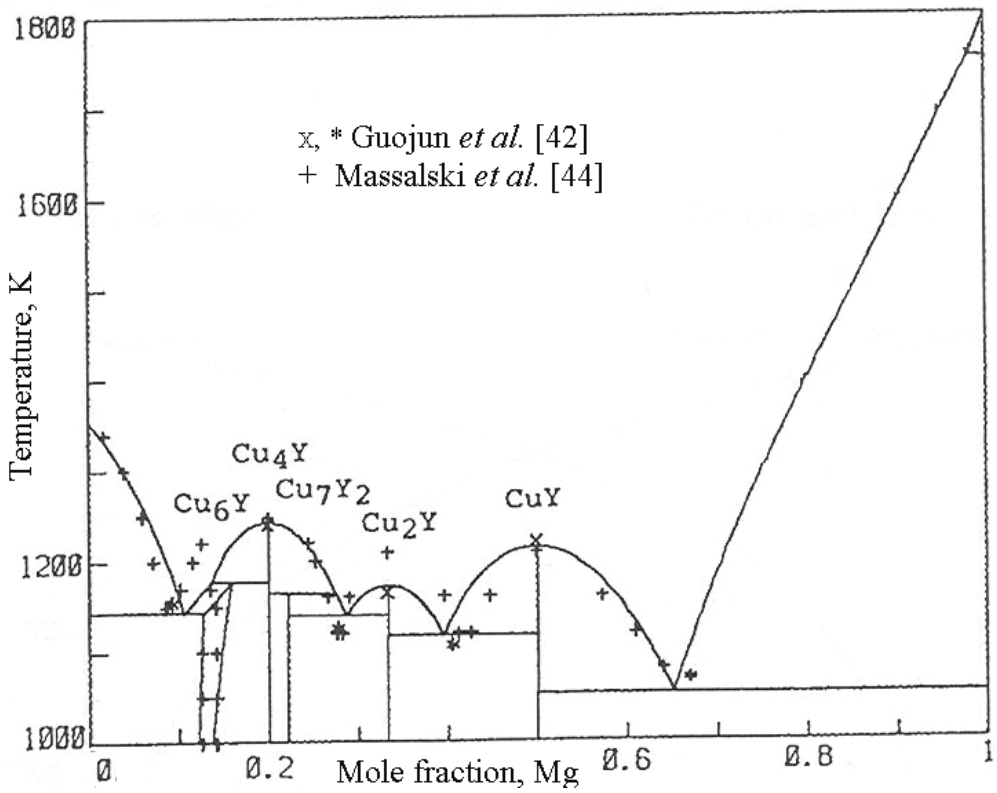

Figure 2.6: Calculated Cu-Y phase diagram [43].

To resolve these controversies Fries *et al.* [45] reinvestigated the Cu-Y system by DTA and XRD analysis, with emphasis on the composition range between 55 to 90 at.% Cu, and proposed a new phase diagram based on thermodynamic modeling. Their calculated phase diagram is shown in Figure 2.7. Their [45] DTA results provide evidence for the possible existence of a high temperature phase transformation in the Cu_2Y compound {Cu_2Y (h) ↔ Cu_2Y (r)}, which is included in their optimization. They reported five intermetallic compounds: CuY, Cu_2Y, Cu_4Y, Cu_6Y and Cu_7Y_2. Apart from Cu_6Y and Cu_7Y_2 all compounds melt congruently. The invariant points obtained by them [45] show fair agreement with the experimental data of [42] but along the (α-Y) liquidus line differs markedly from those of Domagala *et al.* [38]. More experimental data is required for better understanding of this region.

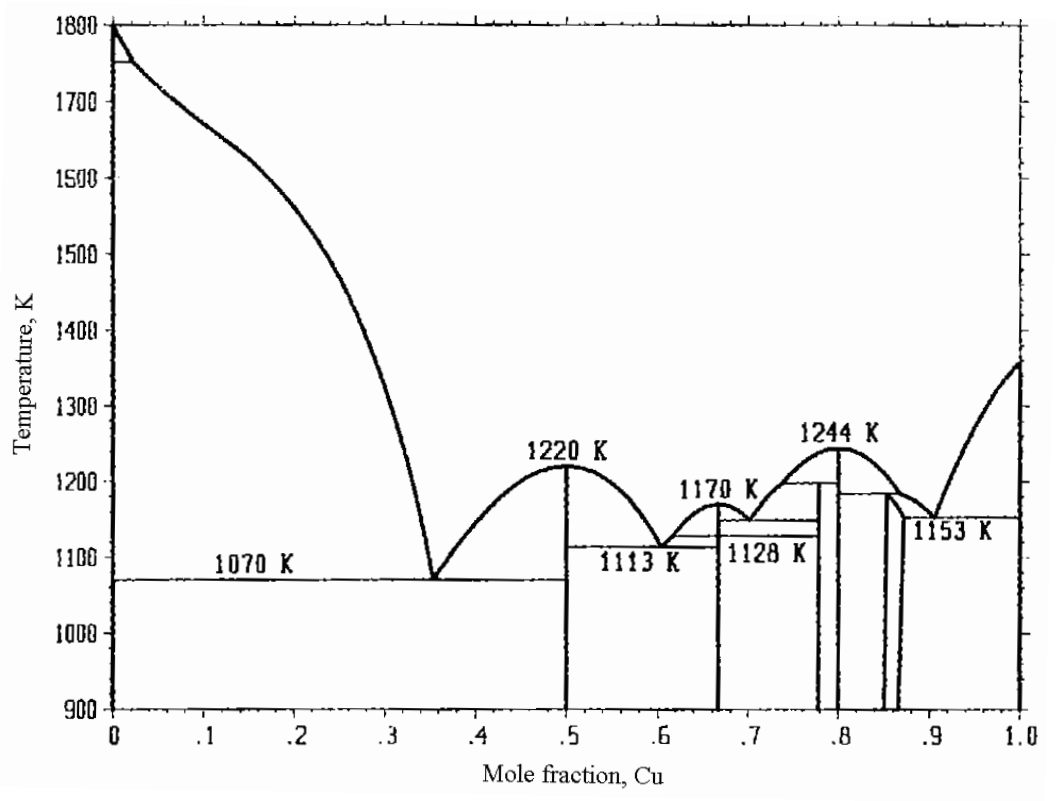

Figure 2.7: Calculated Cu-Y phase diagram [45].

Later, Abend *et al.* [46] reinvestigated the Cu-Y system in the composition range of 30 to 90 at.% Cu using DTA, X-ray diffraction and EMF (electromagnetic field) measurement. They reported four eutectic points at the compositions of 0.098, 0.298, 0.402 0.675 at.% Y at 1150 K, 1143 K, 1102 K and 1071 K which are consistent with those of Guojun *et al.* [42] but differs from the data of Massalski *et al.* [44]. The melting temperatures of the five intermediate compounds agree well with the reported values of Fries *et al.* [45].

There is a point of doubt about the composition of Cu_6Y phase. It was defined as Cu_7Y by Buschow and Goot [39]. According to Fries *et al.* [45], Cu_6Y would be more appropriate description for this phase because the formula Cu_7Y does not represent the composition where this solid solution melts, but the maximum Cu content instead. This is, also, supported by Abend and Schaller [46] and Okamoto [47]. The XRD results of [45] confirmed a range of solubility for the Cu_6Y phase. The limit at Y-rich and Cu-rich sides were determined to be 84.5± 0.5 at.% Cu and 87.0±0.5 at.% Cu respectively in the temperature range of 973 to 1123 K. This is consistent with the reported values, 85.7 at.% to 87.5 at.% Cu, by Massalski *et al* [44] and 84 at.% to 88 at.% Cu by Okamoto [47]. Also, the EMF measurement by [46] showed similar range of homogeneity.

For Cu_4Y phase, Fries *et al.* [45] could not obtain any X-ray with sharp peaks which suggests that the crystal structure of this phase has some defects. They found some similarities in the X-ray spectrum of Cu_4Y with that of Cu_6Y and concluded that Cu_4Y has the $CaCu_5$ type crystal structure with random, nonperiodic defects. They were unable to find any homogeneity range for Cu_4Y phase. Same crystal structure for the Cu_4Y phase was reported by Chakrabarti and Laughlin [40] and Buschow and Goot [39].

The experimental data available for the Cu-Y system is not in good accord with each other. More experimental data is required for the liquidus curve near the Y-rich region. However after reviewing all the available data of this system, it appears that the data of Fries *et al.* [45] and Guojun *et al.* [42] are more reliable than the others and will be used in this work.

2.2.2 Thermodynamic properties

The amount of thermodynamic data for the Cu-Y system is limited. Y is highly reactive and hence it is very difficult to handle the alloys during high temperature experimental process. However, enthalpy of mixing of liquid alloys have been determined calorimetrically by Sudavtsova *et al*. [41] at 1415 K, Watanabe *et al*. [48] at 1373 K, and also by Sidorov *et al.* [49] at 1963 K. Figure 2.8 shows the calculated heat of mixing for liquid Cu-Y alloys by [46]. The curve fits well with the measured values of [48] and [49] but shows a little bit discrepancy with those of [41].

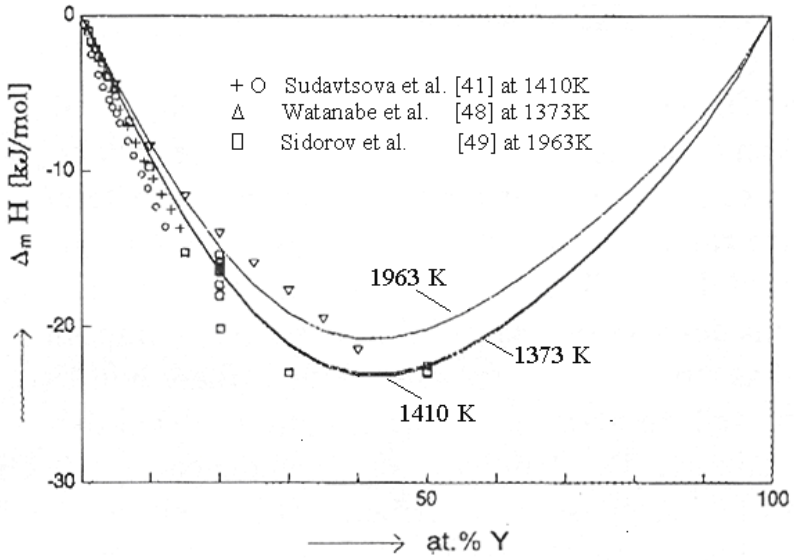

Figure 2.8: Calculated Enthalpy of mixing of liquid Cu-Y at 1373, 1410 and 1963 K [46].

Berezutskii and Lukashenko [50] measured the vapor pressure and activity coefficients of liquid Cu in the composition range of 19.8 to 100 at.% Cu at 1623 K. The calculated values of Ganesan *et al.* [51] show good agreement with the measured values of [50] as shown in Figure 2.9.

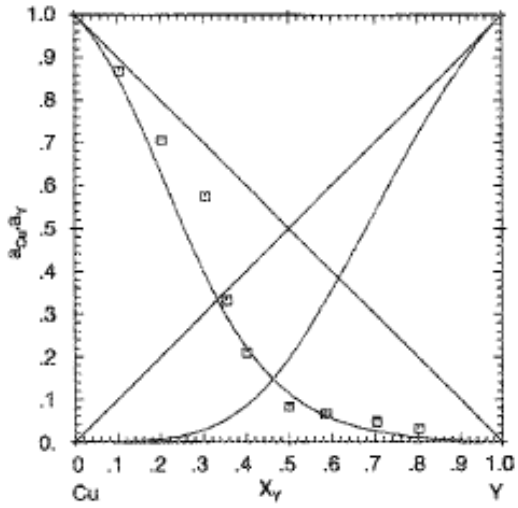

*Figure 2.9***:** *Activity of liquid Cu and Y at 1623 K [51].*

By thermodynamic evaluation Itagaki *et al.* [43] have calculated entropy of mixing of liquid alloys at 1823 K as shown in Figure 2.10. The curve shows clear m-shape which is one of the indications of the presence of short range ordering in the liquid.

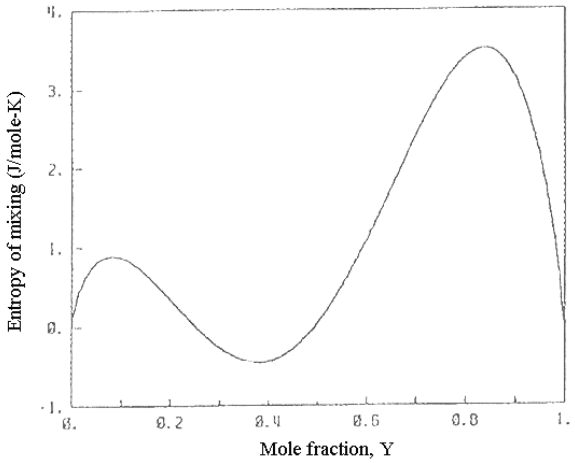

Figure 2.10: Calculated entropy of mixing of liquid Cu-Y at 1823 K [43].

Watanabe *et al.* [48] determined the enthalpy of formation of CuY, Cu_2Y and Cu_4Y. These values along with the reported values of Cu_6Y and Cu_7Y_2 by Itagaki *et al.* [43] are summarized in Table 2.2. These values are reasonably close with each other.

Table 2.2: Enthalpies of formation of the compounds in Cu-Y system

.

Phase	**ΔH^{o}_{298} (kJ/mol)**	**Ref.**
Cu_6Y	-67.0	[43]
Cu_4Y	-80.21±3.13	[48]
	-70.34	[43]
Cu_7Y_2	-133.22	[43]
Cu_2Y	-58.5	[48]
	-52.18	[43]
CuY	-38.68±0.43	[48]
	-36.40	[43]

2.3 Mg-Y Binary System

2.3.1 Phase Diagram

Magnesium alloys are becoming more important due to their potential weight saving characteristics compared to Aluminium based alloys. Addition of Yttrium enhances the high-temperature properties and casting characteristic of Mg. Also, Mg-Y alloys show higher creep resistance, better corrosion resistance and a considerable age hardening response [52]. Thus it is very important to know the phase diagram as well as the thermodynamic properties of this system.

Gibson *et al.* [53] were the first researchers who reported the Mg-Y phase diagram. They investigated the system by thermal, microscopic and x-ray diffraction

methods in the temperature range of 673 to 1223 K. They determined the maximum primary solid solubility of Yttrium in Magnesium as 9 wt.% Y at the eutectic temperature (840 K). This agrees well with the data of Sviderskaya and Padezhnova [54] who used thermal analysis to study the Mg-rich region of Mg-Y system. Another investigation by Mizer and Clark [55] on the Mg-Y system using thermal analysis and metallography showed that the maximum solubility of Y in solid Mg was approximately 12.6 wt% Y at the eutectic temperature 838.5 K. This is also in good agreement with those of [53] and [54].

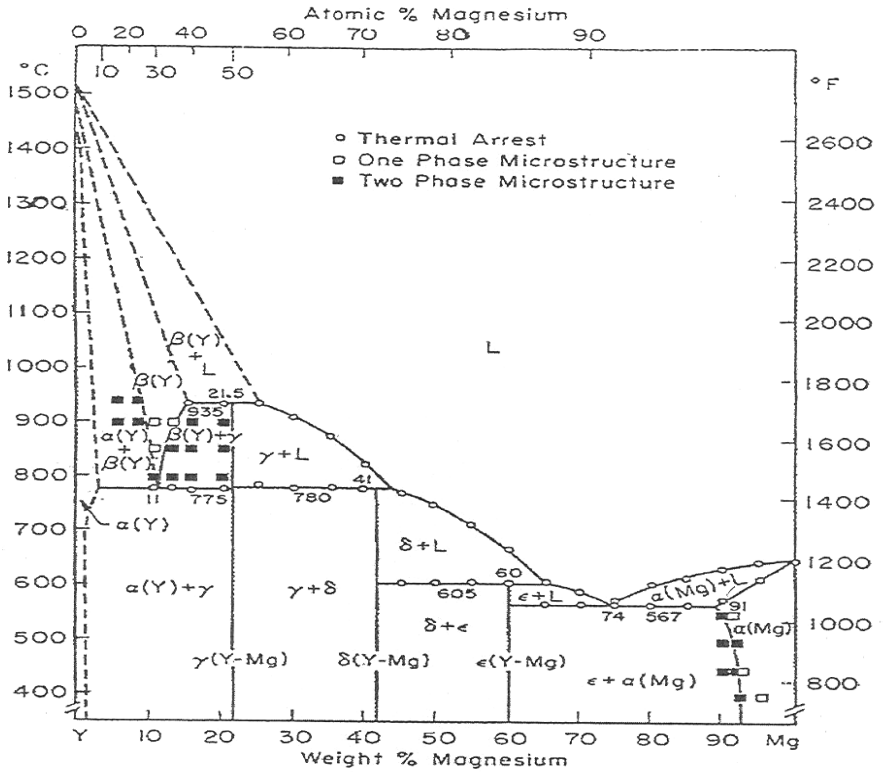

Figure 2.11: Proposed Mg-Y phase diagram [53].

As reported by Gibson *et al.* [53], there is one eutectic reaction at 74 wt.% Mg at 840 K and one eutectoid reaction at 11 wt.% Mg at 1048 K. The latter reaction was associated with a high temperature allotropic transformation of Yttrium. The proposed

phase diagram by [53] is shown in Figure 2.11. Three intermediate phases were identified as γ at 21.5 wt.% Mg, δ at 41 wt.% Mg and ε at 60 wt.% Mg. All these are peritectic compounds and decompose at 1208 K, 1053 K and 878 K, respectively. They did not mention any definite composition for the intermediate phases. However, ε and γ were reported [54] to have a composition of $Mg_{24}Y_5$ and MgY, respectively. The thermodynamic optimization of Ran *et al.* [56] showed a very good agreement with the measured values of [53].

Massalski [57] assessed the Mg-Y phase diagram using the experimental work in the literature. He used the experimental data of Sviderskaya and Padezhnova [54] for the Mg-rich region and his calculated phase diagram is shown in Figure 2.12.

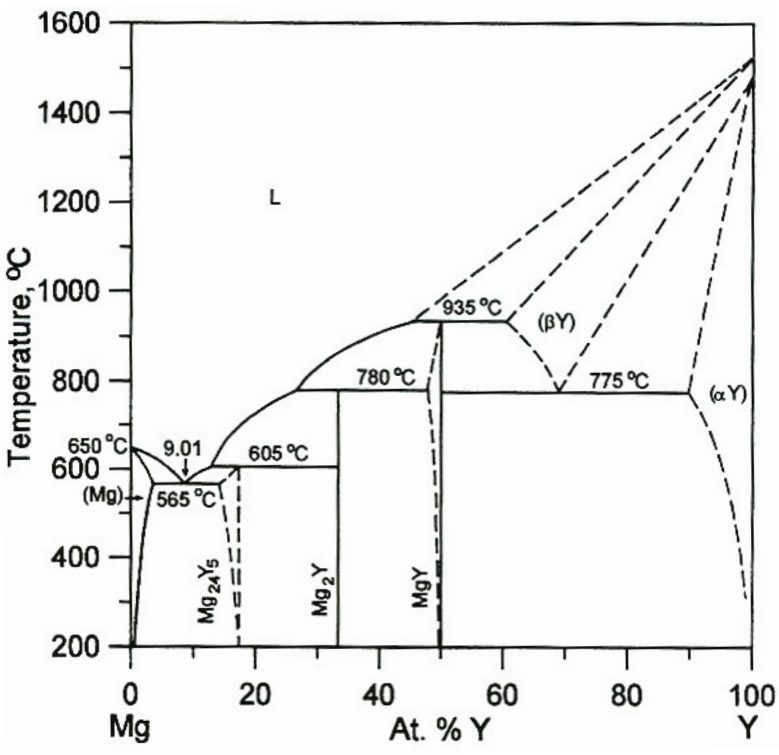

Figure 2.12: The estimated Mg-Y phase diagram [57].

Smith *et al.* [58] investigated the crystallography of MgY (γ), Mg_2Y (δ) and $Mg_{24}Y_5$ (ε) intermediate phases. The tangible homogeneity range of ε and γ determined

by them is shown in Table 2.3. δ phase was predicted as a stoichiometric compound by [53, 57, 58]. Their results do not agree with Flandorfer *et al.* [59], who employed XRD, optical microscopy, and microprobe analyses to study the Ce-Mg-Y isothermal section at 773 K. Based on the experimental work of [59], the range of homogeneity of δ was obtained and mentioned in Table 2.3.

Table 2.3: The homogeneity ranges of the ε, δ, and γ phase.

Phase	**Temperatures range (K)**	**Range of homogeneity at.%Y**	**Ref.**
γ, MgY	<1208	48-50	[58]
ε, $Mg_{24}Y_5$	<878	13-16	[58]
δ, Mg_2Y	<1053	33.2-34.2	[59]

The crystal structures of δ, ε, and γ were determined by Smith *et al.* [58] using X-ray diffraction. They reported that γ-phase has CsCl type structure, δ-phase has $MgZn_2$ structure, and ε-phase has α-Mn structure. Another investigation on the crystal structure of ε by Zhang and Kelly [60] using TEM (Transmission electron microscopy) micrographs, showed the same structure as found by Smith *et al.* [58] but with one difference in the occupying atoms at the *2a* Wyckoff position. However since the work of [60] used TEM, it is considered more precise than that of [58] who used XRD.

Fabrichnaya *et al.* [52] carried out thermodynamic optimization on the Mg-Y system. They treated Mg-hcp and Y-hcp as one phase forming a wide miscibility gap. They used sublattice model to reproduce the homogeneity ranges of $Mg_{24}Y_5$, MgY and Mg_2Y. But they did not consider the crystallographic data for the intermediate phases in their analysis.

Recently, Shakhshir and Medraj [61] reoptimized the Mg-Y system using available experimental data. Their calculated phase diagram is shown in Figure 2.13

which is in good agreement with the experimental data. They considered the liquid phase as random solution and used Redlich-Kister polynomial [25] to model it. They used Sublattice model for the intermetallic phases and based their analysis on the crystallographic data.

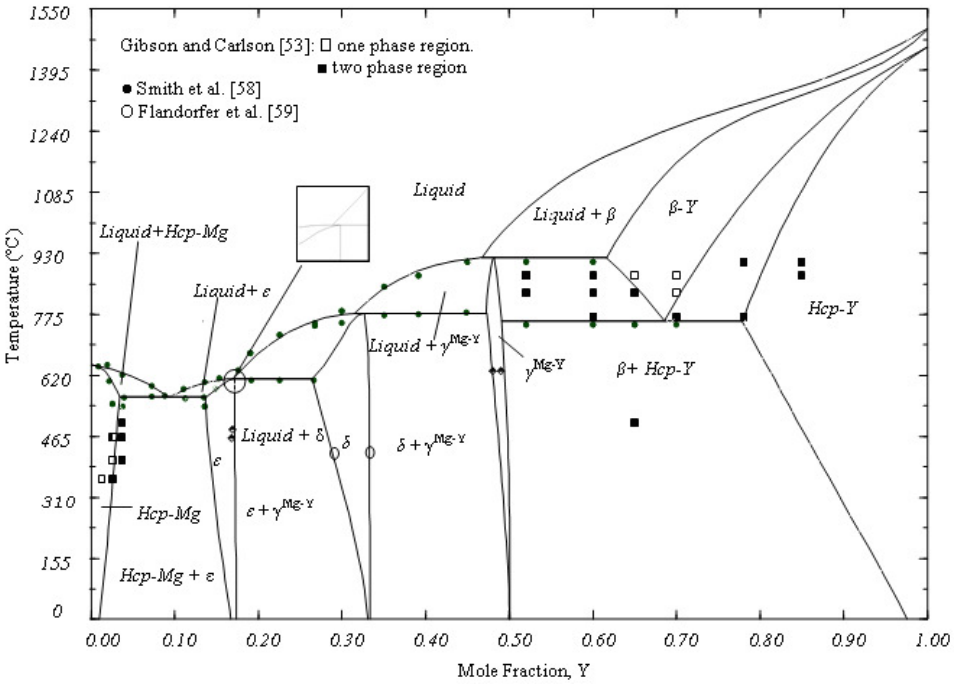

Figure 2.13: Calculated Mg-Y phase diagram [61].

2.3.2 Thermodynamic Data

Agrawal *et al*. [62] measured calorimetrically the enthalpy of mixing of the liquid Mg-Y alloy near the Mg-rich region (upto 21.8 at.% Y) at different temperatures. They extrapolated the values of the heat of mixing over the remaining composition range using the association model as shown in Figure 2.14.

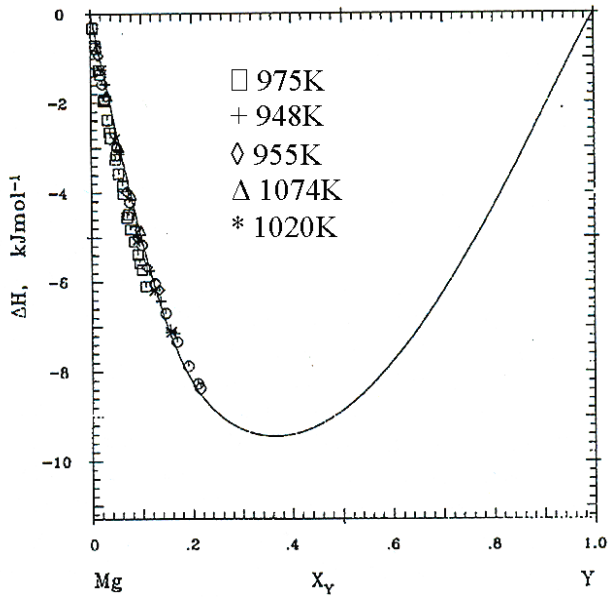

Figure 2.14: Calculated enthalpy of mixing of the Mg-Y liquid at 1000K with experimental Data [62].

Activities of Mg were measured by Ganesan and Ipser [63] using the vapor pressure technique. The activities calculated by Fabrichanya *et al.* [52] as shown in Figure 2.15 agree well with the experimental data [63].

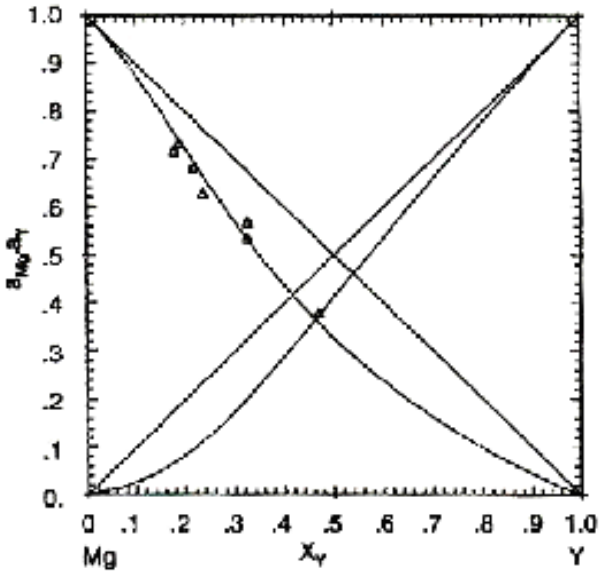

Figure 2.15: Calculated activity of liquid Mg and Y at 1173 K with the experimental data [52].

Shakhshir and Medraj [61] calculated the partial free Gibbs energy of Mg and Y in Mg-Y liquid at 900°C, which is shown in Figure 2.16. Their model could reproduce the experimental data of [63].

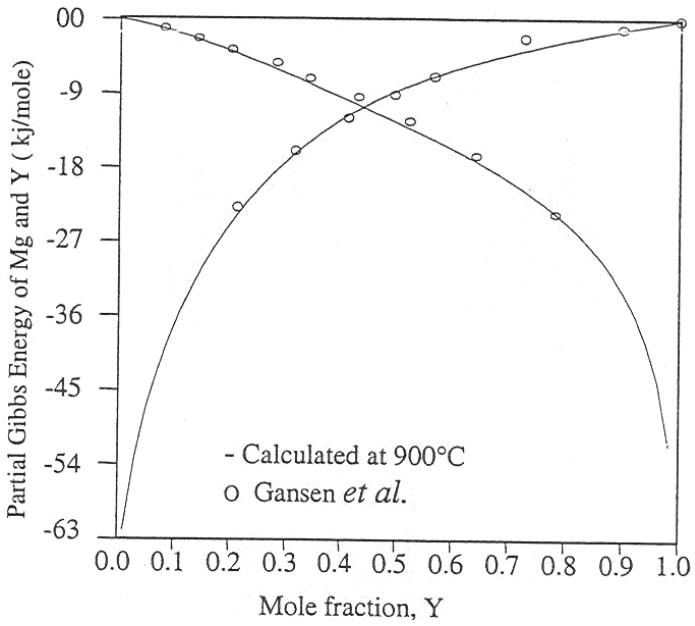

Figure 2.16: Calculated partial Gibbs energy of Mg and Y in Mg-Y alloy at 900°C with the experimental data [61].

The enthalpies of formation of all three compounds were determined calorimetrically by Pyagai *et al.* [64]. These data are in reasonable agreement with the calorimetric data of Smith *et al.* [58] except for the γ-phase, for which the value of [64] is twice more negative than that obtained by [58]. This is due to the difficulties in measuring the heat of formation when the yttrium content increases and hence the reactions become more exothermic. Also, Y has a high melting point compared to Mg and this leads to the sublimation of Mg during fusion of the metals [62]. The experimental data for enthalpies of formation of the compounds are summarized in Table 2.4.

Table 2.4: Enthalpy of formation of the intermediate phases.

Phase	ΔH^{o}_{298} (kJ/mol- atom)	Ref.
YMg	-12.60 -30.30	[58] [64]
YMg_2	-14.20 -12.00	[58] [64]
Y_5Mg_{24}	-7.53 -6.10	[58] [64]

Fabrichanya *et al.* [52] and Shakhshir and Medraj [61] calculated the heat of formation of the three intermediate compounds and their results showed a reasonable agreement with those measured by [58] and [64]. Figure 2.17 shows a comparison between the calculated values of [61] with the experimental results.

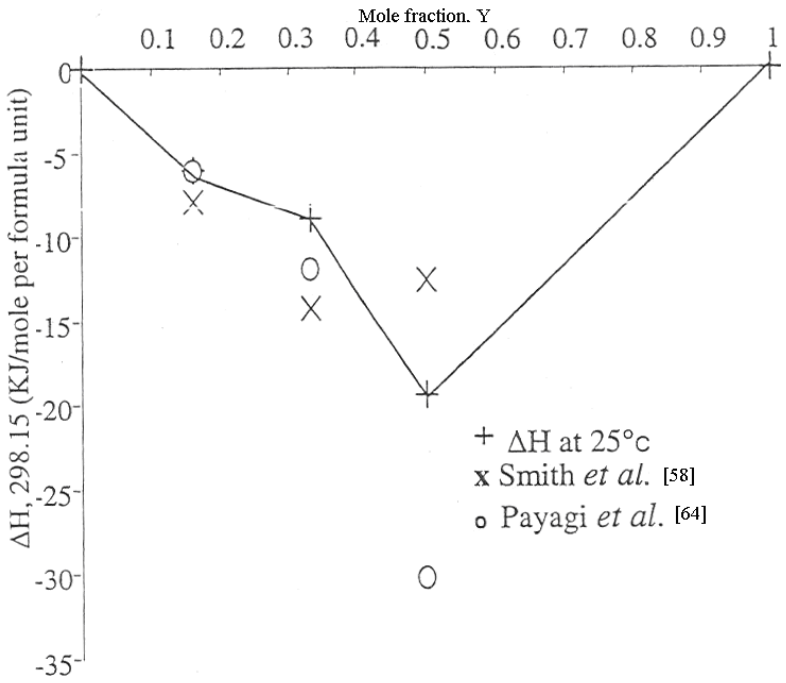

Figure 2.17: Calculated enthalpies of formation of the stoichiometric compounds with the experimental data [61].

2.4 Mg-Cu-Y Ternary System

The Mg-Cu-Y system is becoming a major industrial alloy system and attracted a lot of attention from researchers due to its unique nature to form metallic glass. Several alloy compositions were identified which showed interesting mechanical properties coupled with low density as metallic glass. But a complete investigation on this system is not yet done. Inoue *et al.* [5], Busch *et al.* [65], Ma *et al.* [66] made some experimental investigation on the Mg-Cu-Y system to find the glass forming ability of different compositions. Their reported data cannot be used in this work since equilibrium condition was not achieved during the preparation of the alloys.

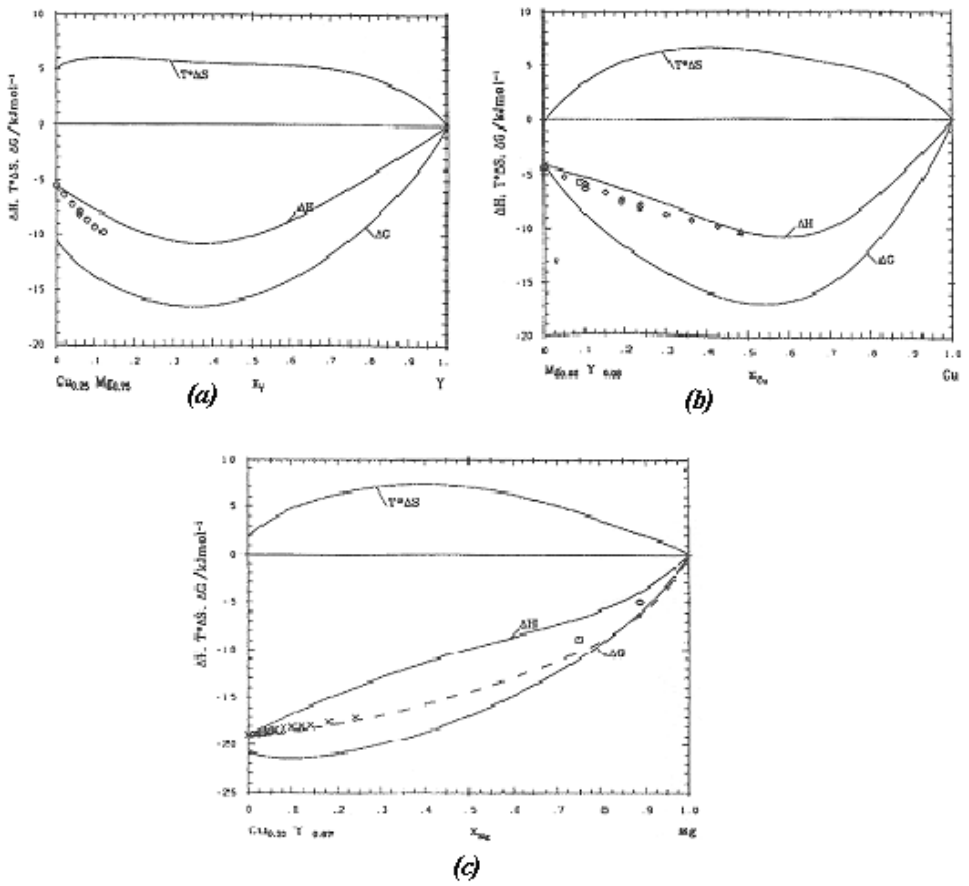

Figure 2.18: Integral enthalpy, entropy and Gibbs energy of mixing of (a) $(Cu_{0.25}Mg_{0.75})_{1-x}Y_x$ ternary liquid at 1023 K, (b) $(Mg_{0.92}Y_{0.08})_{1-x}Cu_x$ ternary liquid at 1023 K and (c)$(Cu_{0.33}Y_{0.67})_{1-x}Mg_x$ ternary liquid at 1107 K [51].

Ganesan *et al.* [51] measured the enthalpy of mixing and activity of liquid Mg-Cu-Y system by calorimetric method along five different isopleths. The composition dependence of the resulting enthalpies of the liquid alloys along three different isopleths is shown in Figures 2.18.

Activity of magnesium in the ternary liquid Mg-Cu-Y reported by [51] is shown in Figure 2.19. The dotted line represents the experimental data. It can be seen from this figure that the calculated values showed negative deviation and are not consistent with the experimental data. The authors could not explain the reasons behind this.

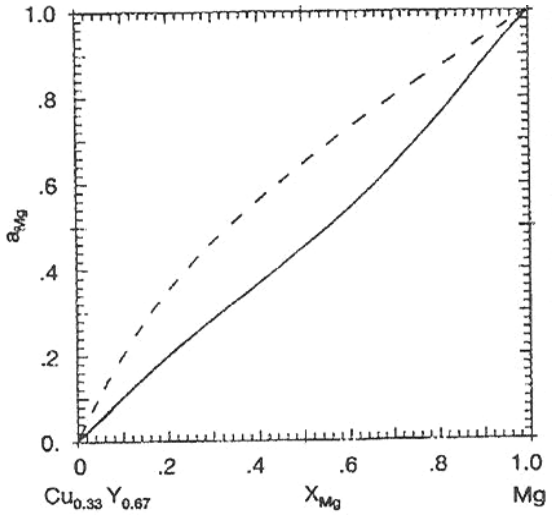

Figure 2.19: Activity of magnesium in the isopleth $x_{Cu}/x_Y = 0.5$ at 1173 K [51].

One ternary compound of composition Y_2Cu_2Mg was identified by Mishra *et al.* [67]. They used X-ray powder diffraction to determine crystallographic information. Another ternary compound of composition YCu_9Mg_2 was identified by Solokha *et al.* [68] who used optical microscopy, scanning electron microscopy and X-ray spectroscopy analysis to examine the microstructure and phase composition. But no thermodynamic property is available about these compounds. For this reason it was not possible to

include them in the present work by conventional method. But for better understanding of the ternary system, these two compounds were included in the optimization by an alternative method which will be discussed elaborately in chapter 4.

A thermodynamic calculation was carried out by Palumbo *et al.* [6] on Mg-Cu-Y system. They proposed a new modeling approach for the description of the specific heat of the liquid to include the glass transition phenomenon of the liquid. They did not consider the presence of short range ordering in the liquid. Also, the ternary compounds were not included in their assessment.

A complete thermodynamic modeling for the Mg-Cu-Y ternary system is still unknown. Also the liquid phases of the three constituent binary systems Mg-Cu, Cu-Y and Mg-Y need to be remodeled in order to consider the presence of short range ordering.

CHAPTER 3

Thermodynamic Modeling

3.1 Methodology of Thermodynamic Modeling

Thermodynamic modeling for any alloy system is nothing but a process of finding appropriate Gibbs energy equations for different phases in terms of temperature and composition of the constituent elements. By minimizing the total Gibbs energy, of all the phases present in equilibrium, phase diagrams can be calculated for a multicomponent system [1]. The total molar Gibbs energy is equal to the sum of the molar Gibbs energies of all phases multiplied by their molar fractions i.e.,

$$G = \sum_{i=1}^{p} n_i G_i^{\varphi} = \text{minimum} \quad \text{(3.1)}$$

Where n_i is the number of moles, p is the number of phases and G_i^{φ} is the Gibbs energy of phase i. G_i^{φ} for a multicomponent system can be define by equation 3.2

$$G_i^{\varphi} = G^{o} + G^{ideal} + G^{ex} \quad \text{(3.2)}$$

Where, G^{o} is the contribution from the mechanical mixing of pure components, G^{ideal} is the ideal mixing contribution, and G^{ex} is the excess Gibbs free energy contribution due to the interactions between the components. To expand the individual terms in equation 3.2, let us consider a binary system with components A and B. Thus mechanical mixing

and ideal mixing contribution of this system can be expressed by equation 3.3 and 3.4, respectively.

$$G^0 = x_A G_A^0 + x_B G_B^0 \quad \ldots\ldots\ldots\ldots\ldots\ldots\ldots\ldots\ldots\ldots\ldots\ldots\ldots\ldots\ldots\ldots \text{(3.3)}$$

$$G^{ideal} = H_{mix}^{ideal} - T\,S_{mix}^{ideal}$$

$$= 0 - RT\,(x_A \ln x_A + x_B \ln x_B)$$

$$= - RT\,(x_A \ln x_A + x_B \ln x_B) \quad \ldots\ldots\ldots\ldots\ldots\ldots\ldots\ldots\ldots\ldots\ldots \text{(3.4)}$$

Where, x_A, x_B are the compositions of the components A and B respectively, and G_A^0, G_B^0 are the Gibbs free energy of the pure components A and B at standard state (298.15 K and 1 bar), R is the universal gas constant. The contribution of ideal enthalpy of mixing, H_{mix}^{ideal}, is zero since there is no change in bond energy or volume upon mixing. The excess Gibbs energy, G^{ex}, can be described by different models and will be discuss in the later part of this chapter.

Thus calculation of phase diagram is actually a process of determining the appropriate minimum Gibbs energy for different phases of a system. This is usually done by a computer-assisted statistical procedure using experimental thermochemical and constitutional data as input. The CALPHAD (Calculation of phase diagram) method, introduced by Kaufman and Bernstien [69], is the most scientific technique of optimization. Komar and Wollants [70] illustrated the CALPHAD method in a befitting way. Figure 3.1 shows a flowchart of this method.

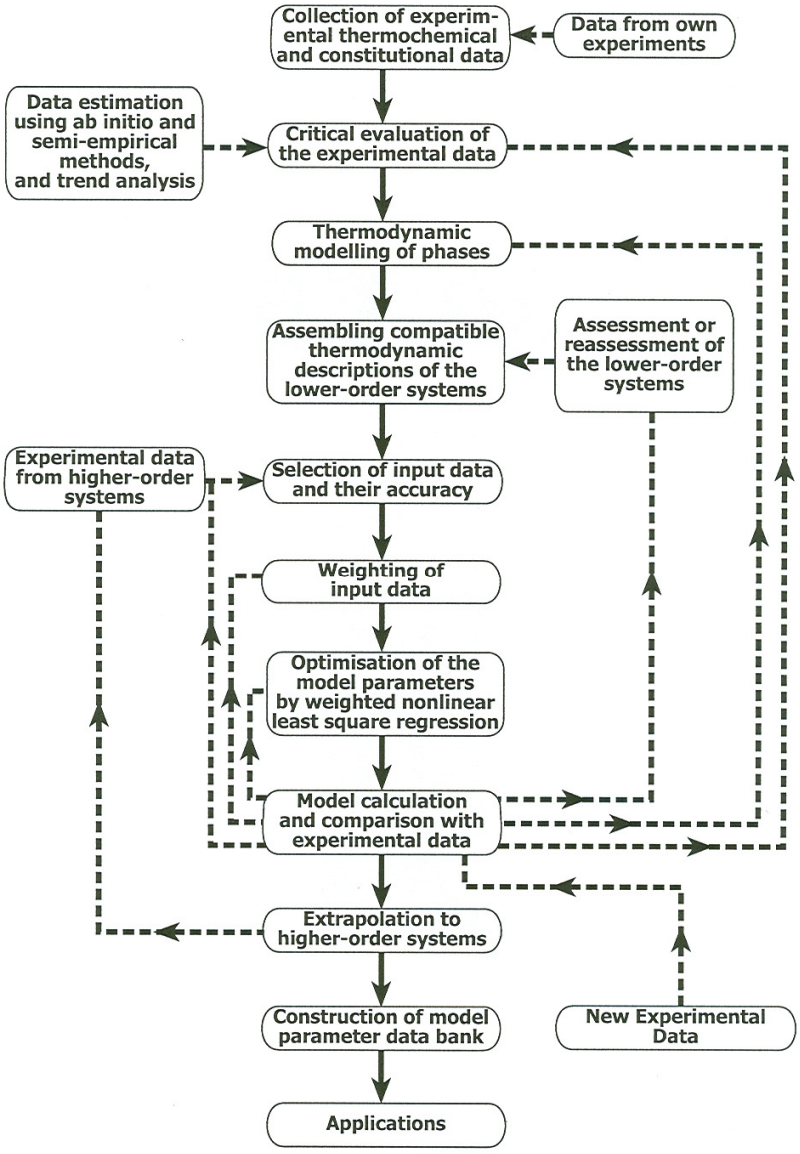

Figure 3.1: Flowchart of the CALPHAD method [70].

The first step of the thermodynamic optimization according to CALPHAD method is to collect the experimental data from the relevant literature. Critical evaluation of these data is the second step as discussed in Chapter 2. The next step is to select a suitable thermodynamic model for each phase. The selected model should be physically sound and it should be able to represent the *P-T-x* domain in which the phase is stable. Also, the model should have reasonable extrapolation characteristics in the higher order

systems [70]. Before starting the optimization, it is essential to select the appropriate input data set for the calculation and it is better to assign a weighing factor based on the accuracy of the measurement. The following steps are: the determination of the model parameters using the experimental data, and reproducing the phase diagram and the thermodynamic data, to verify the agreement between the calculations and the experimental data. The last two steps are iterative until a good agreement with the experimental data is achieved. After satisfactory optimization of the binaries the excess Gibbs energy parameters are then used for the extrapolation of the higher order system. In this step selection of a suitable geometric model is very important for reliable calculation. To make the calculations easy and accurate several software packages are available. FactSage 5.4.1 program [71] has been used in this work.

3.2 Analytical Description of the Employed Thermodynamic Models

Different thermodynamic models were used in the present work. A brief idea about these is presented here.

3.2.1 Unary Phases

The Gibbs Energy function used for the pure elements i (i = Mg, Cu, and Y) in a phase ϕ is described by the following equation:

$${}^{0}G_i^{\phi}(T) = a + bT + cT\ln T + dT^2 + eT^3 + fT^{-1} + gT^7 + hT^{-9} \quad \text{.....} \quad (3.5)$$

Where, $G_i^{\phi}(T)$ is the Gibbs energy of the pure element at standard state, T is the absolute temperature. The values of the coefficients a to h are taken from the SGTE (Scientific Group Thermodata Europe) compilation of Dinsdale [28].

3.2.2 Stoichiometric Phases

The Gibbs energy of a binary stoichiometric phase is given by

$$G^{\phi} = x_i {}^0G_i^{\phi_1} + x_j {}^0G_j^{\phi_2} + \Delta G_f \quad \text{..... (3.6)}$$

Where, x_i and x_j are mole fractions of elements i and j and are given by the stoichiometry of the compound, ${}^0G_i^{\phi_1}$ and ${}^0G_j^{\phi_2}$ are the respective reference states of elements i and j, and ΔG_f is the Gibbs energy of formation per mole of atoms of the stoichiometric compound, which is expressed by the following equation:

$$\Delta G_f = a + b.T \quad \text{..... (3.7)}$$

The parameters a and b were obtained by optimization using experimental results of phase equilibria and thermodynamic data.

3.2.3 Disordered Solution Phases

To model the disordered solution phases present in Mg-Cu, Cu-Y and Mg-Y systems two different types of solution models were used. To describe the terminal solid solution phases the random solution model with Redlich-Kister polynomial [25] was used and the Modified Quasichemical model was used to describe the liquid phase in order to consider the presence of short range ordering.

3.2.3.1 Random Model for Terminal Solid Solutions. The Gibbs energy can be described by the following equation:

$$G^{\phi} = x_i {}^{0}G_i^{\phi} + x_i {}^{0}G_j^{\phi} + RT[x_i \ln x_i + x_j \ln x_j] + {}^{ex}G^{\phi} \quad \text{... ..... (3.8)}$$

where ϕ denotes the phase of interest and x_i, x_j denote the mole fraction of component i and j, respectively. The first two terms on the right hand side of equation 3.8 represent the Gibbs energy of the mechanical mixture of the components, the third term is the ideal Gibbs energy of mixing, and the fourth term is the excess Gibbs energy, which is described by the Redlich-Kister polynomial model [61] in this work and can be represented as:

$${}^{ex}G^{\phi} = x_i . x_j \sum_{n=0}^{n=m} {}^{n}L_{i,j}^{\phi} (x_i - x_j)^n \quad \text{.....……..……..... (3.9)}$$

$${}^{n}L_{i,j}^{\phi} = a_n + b_n \times T \quad \text{..... (3.10)}$$

Where n is the number of terms, a_n and b_n are the parameters of the model that need to be optimized considering the experimental phase diagram and thermodynamic data.

3.2.3.2 Modified Quasichemical Model. The modified Quasichemical model [72, 73, 74] was chosen to describe the liquid phases of the three constituent binaries of the Mg-Cu-Y ternary system. From the literature survey, it was found that all the three binary systems have very high negative enthalpy of mixing curves. Also, the calculated entropy of mixing curves of Cu-Y and Mg-Y system assume m-shaped characteristic. All these are indications of the presence of short range ordering [72] and the modified Quasichemical model has the most scientific approach to describe this kind of phenomenon in the liquid phase.

The modified Quasichemical model has three distinct characteristics [72-74]

i) It permits the composition of maximum short range ordering in a binary system to be freely chosen.

ii) It expresses the energy of pair formation as a function of composition which can be expanded as a polynomial in the pair fraction. Also, the coordination numbers are permitted to vary with the composition.

iii) The model can be extended to multicomponent system.

To elaborate this model let us consider the following pair exchange reaction

$$(A\text{-}A) + (B\text{-}B) = 2\,(A\text{-}B);\ \Delta g_{AB} \quad \text{..... (3.11)}$$

In equation 3.11, (A-B) represents a first-nearest-neighbor pair and Δg_{AB} is the non-configurational Gibbs energy change for the formation of 2 moles of (A-B) pair.

The Gibbs energy of a binary A-B solution, according to Pelton *et al.* [72-74], can be written as:

$$G = (n_A g_A^o + n_B g_B^o) - T\Delta S^{config} + (\frac{n_{AB}}{2})\Delta g_{AB} \quad \text{.....} \quad (3.12)$$

Here, g_A^o and g_B^o are the molar Gibbs energies of the pure components, and ΔS^{config} is the configurational entropy of mixing given by random distribution of (A-A), (B-B) and (A-B) pairs which can be expressed as equation 3.13.

$$\Delta S^{config} = -R(n_A \ln x_A + n_B \ln x_B)$$
$$-R[n_{AA} \ln(X_{AA}/Y_A^2) + n_{BB} \ln(X_{BB}/Y_B^2) + n_{AB} \ln(X_{AB}/2Y_AY_B)]$$

..... (3.13)

Where,

x_A and x_B are the mole fractions of A and B.

X_{AA}, X_{BB} and X_{AB} are the pair fractions and can be expressed as in equation 3.14

$$X_{ij} = \frac{n_{ij}}{n_{AA} + n_{BB} + n_{AB}} \quad \text{..... (3.14)}$$

Y_A and Y_B in equation 3.13 are the coordination equivalent fraction and can be expressed as in equation 3.15.

$$Y_A = \frac{Z_A n_A}{Z_A n_A + Z_B n_B} = \frac{Z_A X_A}{Z_A X_A + Z_B X_B}$$

$$= 1 - Y_B \quad \text{..... (3.15)}$$

Where, Z_A and Z_B are the coordination numbers of A and B which can be represented by equations 3.16 and 3.17.

$$\frac{1}{Z_A} = \frac{1}{Z_{AA}^A}\left(\frac{2n_{AA}}{2n_{AA} + n_{AB}}\right) + \frac{1}{Z_{AB}^A}\left(\frac{n_{AB}}{2n_{AA} + n_{AB}}\right) \quad \text{.....(3.16)}$$

$$\frac{1}{Z_B} = \frac{1}{Z_{BB}^B}\left(\frac{2n_{BB}}{2n_{BB} + n_{AB}}\right) + \frac{1}{Z_{BA}^B}\left(\frac{n_{AB}}{2n_{BB} + n_{AB}}\right) \text{..... (3.17)}$$

Z_{AA}^A and Z_{AB}^A are the values of Z_A when all nearest neighbors of an A atom are A's, and when all nearest neighbors of A atom are B's, respectively. Similarly for Z_{BB}^B and Z_{BA}^B.

The composition of maximum short range ordering is determined by the ratio $\frac{Z_{BA}^{B}}{Z_{AB}^{A}}$. Values of Z_{AB}^{A} and Z_{BA}^{B} are unique to the A-B binary system and should be carefully determined to fit the thermodynamic experimental data (enthalpy of mixing, activity etc.). The values of Z_{AA}^{A} is common for all systems containing A as a component. For this work 6 was chosen for Z_{MgMg}^{Mg} , Z_{CuCu}^{Cu} and Z_{YY}^{Y}. The value 6 was chosen because it gave the best possible fit for many binary systems and is recommended by Dr. Pelton's group [72]. The values of Z_{MgCu}^{Mg}, Z_{CuMg}^{Cu}, Z_{MgY}^{Mg}, Z_{YMg}^{Y}, Z_{CuY}^{Cu} and Z_{YCu}^{Y} will be discussed latter.

Now, the energy of pair formation in equation 3.11 can be expressed as a polynomial in terms of the pair fraction X_{AA} and X_{BB} as shown in equation 3.18

$$\Delta g_{AB} = \Delta g_{AB}^{o} + \sum_{i\geq 1} g_{AB}^{i0} X_{AA}^{i} + \sum_{j\geq 1} g_{AB}^{0j} X_{BB}^{j} \quad \text{..... (3.18)}$$

Where, Δg_{AB}^{o}, Δg_{AB}^{i0} and Δg_{AB}^{0j} are the parameters of the model and can be expressed as functions of temperature ($\Delta g_{AB}^{o} = a + bT$) .

For a very high degree of short range ordering especially for salt or oxide systems this model can be further extended. In these cases the solution is assumed to have two sublattices. One of which is considered to have the species A, B, C……. and the other have X, Y, Z… As for a salt system like LiCl-NaCl all the cations (Li and Na) are assumed to reside on sublattice I and the anion (Cl) on sublattice II. For this work, only vacancies are considered to reside on the second sublattice and thus the model actually reduces to a single sublattice modified Quasichemical model.

3.2.4 Solid Solution Phases

The Gibbs energy of an ordered solution phase is described by the compound energy formalism as shown in the following equations:

$$G = G^{ref} + G^{ideal} + G^{excess} \quad \text{.....} \quad (3.19)$$

$$G^{ref} = \sum y_i^l y_j^m ....y_k^q {}^0G_{(i:j:..:k)} \quad \text{.....} \quad (3.20)$$

$$G^{ideal} = RT\sum_l f_l \sum_i y_i^l \ln y_i^l \quad \text{.....} \quad (3.21)$$

$$G^{excess} = \sum y_i^l y_j^l y_k^m \sum_{\gamma=0} {}^{\gamma}L_{(i,j):k} \times (y_i^l - y_j^l)^{\gamma} \quad \text{.....} \quad (3.22)$$

Where *i, j, …k* represent components or vacancy, *l, m* and *q* represent sublattices. y_i^l is the site fraction of component *i* on sublattice *l*. f_l is the fraction of sublattice *l* relative to the total lattice sites. ${}^0G_{(i:j:..k)}$ represents a real or a hypothetical compound (end member) energy. ${}^{\gamma}L_{(i,j)}$ represent the interaction parameters which describe the interaction within the sublattice.

3.3 Extrapolation for Ternary System

The thermodynamic properties of a Ternary solution can be calculated from the optimized data of its binary subsystems. To obtain a precise ternary system different 'Geometric' extrapolation techniques had been proposed. Some of these are symmetric and some are asymmetric. The Kohler [75] and Muggianu [76] are well known symmetric models while Toop [77] is an asymmetric model. In the asymmetric model

one component is singled out. The choice of the asymmetric component is a matter of experience. For systems with strong interactions, different models (or extrapolation techniques) can give quite different results. In particular, asymmetric models can give better results for some systems, while symmetric models can be better for other systems. Different opinions, on the choice of the asymmetric component for the asymmetric models, can also be found in the literature [78, 79, 80]. Some of the geometric models are shown in Figure 3.2.

The analytical interpretations of the Kohler Model [75], as shown in Figure 3.2 (a), can be expressed as:

$$\Delta G^E = (x_1 + x_2)^2 \Delta G_{12}^E \left(\frac{x_1}{x_1 + x_2}; \frac{x_2}{x_1 + x_3} \right) + (x_2 + x_3)^2 \Delta G_{23}^E \left(\frac{x_2}{x_2 + x_3}; \frac{x_3}{x_2 + x_3} \right) + (x_3 + x_1)^2 \Delta G_{31}^E \left(\frac{x_3}{x_1 + x_3}; \frac{x_1}{x_1 + x_3} \right)$$

..... (3.23)

Muggianu model [75] uses the following expression:

$$\Delta G^E = \frac{4x_1x_2}{(1+x_1-x_2)(1+x_2-x_1)} \Delta G_{12}^E \left(\frac{1+x_1-x_2}{2}; \frac{1+x_2-x_1}{2}\right) + \frac{4x_2x_3}{(1+x_2-x_3)(1+x_3-x_2)} \Delta G_{23}^E \left(\frac{1+x_2-x_3}{2}; \frac{1+x_3-x_2}{2}\right) + \frac{4x_3x_1}{(1+x_3-x_1)(1+x_1-x_3)} \Delta G_{31}^E \left(\frac{1+x_3-x_1}{2}; \frac{1+x_1-x_3}{2}\right)$$

..... (3.24)

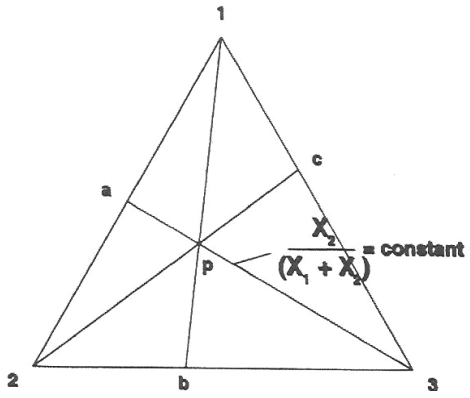

(a)

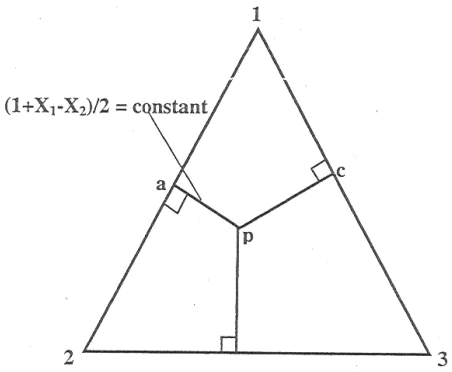

(b)

(c)

Figure 3.2: Different *ıpolation: (a) Kohler (b)*

While Toop model [77] u

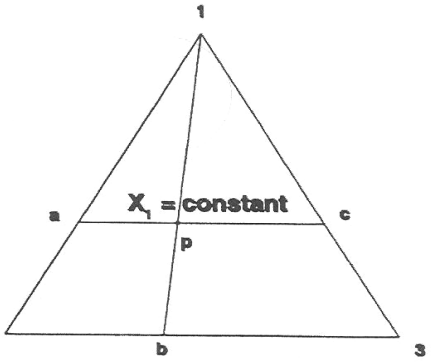

$$\Delta G^E = \quad (x_1;1-x_1)$$

$$+(x_2+x_3)^2 \Delta G_{23}^E\left(\frac{x_2}{x_2+x_3};\frac{x_3}{x_2+x_3}\right)$$

……..... (3.25)

In equations 3.23 to 3.25, ΔG^E and ΔG_{ij}^E correspond to the integral molar excess Gibbs energy for ternary and binary systems, respectively, and x_1, x_2, x_3 are the mole fraction of components.

A polynomial ternary term (some times referred to as ternary interaction parameter) can be added to any of the above equations to fit the experimental data. However, with no ternary terms the extrapolation should provide a reasonable first estimation of the ternary molar excess Gibbs energy.

3.3.1 Comparison between Muggianu, Kohler and Toop Model

The choice of extrapolation technique some times become vital for the thermodynamic calculation of a ternary system since each of them is unique in their approach. It could be noticed from the literature that, in most cases, the Muguannu model was chosen to describe a system since it was simpler than other models. But there are several cases where Toop model is to be preferred. It was mentioned by Chartrand and Pelton [78] that in the case of a dilute solution the geometric configuration associated with Kohler or Toop model will give a more reliable representation of the partial properties in the ternary system than the Muggianu model. Figure 3.3 explains the reasons behind this. Let us consider a ternary solution 1-2-3, dilute in component 1. For this system the Kohler model predicts the excess Gibbs energy values of 1-2 and 3-1 from values in the binary systems at compositions that are also dilute in component 1, which is reasonable. The toop model also produces similar result. But the Muggianu model uses values from the binary systems at compositions which are far away from dilute. If the binaries l-2 and 3-1 display strong asymmetry, the problem will be more pronounced. Thus it can be said that if the choice of the thermodynamic model is wrong during the calculation of phase diagram, significant discrepancies between calculated and

experimental thermodynamic values may result, especially in the dilute ranges of the system.

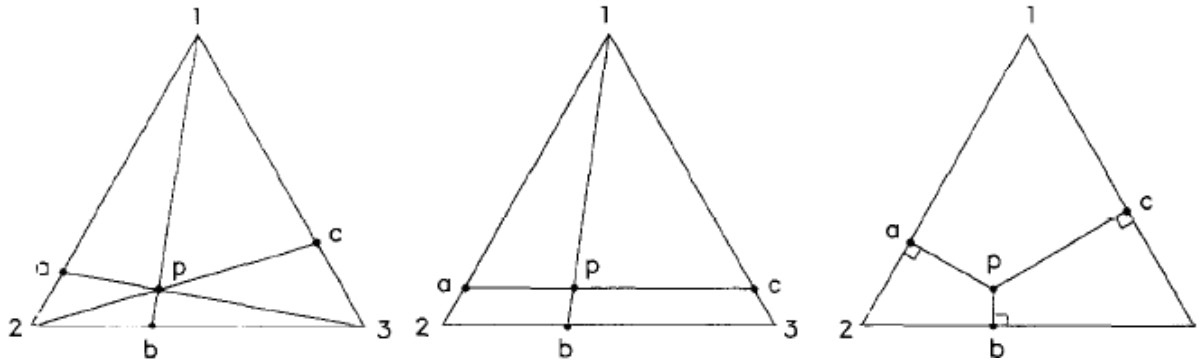

[a] Kohler Model [b]: Toop Model [c]: Muggianu Model

Figure 3.3: Different thermodynamic models showing the extrapolation from dilute concentrations [79].

Chartrand and Pelton [78] suggested that if any of the two binaries of a ternary system show similar properties and the third binary system is different from them then it is better to use one of the asymmetric models. It was found in this work that the binary excess Gibbs energies for Mg-Cu, Cu-Y and Mg-Y systems are fairly similar to one another. Also, all the systems exhibit highly negative heat of mixing. None of the system showed any indication of dissimilarity in terms of thermodynamic property. Hence, for this work, Kohler geometric model which is a symmetric one was chosen for the ternary extrapolation of the Mg-Cu-Y system.

CHAPTER 4

Results and Discussions

4.1 Mg-Cu System

4.1.1 Phase Diagram

In 1991, Coughanowr *et al.* [24] calculated the Mg-Cu phase diagram which showed reasonable agreement with the experimental work. But they did not considered short range ordering in the liquid phase during their modeling. Also, they used too many adjustable parameters to model the $MgCu_2$ phase. In 1993, Zuo and Chang [27] reoptimized the Mg-Cu system. They used less number of parameters to model the system. But they also did not considered short range ordering in the liquid phase. Therefore, this system will be reoptimized during the course of this work.

The liquid phase was modeled by the modified Quasichemical model, according to equation 3.12, to account for the presence of short range ordering. Thus, according to, equation 3.18, the optimized energy of pair formation for the Mg-Cu liquid can be expressed as:

$$\Delta g^{l}_{CuMg} = -12{,}975.95 - (6{,}153.13 - 1.26\,T)X_{CuCu} - 13{,}528.50\,X_{MgMg} \quad \text{J/mole} \quad (4.1)$$

The parameters Z^{Cu}_{CuCu} and Z^{Mg}_{MgMg} were both set equal to 6. The tendency to maximum short range ordering in the composition range of 35 to 45 at.% Mg, was modeled by setting $Z^{Cu}_{CuMg} = 2$ and $Z^{Mg}_{CuMg} = 4$.

The Redlich-Kister polynomial was used to model the Mg-hcp and Cu-fcc phases, Stoichiometric model was used for the Mg_2Cu compound and the general compound energy formalism (CEF) or sublattice model for the $MgCu_2$ solid solution. All the optimized parameters are shown in Table 4.1. The Gibbs energy of pure Mg and Cu were taken from SGTE database [28] as mentioned earlier.

Table 4.1: Optimized model parameters for liquid, Mg-hcp, Cu-fcc, Mg_2Cu and $MgCu_2$ phases in Mg-Cu system.

Phase	**Terms**	**a (J.mole^{-1})**	**b (J.mole^{-1}K)**
Liquid	Δg^{0}_{MgCu}	-12,975.95	
	g^{i0}_{CuY}	-6,153.13	1.26
	g^{0j}_{CuY}	-13,528.50	
Phase	**Terms**	**a (J.mole^{-1})**	**b (J.mole^{-1}K)**
Mg-hcp	${}^{0}L^{Mg-hcp}$	8,371.60	0
Cu-fcc	${}^{0}L^{Cu-fcc}$	-21,923.39	5.37
Mg_2Cu	ΔG_f	-28,620.00	0.03
$MgCu_2$	$G^{MgCu_2}_{Cu:Cu}$	16,743.20	
	$G^{MgCu_2}_{Mg:Cu}$	-37,684.26	
	$G^{MgCu_2}_{Cu:Mg}$	0	
	$G^{MgCu_2}_{Mg:Mg}$	6,278.7	
	${}^{0}L^{MgCu_2}_{Mg,Cu:Cu}$	13,011.35	
	${}^{0}L^{MgCu_2}_{Mg,Cu:Mg}$	13,011.35	
	${}^{0}L^{MgCu_2}_{Cu:Mg,Cu}$	6,599.45	
	${}^{0}L^{MgCu_2}_{Mg:Mg,Cu}$	6,599.45	

The calculated Mg-Cu phase diagram is shown in Figure 4.1. It shows reasonable agreement with the experimental data provided in the literature. The maximum solid solubility of Mg in Cu was found to be 6.85 at.% Mg, which is in good agreement with the experimental value of 6.93 at.% Mg reported by Bagnoud and Feschotte [17].

However, Jones [10] reported this as 6.5 at.% Mg. The solubility obtained in the current work lies between the two values reported by Jones [10] and Bagnoud and Feschotte [17]. The congruent melting temperature of $MgCu_2$ was calculated to be 1061 K. The experimental values reported by Sahmen [8], Bagnoud and Feschotte [17] and Urasow [9] are 1070 K, 1066±4 K and 1072 K, respectively. However Jones [10] determined this value to be 1092 K but he considered $MgCu_2$ as stoichiometric compound which might have consequently resulted in steeper liquidus around this compound and thus higher melting point. The melting temperature of Mg_2Cu was determined as 844 K, 841 K, 841±2 K and 843 K by Sahmen [8], Jones [10], Bagnoud and Feschotte [17] and Urasow [9], respectively. These are in good agreement with the current calculated value of 844K.

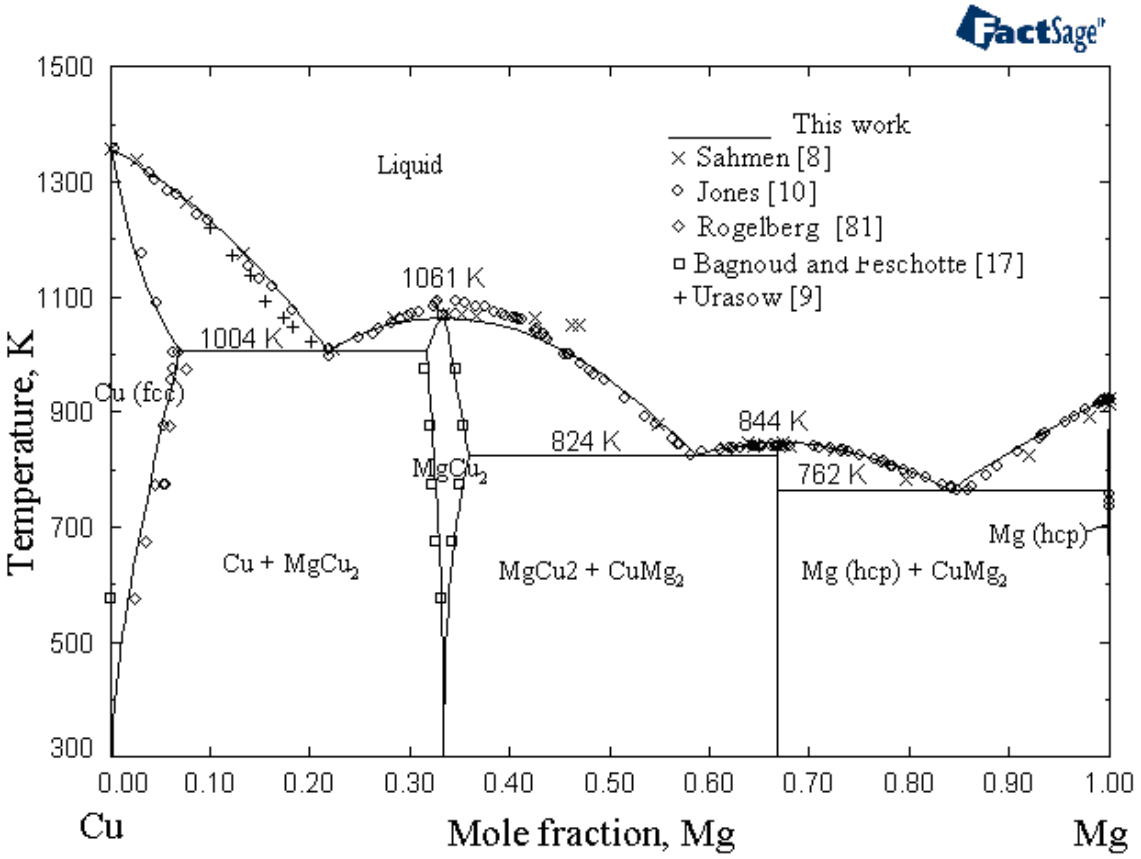

Figure 4.1: Optimized Mg-Cu phase diagram with experimental data form literature.

All the three eutectic temperatures and compositions are in good agreement with the reported experimental values of different researchers [8, 9, 10, 17] except the composition of the eutectic near Mg rich region. The calculated value from this work is 84.07 at.% Mg while the experimental values are 85.4 and 85.5 at.% Mg reported by [8] and [10], respectively. Since the thermodynamic properties are in very good agreement with the experimental values this amount of error can be acceptable. It is worth noting that trying to be consistent with the experimental eutectic composition resulted in deviation from the experimental thermodynamic properties of the Mg-Cu liquid. Also, Zuo and Chang [27] calculated this value to be 84.1 at.% Mg.

4.1.2 Thermodynamic Modeling of the $MgCu_2$ (laves) Phase

To model the $MgCu_2$ two types of information are required; the Crystallographic data and the homogeneity range. The crystallographic data for the $MgCu_2$ phase are summarized in Table 4.2.

Table 4.2: Crystal structure and lattice parameters of $MgCu_2$ -phase.

Phase	**Crystal data**		**Atom**	**WP[1]**	**CN[2]**	**PS[3]**	**Atomic position**			**Ref.**
							X	**Y**	**Z**	
$MgCu_2$	Prototype	$MgCu_2$	Cu	16d	12	-	0.625	0.625	0.625	[82]
	Pearson Symbol	cF24	Mg	8a	16	-	0	0	0	
	Space Group	$Fd\bar{3}m$								
	Space Group No.	227								
	Lattice parameter (nm)	a=0.7035								[17]
	Angles: α= 90, β=90, γ=90									

[1]WP= Wyckoff Position, [2]CN=Coordination Number and [3]PS=Point Symmetry

Powder cell software [83] along with the crystallographic information provided in Table 4.2, are used to determine the substructures in the $MgCu_2$ solid solution as shown in Figure 4.2, in order to model this phase using the sublattice model.

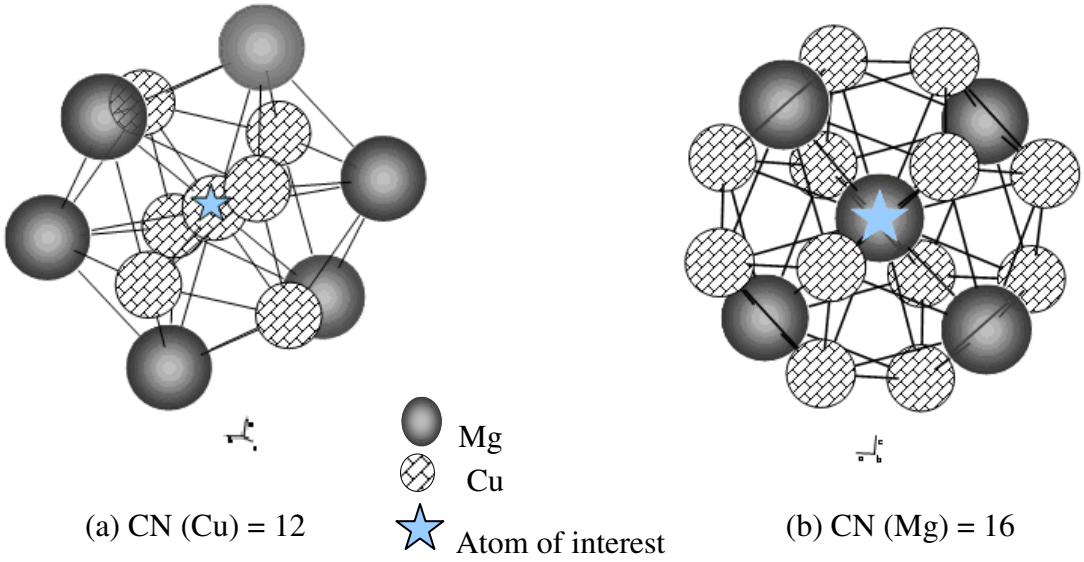

Figure 4.2: Substructure of (a) Cu and (b) Mg atoms in Laves ($MgCu_2$) phase unit cell with the coordination number (CN).

The crystallographic data indicate that the unit cell of $MgCu_2$ phase has 24 atomic positions; 16 for Cu and 8 for Mg atom. Hence the direct sublattice model based on the crystallographic data is:

$$(Mg)_8 : (Cu)_{16}$$

This model represents the stoichiometry of $MgCu_2$ phase. To obtain a deviation from this stoichiometry, mixing of constituents is applied. Mixing of Cu antistructure atom in the first sublattice and Mg antistructure atom in the second sublattice is applied. Thus the model is represented as follows:

$$(Mg\%, Cu)_8 : (Cu\%, Mg)_{16}$$

This model covers the $0 \leq X_{Mg} \leq 1$ composition range and, of course, includes the homogeneity range of $0.31 \leq X_{Mg} \leq .353$ which was reported by Bagnoud and Feschotte [17].

Based on this model, the Gibbs energy per mole of formula unit of $MgCu_2$ phase can be written as:

$$G_m^{MgCu_2} = y_{Mg}^I y_{Cu}^{II} {}^0G_{Mg:Cu}^{MgCu_2} + y_{Mg}^I y_{Mg}^{II} {}^0G_{Mg:Mg}^{MgCu_2} + y_{Cu}^I y_{Cu}^{II} {}^0G_{Cu:Cu}^{MgCu_2} + y_{Cu}^I y_{Mg}^{II} {}^0G_{Cu:Mg}^{MgCu_2} + RT(0.33 \sum_{i=Mg}^{Cu} y_i^I \ln y_i^I + 0.67 \sum_{i=Cu}^{Mg} y_i^{II} \ln y_i^{II}) + {}^{ex}G_m^{MgCu_2} \quad \text{..... (4.2)}$$

And,

$$ {}^{ex}G_m^{MgCu_2} = y_{Mg}^I y_{Cu}^I (y_{Cu}^{II} {}^0L_{Mg,Cu:Cu}^{MgCu_2} + y_{Mg}^{II} {}^0L_{Mg,Cu:Mg}^{MgCu_2}) + y_{Cu}^{II} y_{Mg}^{II} (y_{Mg}^I {}^0L_{Mg:Cu,Mg}^{MgCu_2} + y_{Cu}^I {}^0L_{Cu:Cu,Mg}^{MgCu_2}) \quad \text{..... (4.3)}$$

Where, *i* is the lattice species.

y_{Mg}^I, y_{Cu}^I are the site fractions of lattice I.

y_{Mg}^{II}, y_{Cu}^{II} are the site fractions of lattice II.

${}^0G_{Mg:Cu}^{MgCu_2}$, ${}^0G_{Mg:Mg}^{MgCu_2}$, ${}^0G_{Cu:Cu}^{MgCu_2}$ and ${}^0G_{Cu:Mg}^{MgCu_2}$ are the Gibbs energies of the hypothetical and stoichiometric compounds. The interaction parameters within the sublattice can be expressed as:

$$ {}^0L_{Mg,Cu:Cu}^{MgCu_2} = {}^0L_{Mg,Cu:Mg}^{MgCu_2} = \sum_{n=0} [(a_n + b_n T)(y_{Mg}^I - y_{Cu}^I)^n] \quad \text{..... (4.4)}$$

$$ {}^0L_{Mg:Cu,Mg}^{MgCu_2} = {}^0L_{Cu:Cu,Mg}^{MgCu_2} = \sum_{n=0} [(a_n + b_n T)(y_{Mg}^{II} - y_{Cu}^{II})^n] \quad \text{..... (4.5)}$$

$^{0}G^{MgCu_2}_{Mg:Cu}, ^{0}G^{MgCu_2}_{Mg:Mg}, ^{0}G^{MgCu_2}_{Cu:Cu}, ^{0}G^{MgCu_2}_{Cu:Mg}, ^{0}L^{MgCu_2}_{Mg,Cu:Cu}, ^{0}L^{MgCu_2}_{Mg,Cu:Mg}, ^{0}L^{MgCu_2}_{Mg:Cu,Mg}, and\ ^{0}L^{MgCu_2}_{Cu:Cu,MgMg}$ are the parameters which were optimized using the sublattice model with the experimental data from the literature. The optimized values of the parameters are mentioned in Table 4.1.

4.1.3 Thermodynamic Properties:

The calculated heat of mixing at 1100 K, shown in Figure 4.3, is in good agreement with the experimental data of Sommer *et al.* [33]. A small deviation can be seen between the calculated result and the experimental data of Batalin *et al*. [34] near the composition range 20 to 60 at.% Mg. Sommer *et al.* [33] did their experiment at three different temperatures and hence their data would be more reliable. The experimental data of Garg *et al.* [29] and Juneja *et al*. [31] show a large discrepancy with the calculated

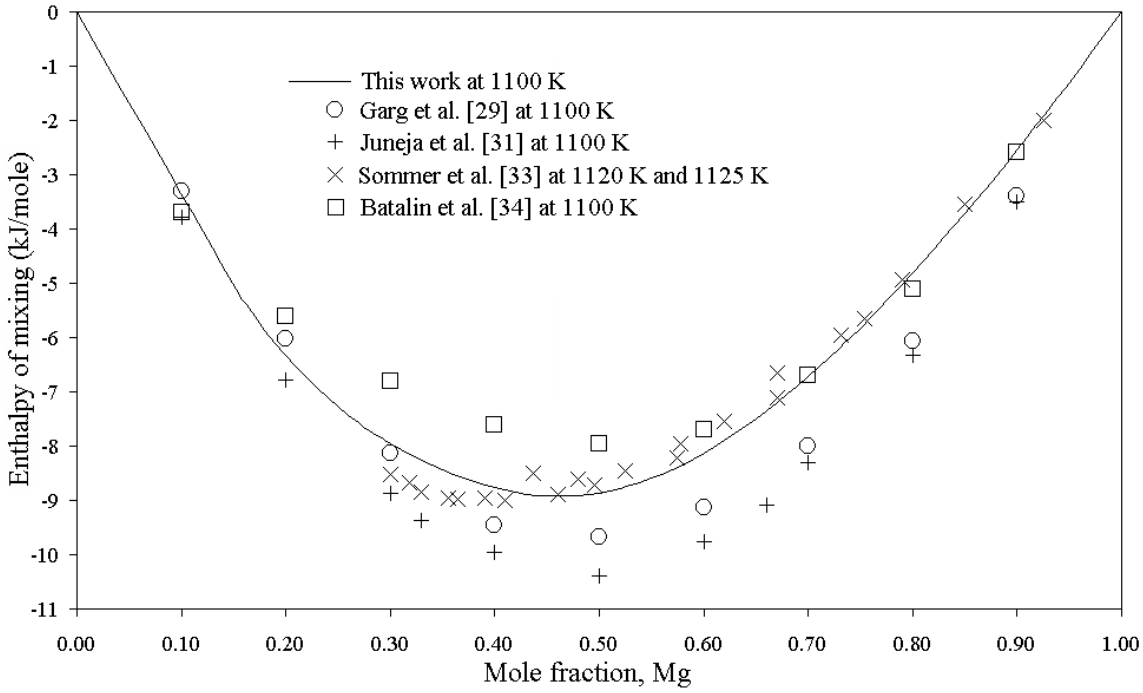

Figure.4.3: Calculated enthalpy of mixing at 1100 K.

values as well as the results of [33] and [34]. This discrepancy is probably due to the less accurate vapor pressure experimental technique used by [29] and [31] than the calorimetric experimental technique which was used by [33] and [34].

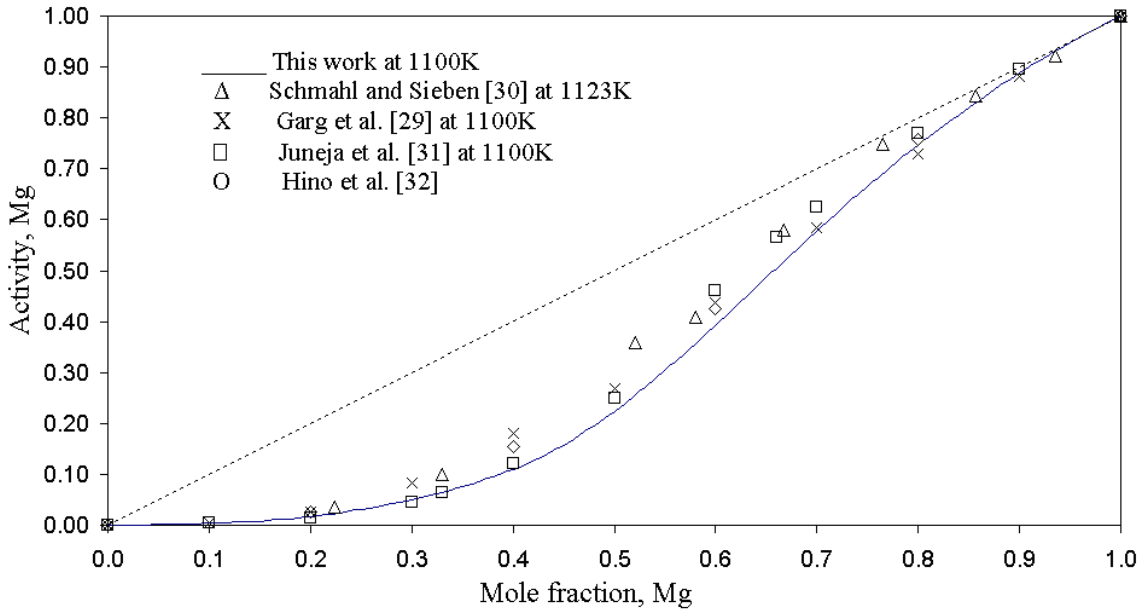

Figure 4.4: Activity of Mg in Mg-Cu liquid.

The calculated activity of Mg in Mg-Cu liquid at 1100K is shown in Figure 4.4. It can be seen from this figure that the calculated Mg activity agrees well with the experimental results from the literature [29-32]. The experimental data for the activity of Cu could not be found in the literature.

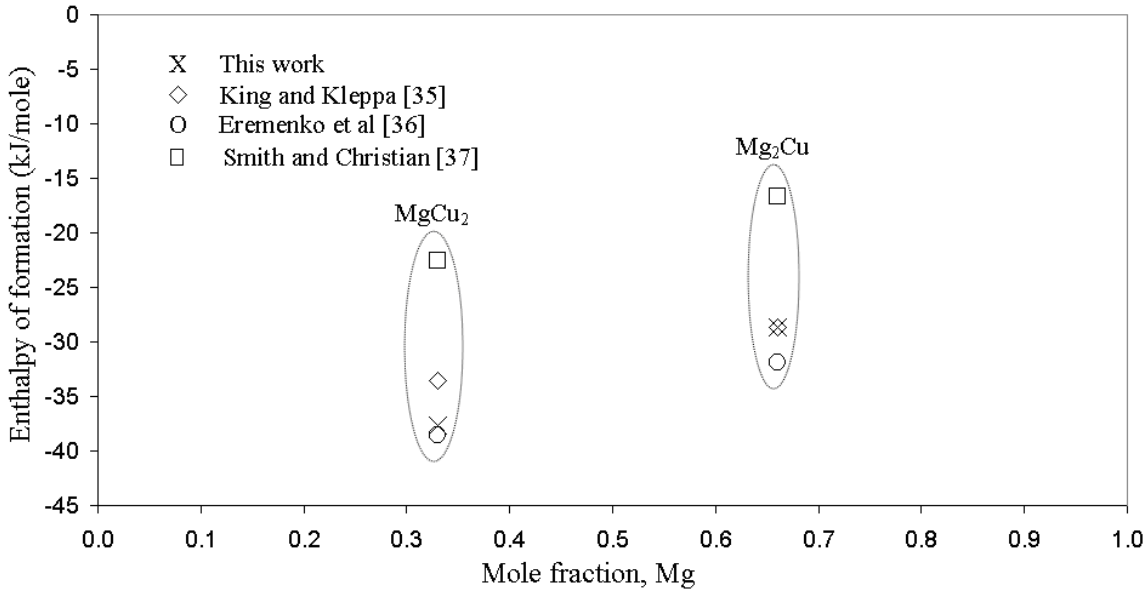

Figure 4.5: Calculated enthalpy of formation of the stoichiometric compounds.

Figure 4.5 shows a good agreement between the calculated heats of formation of $MgCu_2$ and Mg_2Cu, obtained in this study and the experimental results reported by King and Kleppa [35] and Eremenko *et al.* [36]. The measured values of Smith and Christian [37] are less negative than the calculated ones and also inconsistent with other experimental results. This is probably due to the inaccuracy involved in the vapor pressure measurement carried out by [37].

4.2 Cu-Y System

4.2.1 Phase Diagram

In 1990, Itagaki *et al.* [43] carried out thermodynamic assessment of the Cu-Y system. Their calculated phase diagram shows reasonable agreement with the experimental data. But they used too many parameters to describe the Cu_6Y phase. Besides, the modeling of the liquid phase was done without considering the short range ordering. In 1992, Fries *et al.* [45] made an attempt to reoptimize this system. In their calculation, they overcome some of the drawbacks of the previous calculation made by [43]. But in their modeling they too did not account for the presence of short range ordering in the liquid. In 1997, Abend and Schaller [46] made another optimization on Cu-Y system. But their calculated phase diagram did not show good agreement with the experimental data and they did not include the homogeneity range for the Cu_6Y phase. Also short range order in the liquid phase was not considered. Based on these observations, it is decided to reoptimize this system.

The Modified Quasichemical model was used for the liquid phase of the Cu-Y system. This model considers the presence of short range ordering in the liquid. According to equation 3.18, the optimized Gibbs energy of the liquid phase can be written as:

$$\Delta g_{CuY} = -28{,}718.77 + 6.28\,T - (6{,}446.13 - 0.84\,T)\,X_{CuCu} - (6{,}906.57 - 2.09T)\,X_{YY} \quad \text{J/mole.} \qquad \text{..... (4.6)}$$

The coordination numbers for the first nearest neighbor of Cu and Y atoms (Z_{CuCu}^{Cu}, Z_{YY}^{Y}) were both set to 6. The tendency to maximum short range ordering near 30 to 40 at.% Y, was modeled by setting Z_{CuY}^{Cu} = 3 and Z_{CuY}^{Y} = 6. These were determined by trial and error method. Only these values can be used to reproduce the phase diagram while being consistent with the thermodynamic properties

Stoichiometric model was used for CuY, Cu_2Y, Cu_4Y and Cu_7Y_2 compounds and the general compound energy formalism (CEF) was used to reproduce the homogeneity range of Cu_6Y phase. The optimized parameters are shown in Table 4.3. The solid solubilities of Y in Cu and Cu in Y are negligible and hence were not included in this work.

Table 4.3: Optimized model parameters for liquid, CuY, Cu_2Y(h), Cu_2Y (r), Cu_4Y, Cu_7Y_2 and Cu_6Y phases.

Phase	**Terms**	**a (J/mole)**	**b (J/mole K)**
Liquid	Δg_{CuY}^{0}	-28,718.77	6.28
	g_{CuY}^{i0}	-6,278.70	0.84
	g_{CuY}^{0j}	-6,906.57	2.09
Cu_6Y	$G_{Cu:Cu}^{Cu_6Y_2} - 7G_{Cu}^{hcp}$	0	0
	$G_{Cu:Y}^{Cu_6Y_2} - 5G_{Cu}^{hcp} - 2G_{Y}^{hcp}$	65.8	0
	${}^{0}L_{Y,Cu_2:Cu}^{Cu_6Y}$	- 4,794.8	0.45
Phase	**Terms**	**a (J/mole-atom)**	**b (J/mole-atom K)**
CuY	ΔG_f	-22,517.5	-3.311
Cu_2Y (h)	ΔG_f	-17,416.2	1.63
Cu_2Y (r)	ΔG_f	-21,997.9	-2.44
Cu_4Y	ΔG_f	-17,888	-1.65
Cu_7Y_2	ΔG_f	-18,775.5	-1.73

The calculated Cu-Y phase diagram is shown in Figure 4.6 with the available experimental points from the literature. Also, an enlarged portion of the phase diagram is shown in Figure 4.7, for better illustration with the same experimental data points as in Figure 4.6.

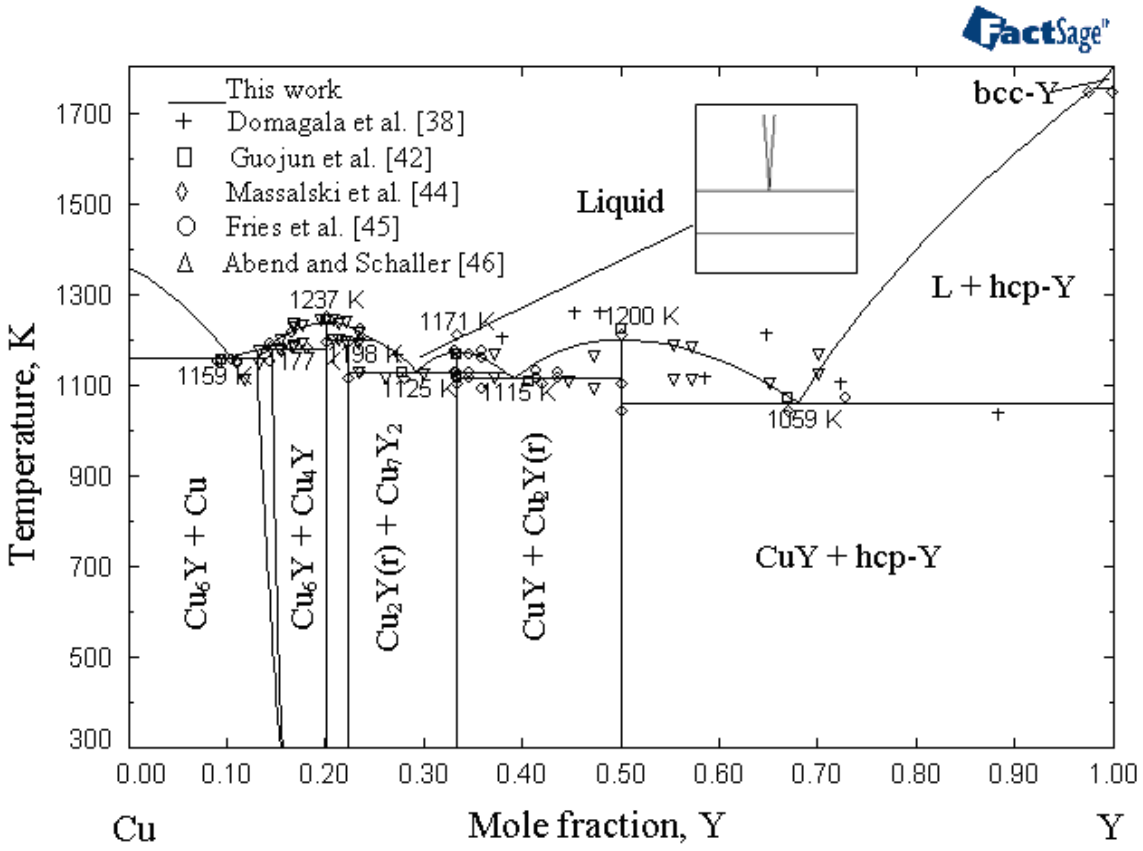

Figure 4.6: Calculated Cu-Y phase diagram with experimental results from the literature

A comparison between the current calculated values and different experimental works on this system is shown in Table 4.4. Except few discrepancies with the data from Domagala [38] the phase diagram shows reasonable agreement with all the experimental points. Composition of the eutectic point near the Cu reach side show small deviation with the experimental data. But the thermodynamic properties especially the enthalpy of

mixing near Cu rich side showed strong agreement with the experimental data; hence this amount of error is acceptable.

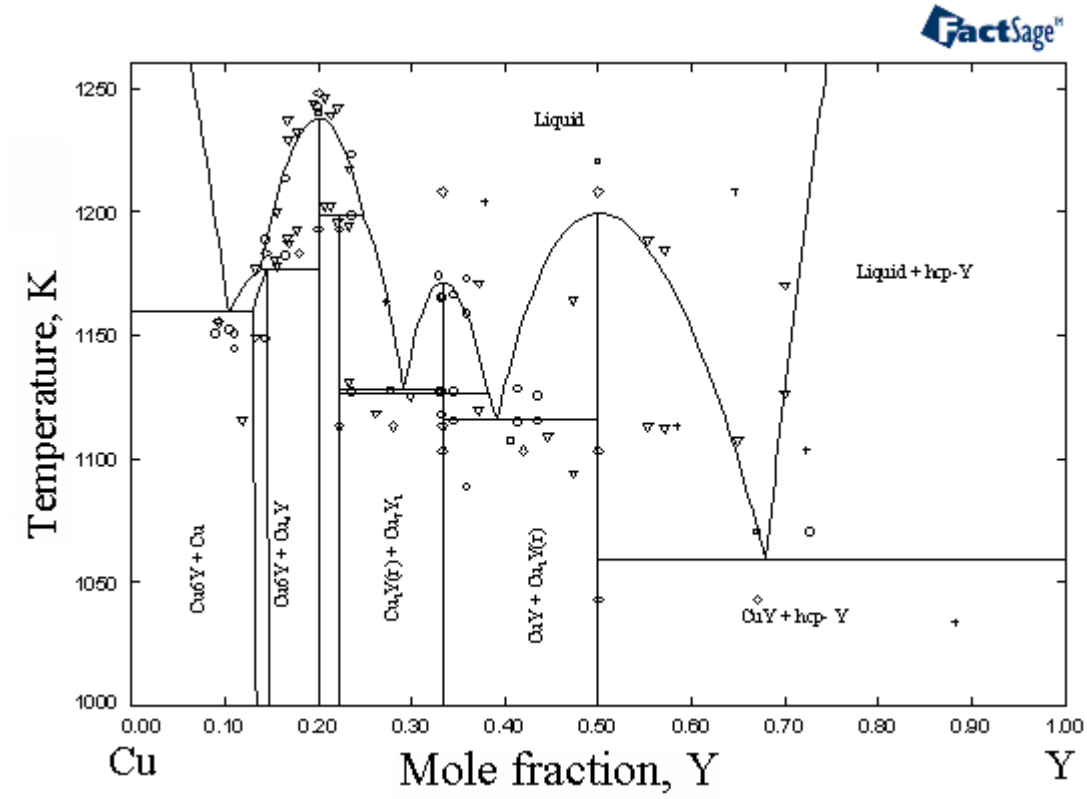

Figure 4.7: Calculated Cu-Y phase diagram with experimental results from the literature.

The solid phase transformation of $Cu_2Y(h) \leftrightarrows Cu_2Y(r)$ was included in the current assessment of this system. Due to this reason there are some discrepancies in temperature and composition of the two eutectic points around this compound. However, they are in good agreement with the calculated values of [43, 45, 46]. The liquidus curve near the Cu-rich side is much better than that of [45] which showed unusual behavior.

Table 4.4: Comparison of the calculated Cu-Y phase diagram and other experimental works.

Reaction	***Temperature (K)***	***Composition (at.% Y)***	***Ref.***
Liquid ⇆ (Cu) +Cu_6Y	1159	10.4	This work
	1163±10	9.3	[38]
	1155±5	9.3	[42]
	1133	9.3	[44]
	1153±2	-	[45]
	1149	-	[46]
Liquid + Cu_4Y ⇆ Cu_6Y	1177	13.7	This work
	1203±20	-	[38]
	1183±5	-	[44]
	1184±5	-	[45]
	1178	-	[46]
Liquid ⇆ Cu_4Y	1237	20	This work
	1258±15	20	[38]
	1240±5	20	[42]
	1248±5	20	[44]
	1244±5	-	[45]
	1246	-	[46]
Liquid + Cu_4Y ⇆ Cu_7Y_2	1198	24.8	This work
	1193±5	-	[44]
	1196	-	[46]
Cu_2Y (h) ⇆ Cu_2Y (r)	1125		This work
	1128±5		[45]
Liquid ⇆ Cu_7Y_2+ Cu_2Y	1128	29.2	This work
	1113±15	28	[38]
	1127±5	27.8	[42]
	1113±15	28	[44]
	1118	-	[46]
Liquid ⇆ Cu_2Y (h)	1171	33.3	This work
	1208±15	33.3	[38]
	1170±5	33.3	[42]
	1208±15	33.3	[44]
	1170±5	-	[45]
Liquid ⇆ Cu_2Y(r) +CuY	1115	39.2	This work
	1103±15	42	[38]
	1110±7	-	[42]
	1103±15	42	[44]
	1116±5	-	[45]
	1109	-	[46]
Liquid ⇆ CuY	1200	50	This work
	1208±15	50	[38]
	1220±5	50	[42]
	1208±15	50	[44]
Liquid ⇆ CuY + hcp-Y	1059	67.9	This work
	1033	67	[38]
	1070±3	67	[42]
	1043	67	[44]

4.2.2 Thermodynamic Modeling of the Cu_6Y Phase

The crystal structure data of the Cu_6Y intermediate solid solution was obtained by Buschow and Goot [39] and is listed in Table 4.5.

Table 4.5: Crystal structure and lattice parameters of Cu_6Y phase.

Phase	Crystal data		Atom	WP[1]	CN[2]	PS[3]	Atomic position			Ref.
							X	Y	Z	
Cu_6Y	Prototype	$TbCu_7$	Y	1a	20	….	0	0	0	[39]
	Pearson Symbol	*hP8*	Cu 1	2e	8	….	0	0	0.306	
	Space Group	*P6/mmm*	Cu 2	2c	12	….	0.333	0.667	0	
	Space Group No.	191	Cu 3	3g	16	….	0.5	0	0.5	
	Lattice parameter (nm)	a=0.494 b=0.4157								
	Angle: α= 90°, β=90°, γ=120°									

[1]WP= Wyckoff Position, [2]CN=Coordination Number and [3]PS=Point Symmetry

The coordination numbers for the different Y and Cu atoms were determined using powder cell software [83] as shown in Figure 4.8. According to [39] some of the Y sites are occupied by a pair of Cu atoms, which can be described by the following model with two sublattices:

$$(Y\%, Cu_2)\ (Cu)_5$$

The '%' indicates the main element of the sublattice. This is actually a Wagner-Schottky type model [26]. This type of model can be used only for intermediate phases with a narrow homogeneity range [70].

The model covers $0.83 \leq X_{Cu} \leq 1$ composition range. This range includes the homogeneity range of $0.84 \leq X_{Cu} \leq 0.87$ which was reported by [45].

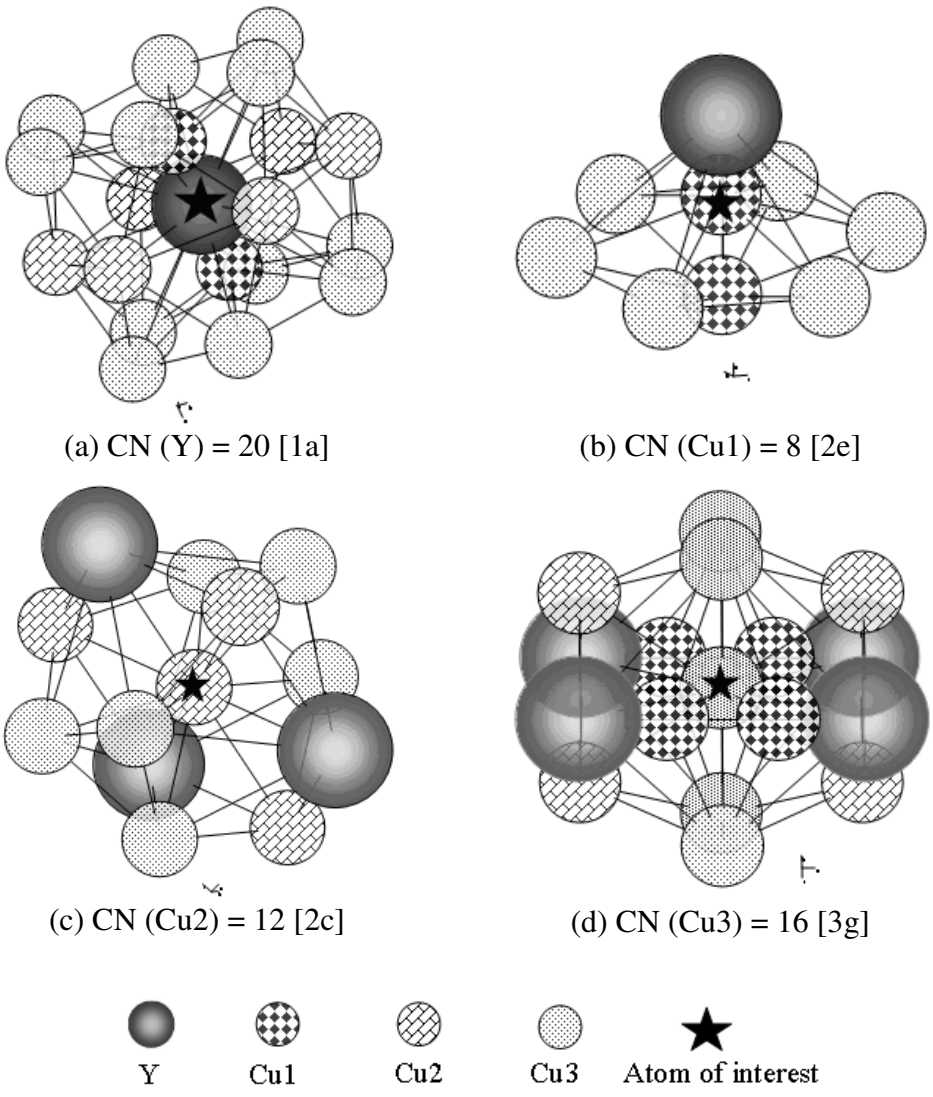

Figure 4.8: Substructure of (a) Y (b) Cu1 (c) Cu2 and (d) Cu3 atoms in Cu_6Y unit cell with the coordination number (CN).

Based on this model, the Gibbs energy per mole of formula unit of Cu_6Y can be written as:

$$G_m^{Cu_6Y} = y_Y^I y_{Cu}^{II} ({}^0G_{Y:Cu}^{Cu_6Y} - {}^0G_{Y-hcp}^{Cu_6Y} - 5\,{}^0G_{Cu-fcc}^{Cu_6Y}) + y_{Cu_2}^I y_{Cu}^{II} ({}^0G_{Cu_2:Cu}^{Cu_6Y} - 7\,{}^0G_{Cu-fcc}^{Cu_6Y}) + RT[(0.167 \sum_{i=Y}^{Cu_2} y_i^I \ln y_i^I)] + {}^0L_{Y,Cu_2:Cu}^{Cu_6Y} \quad \text{.....(4.7)}$$

Where, i is the lattice species, y_Y^I, $y_{Cu_2}^I$ are the site fractions of the species Y and Cu_2 on sublattice I. y_{Cu}^{II} is the site fraction of the species Cu on sublattice II. ${}^0G_{Y:Cu}^{Cu_6Y}$, ${}^0G_{Cu_2:Cu}^{Cu_6Y}$ and ${}^0L_{Y,Cu_2:Cu}^{Cu_6Y}$ are the parameters which were optimized using the compound energy formalism with the experimental data from the literature.

4.2.3 Thermodynamic Properties

The calculated enthalpy of mixing of the Cu-Y liquid at 1410 K in relation to the experimental results from the literature is shown in Figure 4.9. It is in very good agreement with the experimental results of Sudavtsova *et al.* [41] and Watanabe *et al.* [48]. However the deviation from the experimental data of Sidorov *et al.* [49] is due to the considerable difference in the temperature at which the measurements were performed.

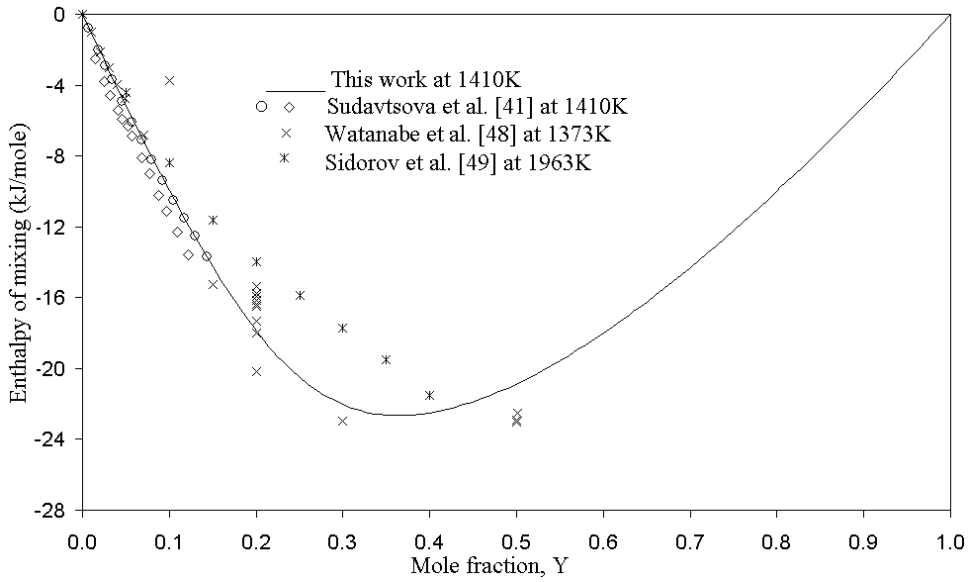

Figure 4.9: Calculated enthalpy of mixing at 1410 K.

The Calculated activity of Cu at 1623 K is shown in Figure 4.10, which is in good agreement with the experimental results of berezutskii and Lukashenko [50] near Y-rich corner. The curve shows some deviation from the experimental values between 20 to 35 at.% Y. This is probably due to the presence of several high melting point compounds in this region which makes measuring the activity difficult. However, the calculation of Ganesan *et al.* [51] showed very similar results to the present calculation.

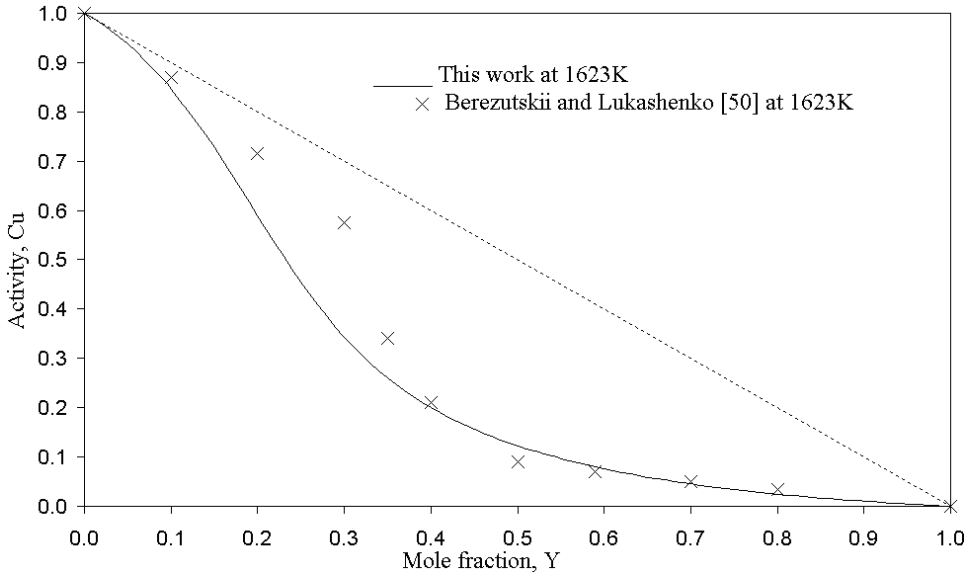

Figure 4.10: Calculated activity of liquid Cu at 1623K.

The calculated entropy of mixing of liquid Cu-Y at 1823 K is shown in Figure 4.11. The m-shape entropy of mixing curve is a perfect indication of the presence of short range ordering in the liquid phase. The calculation of Itagaki *et al.* [43] also showed similar shaped curve but their calculation showed some negative values near Cu rich corner which is corrected in this calculation.

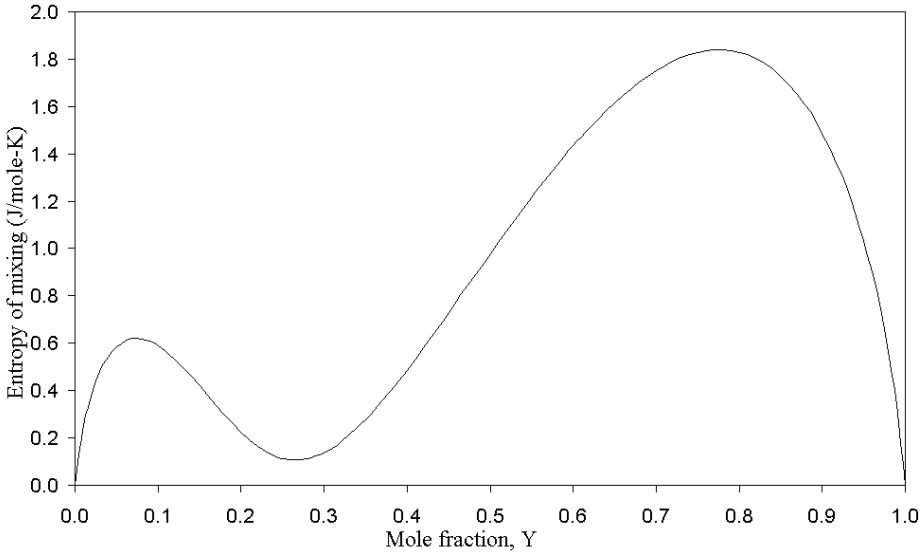

Figure 4.11: Calculated entropy of mixing of liquid Cu-Y at 1823 K.

A comparison between the calculated enthalpy of formation for the stoichiometric compounds in this work and other works are shown in Figure 4.12. Small discrepancy can be seen between the different experimental works which is not unexpected since both Cu and Y are highly reactive elements and it is very difficult to perform any kind of experimental investigation on this system.

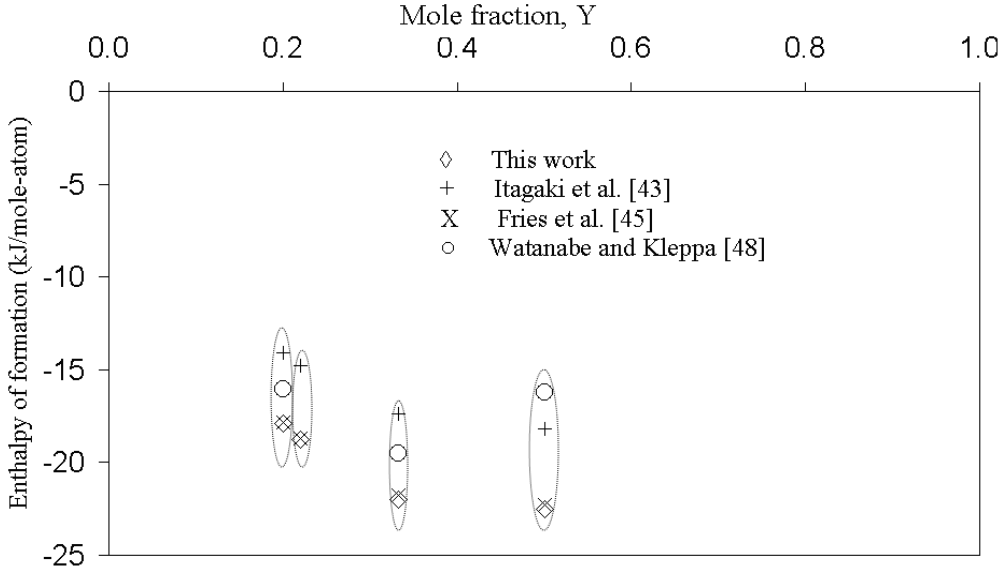

Figure 4.12: The calculated enthalpies of formation of the stoichiometric compounds compared with other works from the literature.

4.3 Mg-Y system

4.3.1 Phase Diagram

Mg-Y system was optimized by different groups. Among them the assessment of Fabrichnaya *et al.* [52] and Shakhshir and Medraj [61] are more reliable. Both of their calculated phase diagrams showed reasonable agreement with the experimental data. But [52] did not consider the crystallographic information to model the ε, δ, and γ phases while [61] considered this. However none of them considered the short range ordering in the liquid during their modeling.

In the current work, the Mg-Y system was reoptimized and the short range ordering in the liquid was taken into account through using the Modified Quasichemical model. According to equation 3.18, the optimized Gibbs energy for the liquid can be written as:

$$\Delta g_{AB} = -13{,}059.70 + 6.45\,T - (13{,}394.56 - 7.20\,T)\,X_{MgMg} - (6{,}529.85 - 1.26\,T)\,X_{YY} \quad \text{J/mole} \qquad (4.8)$$

The tendency to maximum short range ordering in the composition range 20 to 30 at.% Y, was modeled by setting $Z_{MgY}^{Mg} = 2$ and $Z_{MgY}^{Y} = 4$. This was done by iterative process to get the optimum result.

The hcp-Mg, β-Y, ε, δ, and γ phases were reproduced using the same models reported by [61] with small modifications in the excess Gibbs energy parameters as shown in Table 4.6.

Table 4.6: Optimized model parameters for liquid, hcp-Mg, β-Y, ε, δ, and γ phases in Mg-Y system.

Phase	Terms	a (J/mole)	b (J/moleK)
Liquid	Δg^{0}_{MgY}	-13,059.70	6.45
	g^{i0}_{MgY}	-13,394.56	7.20
	g^{0j}_{MgY}	-6,529.85	1.26
Hcp-Mg	${}^{0}L^{Mg-hcp}$	- 12,476.78	7.49
	${}^{1}L^{Mg-hcp}$	-2,724.56	2.4
	${}^{2}L^{Mg-hcp}$	-8,788.22	2
β-Y	${}^{0}L^{Y-\beta}$	-29,760.18	13.49
	${}^{1}L^{Y-\beta}$	-2,005.86	1.5
Phase	**Terms**	**a (J/mole-atom)**	**b (J/moleK)**
$\varepsilon^{Mg_{24}Y_5}$	$G^{\varepsilon}_{Mg:Mg:Mg}$	1,585	0
	$G^{\varepsilon}_{Mg:Y:Mg}$	-5,891.23	0
	$G^{\varepsilon}_{Y:Y:Mg}$	6,000	-0.22
δ^{Mg_2Y}	$G^{\delta}_{Mg:Mg:Mg}$	21,48.82	0
	$G^{\delta}_{Mg:Y:Mg}$	-8,849.07	-0.05
	$G^{\delta}_{Y:Y:Mg}$	4,000	0
	$G^{\delta}_{Y:Mg:Mg}$	-5,000	163.02
	${}^{0}L^{\delta}_{\mathrm{Mg,\,Y:Mg:Mg}}$	-5,000	336.16
	${}^{0}L^{\delta}_{\mathrm{Mg,\,Y:Y:Mg}}$	-8,514.55	20.44
	${}^{0}L^{\delta}_{\mathrm{Mg:Mg,\,Y:Mg}}$	-3,910.07	3.47
	${}^{0}L^{\delta}_{\mathrm{Y:Mg,\,Y:Mg}}$	-5,000	336.44
γ^{MgY}	$G^{\gamma}_{Mg:Y}$	-10,727.25	1.26
	$G^{\gamma}_{Mg:Va}$	5,232.25	0.0
	$G^{\gamma}_{Y:Y}$	33,486	0
	$G^{\gamma}_{Y:Va}$	0	17.50
	${}^{0}L^{\gamma}_{\mathrm{Mg,Y:Y}}$	7,500	8
	${}^{0}L^{\gamma}_{\mathrm{Mg,Y:Va}}$	7,500	7.50
	${}^{0}L^{\gamma}_{\mathrm{Mg:Y,Va}}$	-2,500	3.50
	${}^{0}L^{\gamma}_{\mathrm{Y:Y,Va}}$	-2,500	3.50

The calculated phase diagram is shown in Figure 4.13, along with the experimental data from the literature. For better illustration the Mg rich portion of the phase diagram is magnified and is shown in Figure 4.14. The temperatures and phase composition of invariant reactions are presented in Table 4.7, together with the data of some recent works. The calculated phase diagram shows reasonable agreement with the experimental data from the literature.

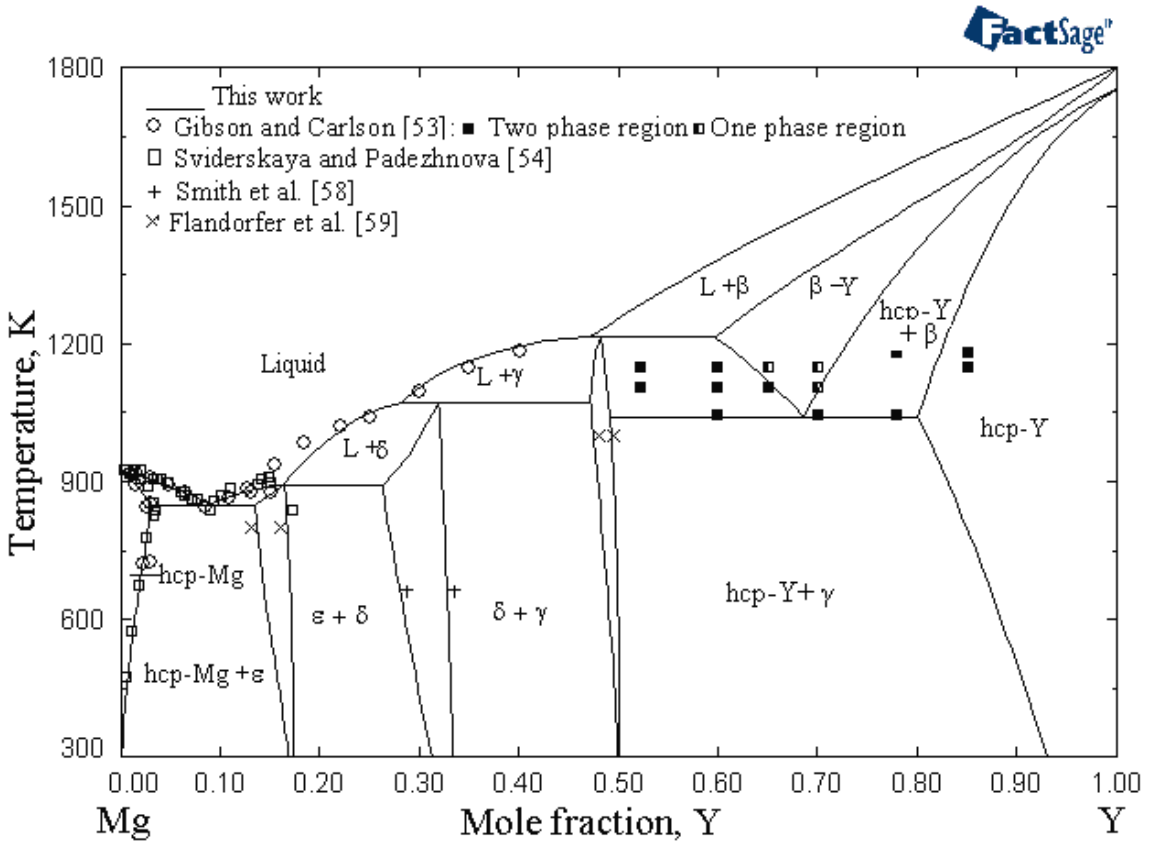

Figure 4.13: Calculated Mg-Y phase diagram with experimental results from the literature.

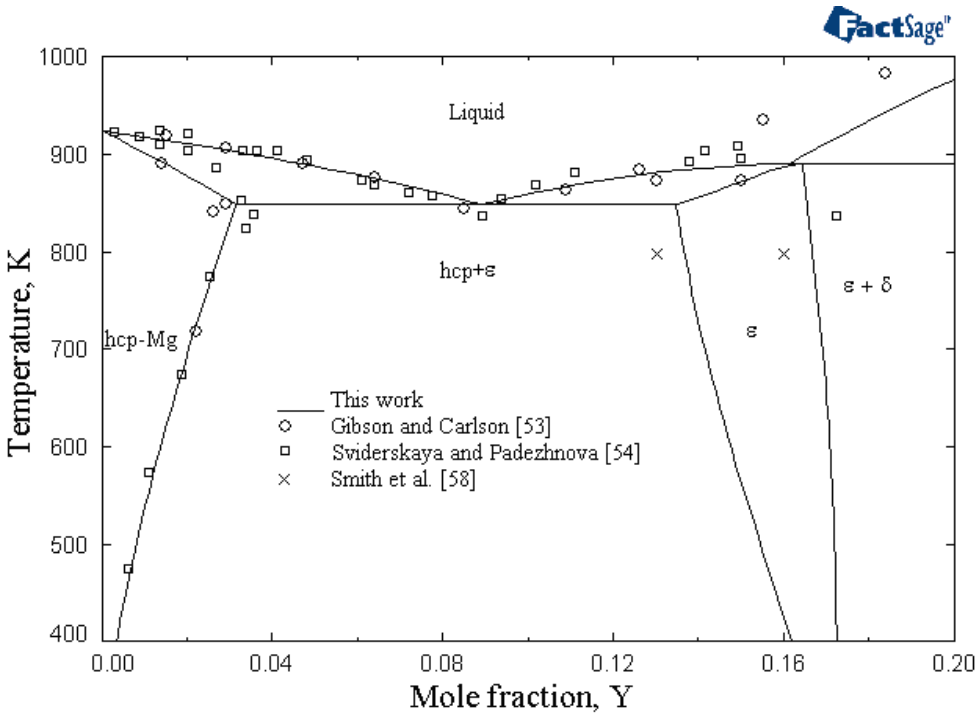

Figure 4.14: Enlarged portion of the Mg-Y phase diagram with experimental results from the literature.

Table 4.7: Comparison of the Calculated Mg-Y phase diagram and other works.

Reaction	***Temp. (°C)***	***Comp. (at. % Y)***	**Ref.**
Liquid ⇆ hcp-Mg + ε	848	8.88	This work
	839	7.85	[61]
	845	8.2	[52]
Liquid + δ ⇆ ε	890	16.14	This work
	898	16.7	[61]
	881	14.1	[52]
Liquid + γ ⇆ δ	1067	28.05	This work
	1053	30.2	[61]
	1056	28.9	[52]
Liquid+ β-Y ⇆ γ	1212	46.94	This work
	1209	47.7	[61]
	1215	47.2	[52]
β-Y ⇆ hcp-Y + γ	1038	68.53	This work
	1046	69	[61]
	1050	69	[52]

4.3.2 Thermodynamic Properties:

The calculated enthalpy of mixing at 984 K is shown in Figure 4.15. Reasonable agreement between the experimental results of Agrawal *et al.* [62] at different temperatures and the calculated one can be seen.

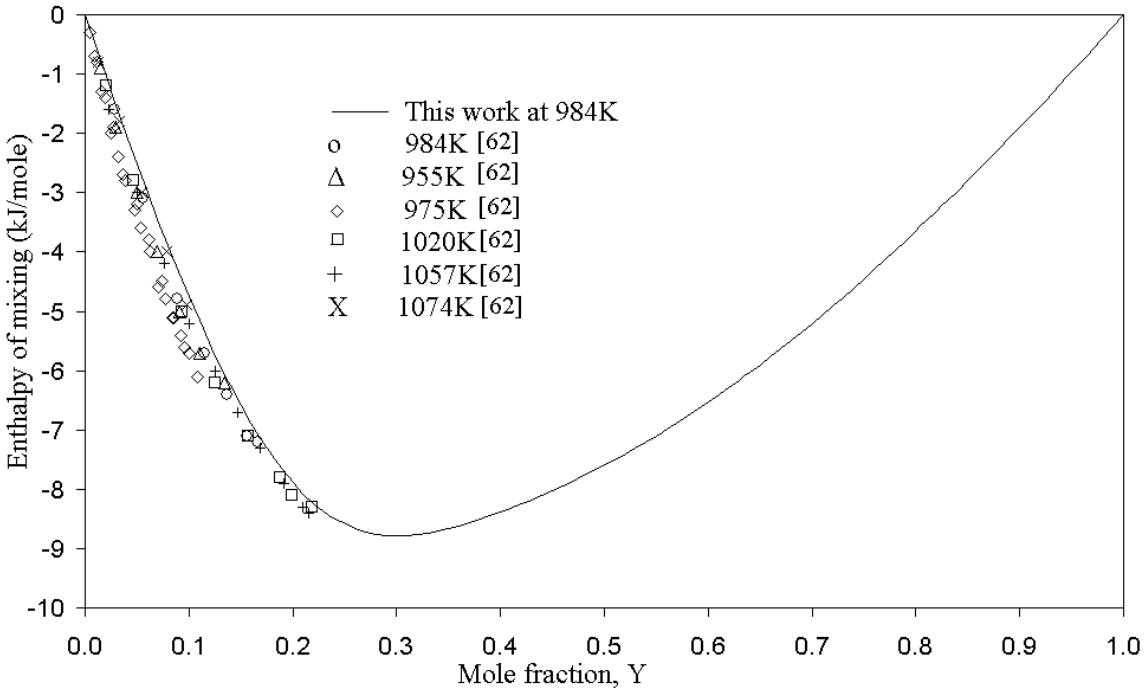

Figure 4.15: Calculated enthalpy of mixing of the Mg-Y liquid at 984K [62].

The activity of Mg in liquid Mg-Y at 1173 K is shown in Figure 4.16. The activity curve shows very good agreement with the experimental work of [51] and [63]. This calculation shows much better fit with the experimental data than that of [52] and [61].

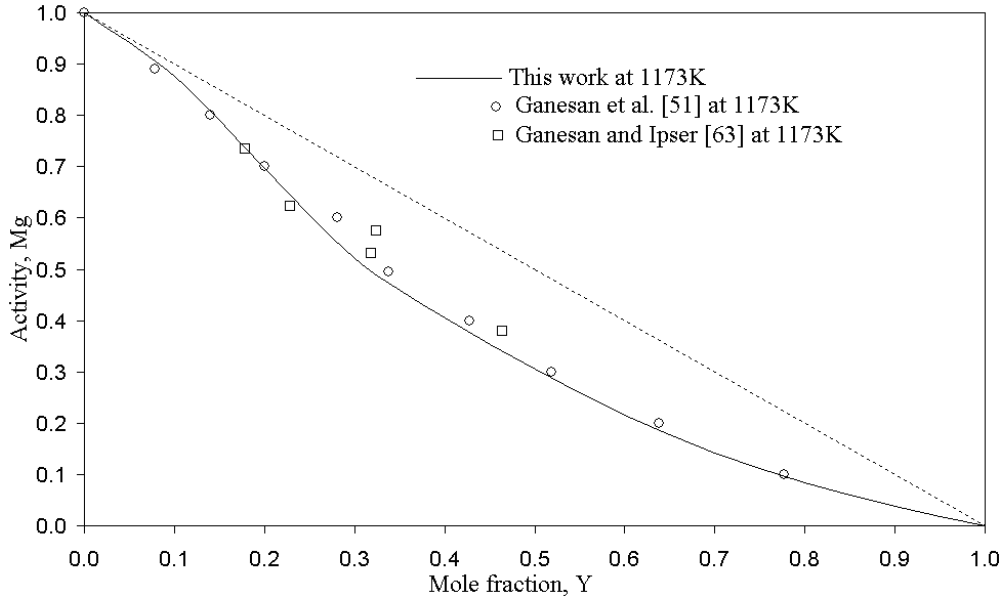

Figure 4.16: Calculated activities of Mg in Mg-Y liquid at 1173K.

The calculated partial Gibbs free energy of Mg and Y in Mg-Y liquid at 1173 K shows good agreement with the experimental results of [51] as shown in Figure 4.17.

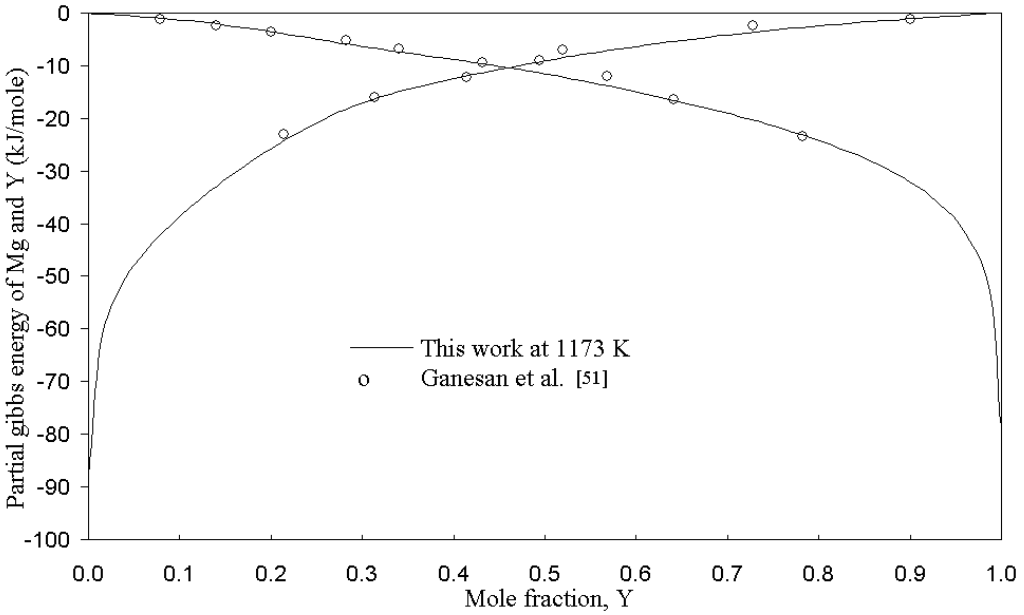

Figure 4.17: Calculated partial Gibbs energy of Mg and Y in Mg-Y alloy at 1173K.

Figure 4.18, shows the calculated enthalpy of formation of the intermediate compounds in the Mg-Y system in relation to the experimental results from the literature.

A good agreement between the calculated and the experimental data of smith *et al.* [58] and Pyagai *et al.* [64] can be seen. But the enthalpy of formation for γ (MgY) phase measured by [64] is not consistent with the experimental value of [58] as well as the calculated value in this work. However, the data of [58] is more reliable since they used both the calorimetric and vapor pressure techniques in their investigation.

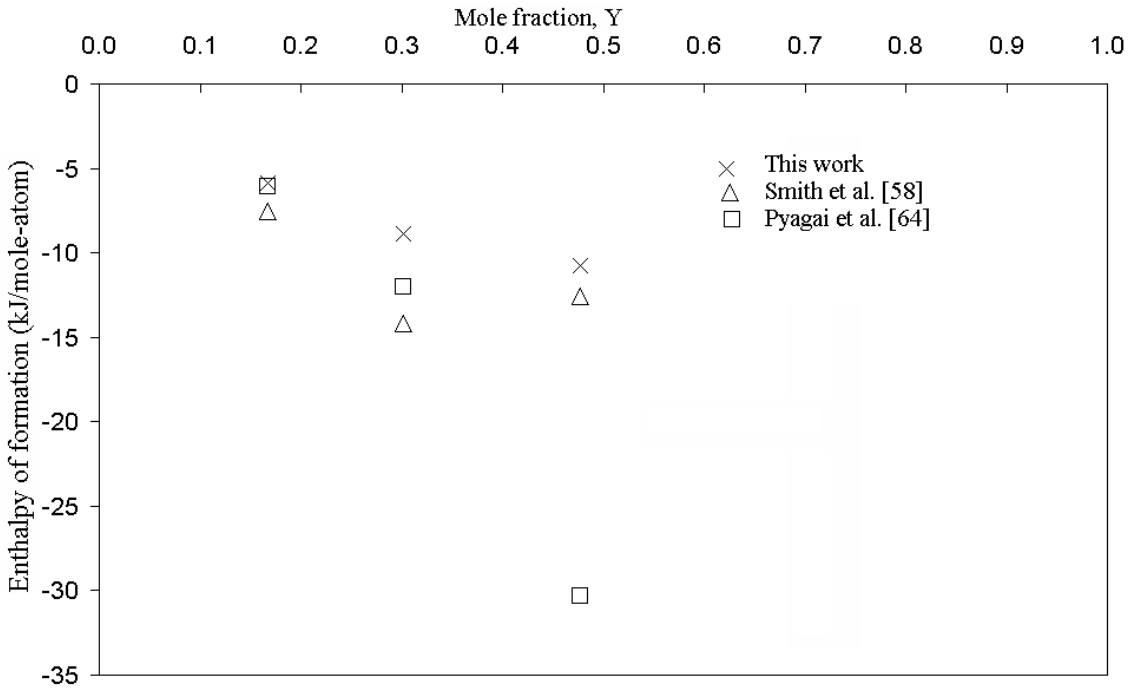

Figure 4.18: The calculated enthalpies of formation of the stoichiometric compounds compared with experimental data from the literature.

4.4 Mg-Cu-Y system

A self-consistent thermodynamic database for the Mg-Cu-Y system has been constructed by combining the thermodynamic descriptions of the three constituent binaries; Mg-Cu, Cu-Y and Mg-Y systems. For the extrapolation of the ternary system Kohler geometric model [75] was used because none of the three subsystems showed much dissimilarity in their thermodynamic characteristics. The liquid enthalpy of mixing for all the subsystems is highly negative. During the optimization no ternary parameters were used.

4.4.1 Phase Diagram

The main features of the ternary Mg-Cu-Y system will be discussed in this section by means of several isothermal sections, vertical sections and liquidus projections.

4.4.1.1 Isothermal Sections. One way to show the phase relationship for a ternary system is isothermal section which is constructed through the diagram, parallel to the base. It represents the stable phases for different compositions at the same quenching temperature. The calculated isothermal sections of the Mg-Cu-Y system are given in Figures 4.19 to 4.22.

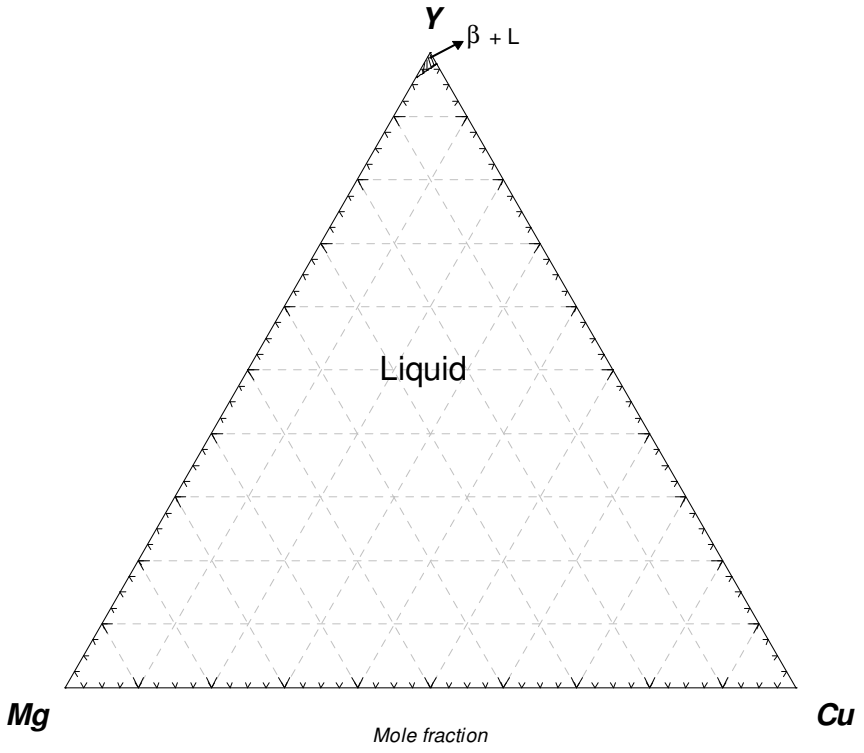

Figure 4.19: Isothermal section of Mg-Cu-Y ternary system at 1760 K.

The solidification starts at 1800 K. At a temperature higher than this there is no phase boundary and the whole concentration triangle is composed of a homogeneous liquid phase. Figure 4.19 shows the isothermal section of Mg-Cu-Y system at 1760 K. Only the crystallization of β-Y phase sets in and it exists in equilibrium with the liquid phase.

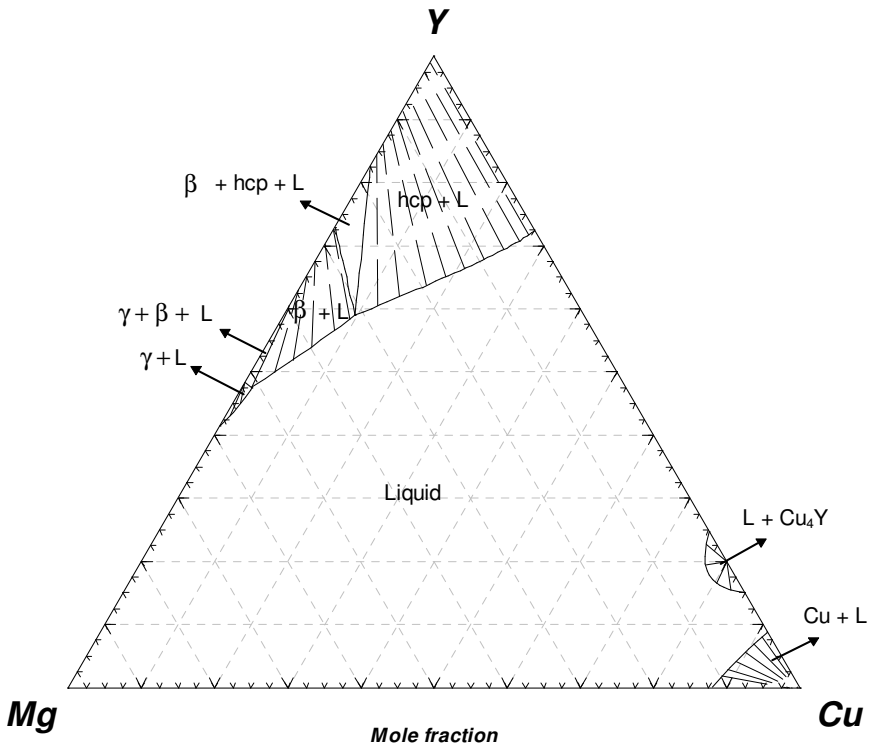

Figure 4.20: Isothermal section of Mg-Cu-Y ternary system at 1200 K.

By cooling from 1760 K to 1200 K solidification of different phases takes place. Figure 4.20, shows the isothermal section at 1200 K. The liquid phase is stable to the greater part of the composition. Primary crystallizations of hcp-Y, γ, Cu_4Y and Cu-fcc take place during the solidification. During cooling to 1200 K the binary peritectic point between Mg and Y has been encountered as can be seen from the region of L+ β + γ and is a result of the following eutectic reaction:

$$\text{Liquid} + \beta\text{-Y} \leftrightarrows \gamma \quad \text{.....(4.9)}$$

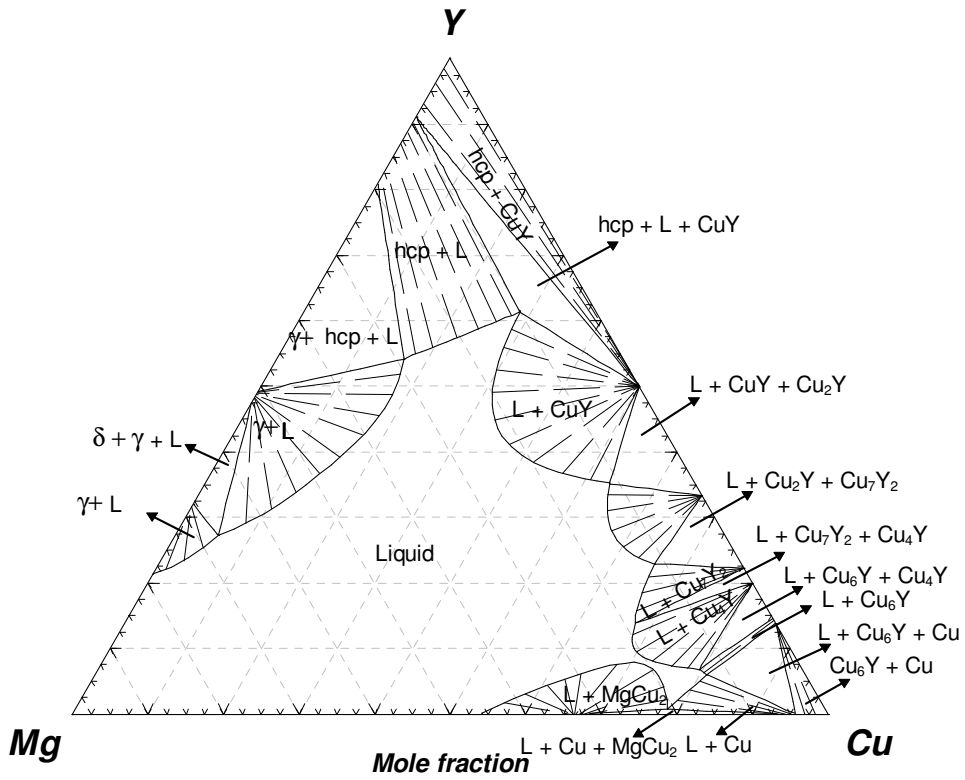

Figure 4.21: Isothermal section of Mg-Cu-Y ternary system at 1000 K.

Further crystallization takes place during cooling from 1200 K to 1000 K. The regions of primary solidification of hcp-Y, CuY, γ, δ, Cu_2Y, Cu_7Y_2, Cu_4Y, Cu_6Y and Cu in equilibrium with the liquid phase can be seen from Figure 4.21. Five binary eutectic and three peritectic reactions are encountered during the cooling.

Liquid ⇆ (Cu) +Cu_6Y (eutectic reaction)..... (4.10)

Liquid ⇆ Cu_7Y_2+ Cu_2 (eutectic reaction)..... (4.11)

Liquid ⇆ Cu_2Y(r) +CuY (eutectic reaction)..... (4.12)

Liquid ⇆ CuY + hcp-Y (eutectic reaction)..... (4.13)

Liquid ⇆ fcc-Cu + $MgCu_2$ (eutectic reaction)..... (4.14)

Liquid + Cu_4Y ⇆ Cu_7Y_2 (peritectic reaction)..... (4.15)

Liquid + Cu_4Y ⇆ Cu_6Y (peritectic reaction)..... (4.16)

Liquid + γ ⇆ δ (peritectic reaction)..... (4.17)

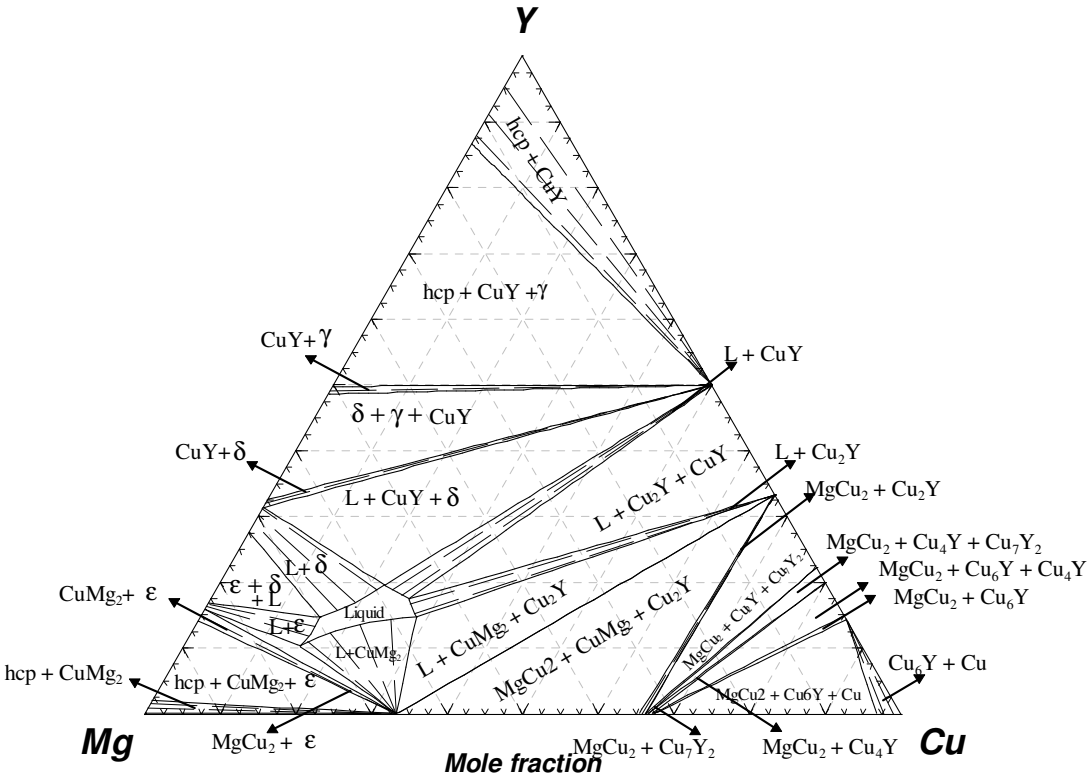

Figure 4.22: Isothermal section of Mg-Cu-Y ternary system at 700 K.

Figure 4.22 shows the isothermal section of Mg-Cu-Y system at 700 K. Primary solidification regions of hcp-Y, CuY, ε, γ, δ, Cu_2Y, Cu_7Y_2, Cu_4Y, Cu_6Y, Cu, hcp-Mg, $CuMg_2$ and Cu_2Mg in equilibrium with the melt can be seen. Eight regions of three-solid phases can be identified in the isothermal section at 700 K. Four ternary eutectic points have been encountered which occur according to the following reactions:

Liquid ⇆ hcp-Mg + ε + $CuMg_2$..... (4.18)

Liquid ⇆ δ + $CuMg_2$ + CuY..... (4.19)

Liquid ⇆ Cu_6Y + $MgCu_2$ + Cu..... (4.20)

Liquid ⇆ γ + hcp-Y + CuY..... (4.21)

Three binary eutectic and one peritectic reactions have also taken place between 1000 K to 700 K as shown below:

Liquid ⇆ $MgCu_2$ + Mg_2Cu (eutectic reaction)..... (4.22)

Liquid ⇆ hcp-Mg + $CuMg_2$ (eutectic reaction)..... (4.23)

Liquid ⇆ hcp-Mg + ε (eutectic reaction)..... (4.24)

Liquid + δ ⇆ ε (peritectic reaction)..... (4.25)

4.4.1.2 Liquidus Projection of the Mg-Cu-Y System. The liquidus projection is a two-dimensional projection of ternary liquidus univariant lines at constant pressure onto a Gibbs triangle plane. The liquidus projection shown in Figure 4.23 is calculated using FactSage 5.4.1 software [71] with the optimized parameters of the three constituent binary systems, Mg-Cu, Cu-Y and Mg-Y. The univariant valleys are shown by the heavier lines and the arrows on these lines indicate the directions of decreasing temperature. There are four ternary eutectic (E_1 to E_4) points, eight ternary quasi-peritectic (U_1 to U_8) points and three maximum (m_1 to m_3) points present in this system. A summary of all the ternary and binary invariant points are given in Table 4.8 and 4.9, respectively.

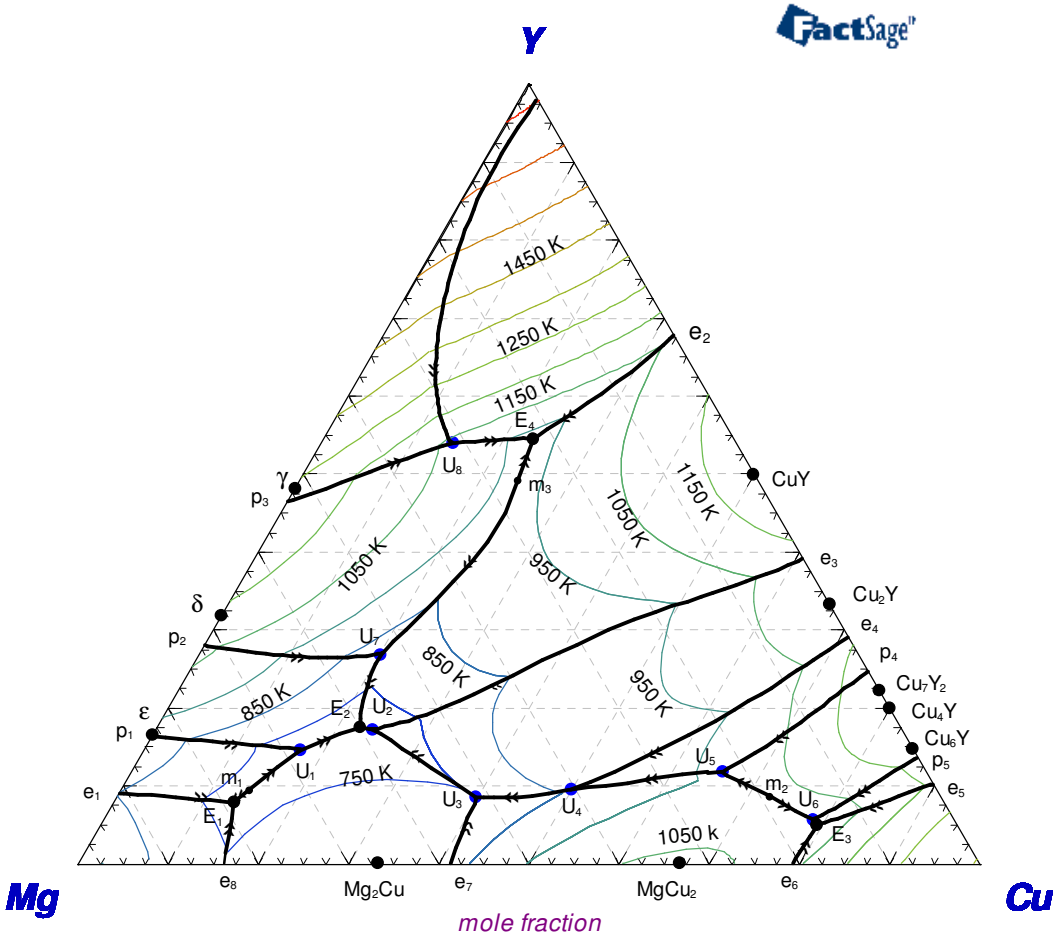

Figure 4.23: Liquidus projection of the Mg-Cu-Y system.

Table 4.8: Calculated 4-phase equilibria points and their reactions in the Mg-Cu-Y system.

No	Reaction	Calculated (this work)				
		Temp. (K)	Type	Y (at.%)	Mg(at.%)	Cu(at.%)
1	Liquid ⇆ hcp-Mg + ε + $CuMg_2$	709.8	E_1	7.7	79.2	13.1
2	Liquid ⇆ δ + $CuMg_2$ + CuY	662.6	E_2	17.8	59.6	22.6
3	Liquid ⇆ Cu_6Y + $MgCu_2$ + Cu	956.3	E_3	5.1	15.9	79.0
4	Liquid ⇆ γ + hcp-Y + CuY	910.1	E_4	54.6	22.4	23.0
5	Liquid + ε ⇆ δ + Mg_2Cu	680.9	U_1	14.7	67.9	17.3
6	Liquid + Cu_2Y ⇆ CuY + $CuMg_2$	672.9	U_2	17.4	58.3	24.3
7	Liquid + $MgCu_2$ ⇆ $CuMg_2$ + Cu_2Y	761.2	U_3	8.8	51.4	39.8
8	Liquid + Cu_7Y_2 ⇆ $MgCu_2$ + Cu_2Y	849.4	U_4	9.8	40.6	49.6
9	Liquid + Cu_4Y ⇆ $MgCu_2$ + Cu_7Y_2	957.4	U_5	10.6	25.2	64.2
10	Liquid + Cu_4Y⇆ Cu_6Y + $MgCu_2$	961.4	U_6	5.8	15.9	78.3
11	Liquid + γ ⇆ δ + CuY	794.2	U_7	27.3	52.2	20.5
12	Liquid + β-Y⇆ hcp-Y + γ	1038	U_8	54.0	32.1	13.9

Table 4.9: Calculated 3-phase equilibria points and their reactions in the Mg-Cu-Y system.

No	Reaction	Calculated (this work)				
		Temp. (K)	Type	Y(at.%)	Mg (at.%)	Cu (at.%)
1	Liquid ⇆ ε + Mg_2Cu	710.5	m_1	8.8	77.4	13.8
2	Liquid ⇆ $MgCu_2$ + Cu_4Y	995.5	m_2	8.0	19.9	72.1
3	Liquid ⇆ γ + CuY	918.3	m_3	49.6	26.1	24.3
4	Liquid ⇆ fcc-Cu + $MgCu_2$	1004	e_1	0.0	21.8	78.2
5	Liquid ⇆ $MgCu_2$ + Mg_2Cu	824	e_2	0.0	58.7	41.3
6	Liquid ⇆ hcp-Mg + $CuMg_2$	762	e_3	0.0	84.1	15.9
7	Liquid ⇆ (Cu) +Cu_6Y	1159	e_4	10.4	0.0	89.6
8	Liquid ⇆ Cu_7Y_2+ Cu_2	1128	e_5	29.2	0.0	70.8
9	Liquid ⇆ Cu_2Y(r) +CuY	1115	e_6	39.2	0.0	60.8
10	Liquid ⇆ CuY + hcp-Y	1059	e_7	69.9	0.0	30.1
11	Liquid ⇆ hcp-Mg + ε	848	e_8	8.9	91.1	0
12	Liquid + Cu_4Y ⇆ Cu_6Y	1177	p_1	13.7	0.0	86.3
13	Liquid + Cu_4Y ⇆ Cu_7Y_2	1198	p_2	24.8	0.0	75.2
14	Liquid + δ ⇆ ε	890	p_3	16.1	83.9	0.0
15	Liquid + γ ⇆ δ	1067	p_4	28.1	71.9	0.0

16	Liquid+ β-Y ⇆ γ	1212	p_5	46.9	53.1	0.0

4.4.2 Thermodynamic Properties

Ganesan *et al.* [51] measured the enthalpy of mixing of the ternary Mg-Cu-Y liquid alloys by calorimetric method along five different isopleths. The calculated enthalpy of mixing showed reasonable agreement with the experimental data. Calculations for three different compositions are shown in Figures 4.24 to 4.26. The initial discrepancy with the experimental data in Figure 4.26, is due to the contribution of the binary Cu-Y liquid enthalpy of mixing.

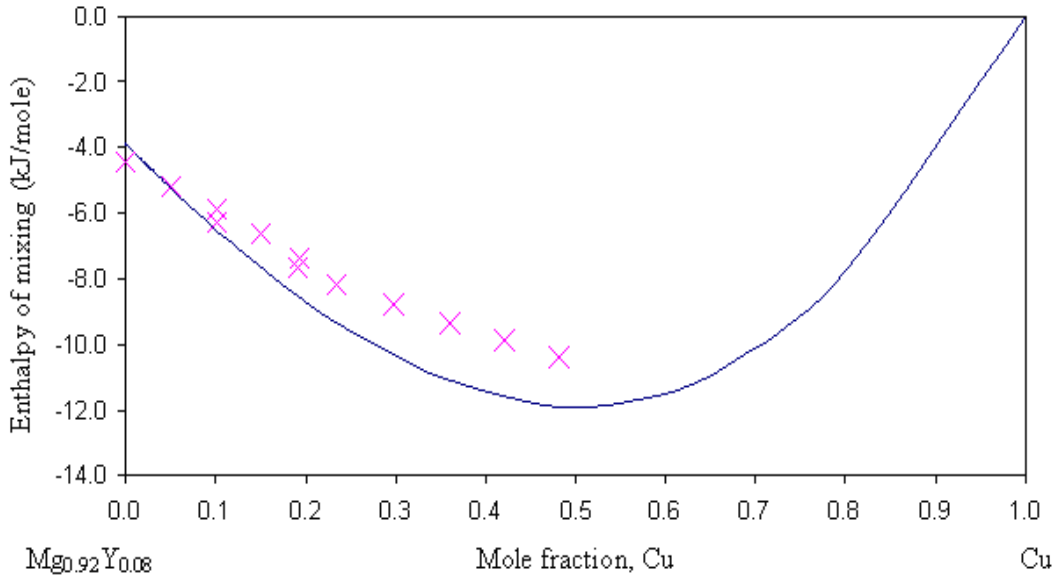

Figure 4.24: Integral enthalpy of mixing of $(Mg_{0.92}Y_{0.08})_{1-x}Cu_x$ ternary liquid alloy at 1023 K with experimental data of [51].

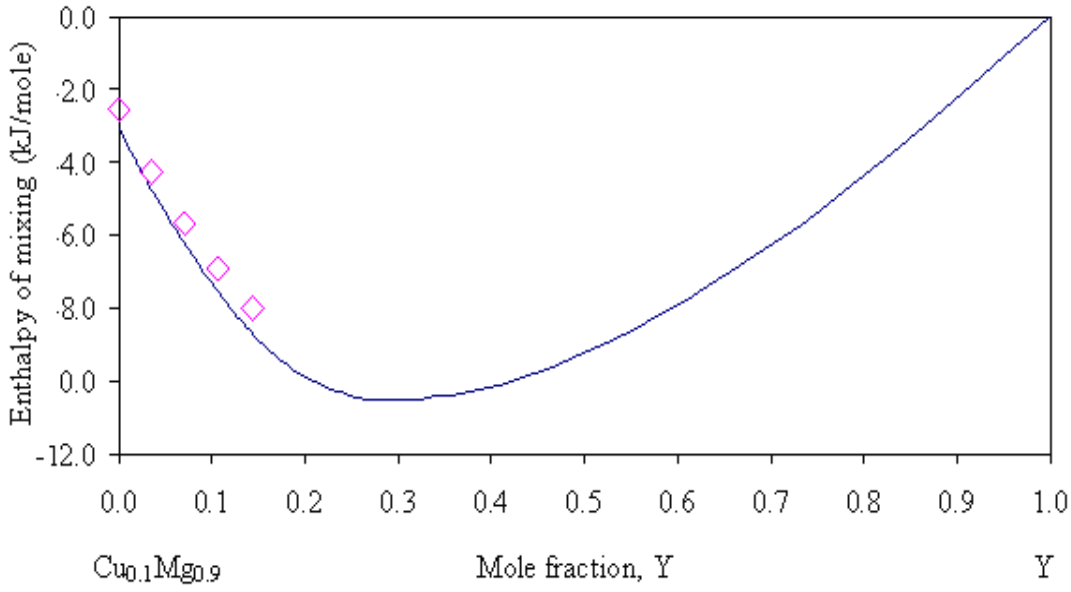

Figure 4.25: Integral enthalpy of mixing of $(Cu_{0.1}Mg_{0.9})_{1-x}Y_x$ ternary liquid alloy at 1023 K with experimental data of [51]

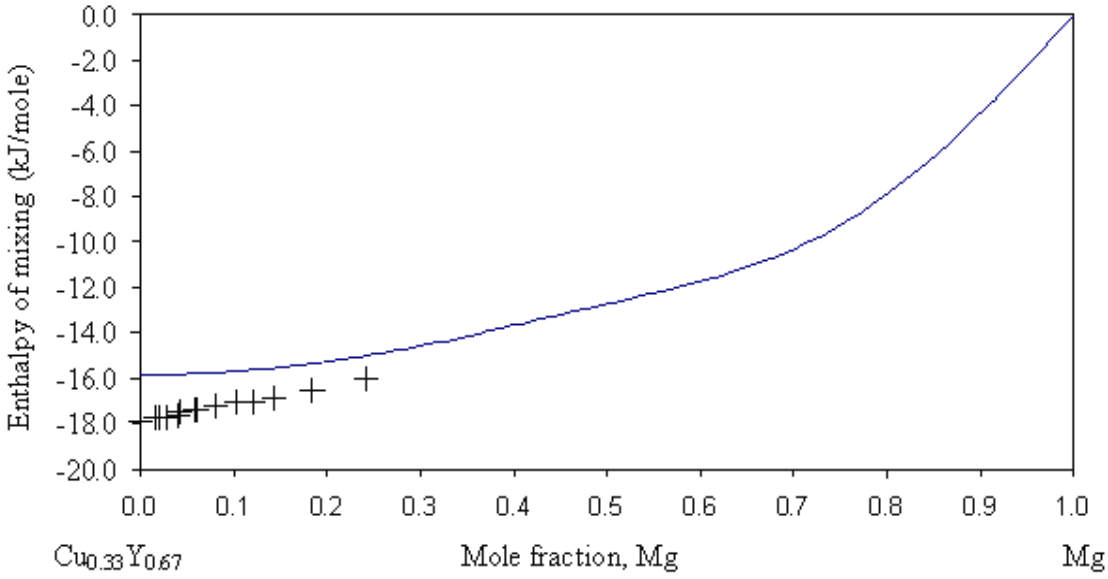

Figure 4.26: Integral enthalpy of mixing of $(Cu_{0.33}Y_{0.67})_{1-x}Mg_x$ ternary liquid alloy at 1107 K with experimental data of [51].

The calculated activity of Mg in the ternary liquid alloy at 1173 K is shown in Figure 4.27 with the experimental data of [51]. Activities measured at different temperatures were converted into same temperature by Ganesan *et al.* [51], using a

mathematical equation, to compare with the calculated one. The present calculated values showed negative deviation from Raoult's law unlike the measured activity that showed positive deviation. The reason for this is unknown. But the present calculated activity of Mg showed similar trend as the one calculated by [51].

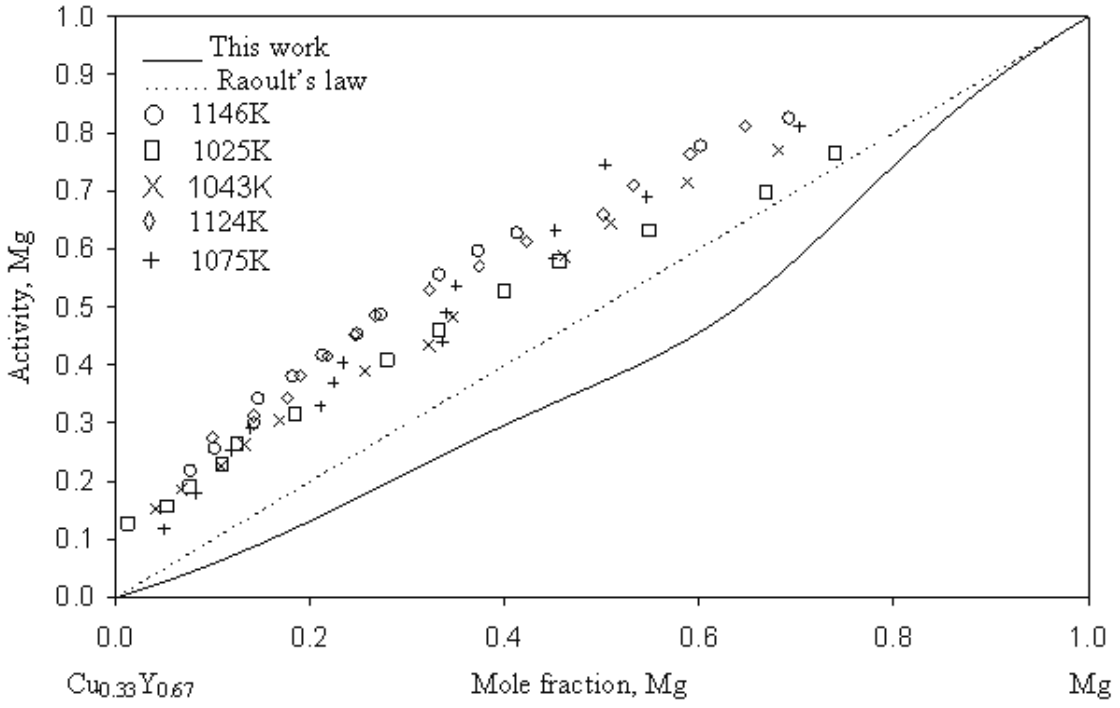

Figure 4.27: Activity of Mg in ternary liquid alloy at 1173 K with experimental data [51].

4.4.3 An alternative approach to include the ternary compounds in the system

An alternative approach has been applied to include the two ternary compounds in the optimization. It was difficult to do so, since there is limited experimental data available. However, it was done by making some assumptions based on available experimental evidences on the amorphous alloys of different compositions in the Mg-Cu-Y system.

The melting temperature or the enthalpy of formation of the two ternary compounds Y_2Cu_2Mg and YCu_9Mg_2, which were reported by Mishra *et al.* [67] and Solokha *et al.* [68], could not be found in the literature. But they [67, 68] mentioned the annealing temperatures of these two compounds which can give an indication of the melting temperature. Annealing is a process usually used to release the residual stress from a material. In this process metals are heated to a temperature below its melting temperature. So, the annealing temperature of these compounds will give a lower limit of a possible melting temperature range. Also the upper limit will not be too far from this temperature since annealing is usually done closer to the actual melting temperature. The reported annealing temperatures of Y_2Cu_2Mg and YCu_9Mg_2 are 900 K and 673 K, respectively.

Inoue *et al.* [5] and Ma *et al.* [66] made some experiments on Mg-Cu-Y system to find suitable compositions for metallic glass. They used XRD and DSC analyses to examine different amorphous samples of Mg-Cu-Y system. During their experiments proper equilibrium conditions were not prevailed, hence their experimental data cannot be used directly in this work. But after reviewing the works of [5] and [66] some information regarding the system can be obtained. The DSC analysis of Ma *et al.* [66] shows that near $Mg_{65}Cu_{25}Y_{11}$ composition one ternary eutectic point exists. Same composition for the eutectic was reported earlier by Inoue *et al.* [5]. Based on these, it can be assumed that the actual eutectic point would be found near this composition at a similar temperature if proper equilibrium conditions are maintained. Depending on this information an approximate melting temperature for the ternary compounds can be

estimated, since the occurrence of ternary compounds greatly hampered the equilibrium phase diagram.

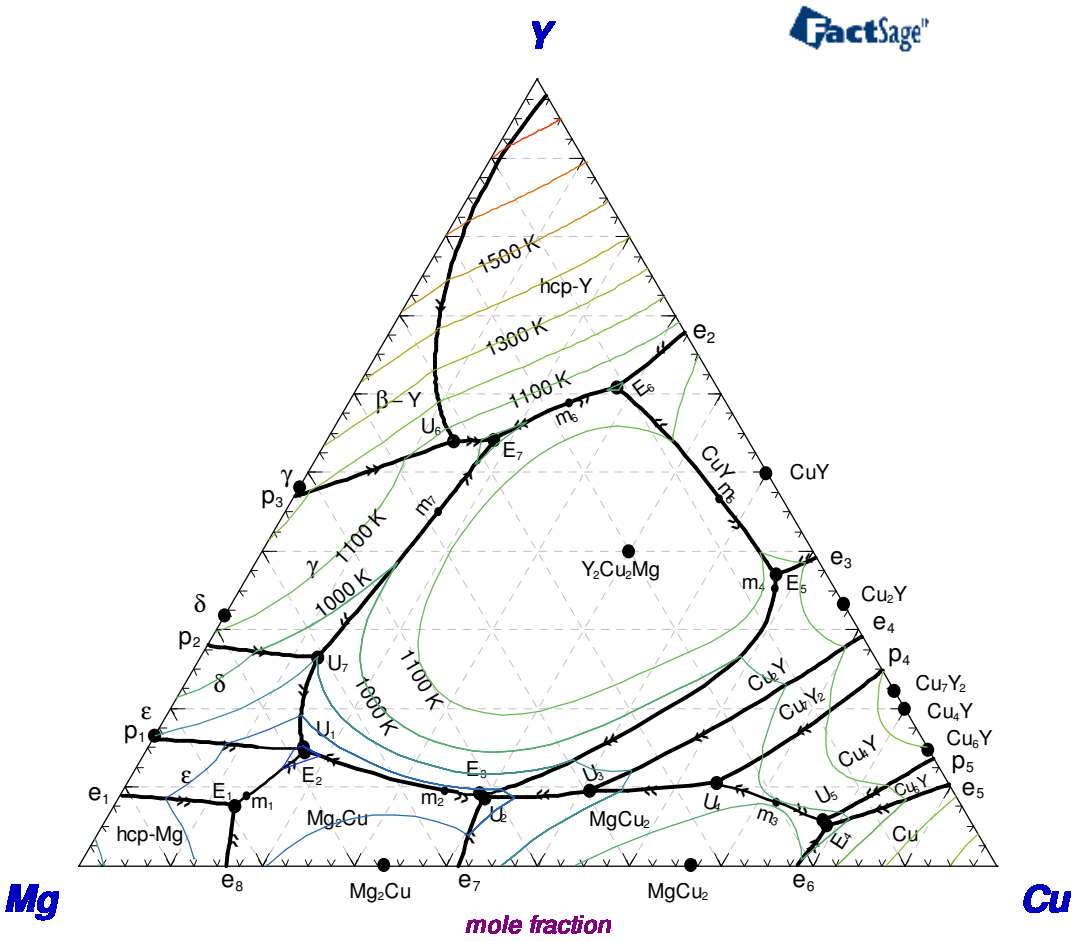

Figure 4.28: Liquidus projection of the Mg-Cu-Y system with the ternary compounds.

Based on the abovementioned assumptions the optimization was done and the resulted liquidus projection is shown in Figure 4.28. The eutectic point (E_2) is observed at a composition of $Mg_{68}Cu_{17.4}Y_{14.6}$ at temperature 682 K. The composition deviates from that of Inoue *et al.* [5] and Ma *et al.* [66] by about 8 at.% Cu and temperature around 50

K. More accurate result can be obtained through introducing some ternary interaction parameters but since the experimental data is not dependable, it is decided to accept the current calculation without using any interaction parameter. All the invariant points calculated after incorporating the ternary compounds are given in table 4.10.

Table 4.10: Calculated equilibria points and their reactions in the Mg-Cu-Y system after including the ternary compounds.

No	Reaction	Calculated (this work)				
		Temp. (K)	Type	Y (at.%)	Mg(at.%)	Cu(at.%)
1	Liquid ⇆ hcp-Mg + ε + $CuMg_2$	709.8	E_1	7.7	79.2	13.1
2	Liquid ⇆ δ + $CuMg_2$ + Y_2Cu_2Mg	682.0	E_2	14.6	68.1	17.3
3	Liquid ⇆ $CuMg_2$ + Cu_2Y + Y_2Cu_2Mg	760.8	E_3	9.0	51.6	39.4
4	Liquid ⇆ Cu_6Y + $MgCu_2$ + Cu	956.3	E_4	5.1	15.9	79.0
5	Liquid ⇆ Cu_2Y + CuY + Y_2Cu_2Mg	1059.9	E_5	37.1	5.5	57.4
6	Liquid ⇆ hcp-Y + CuY + Y_2Cu_2Mg	993.5	E_6	60.8	11.1	28.1
7	Liquid + δ ⇆ ε + $CuMg_2$	684.1	U_1	14.8	68.1	17.1
8	Liquid + Cu_2Mg ⇆ Cu_2Y + $CuMg_2$	761.2	U_2	8.8	51.7	39.5
9	Liquid + Cu_7Y_2 ⇆ $MgCu_2$ + Cu_2Y	868.0	U_3	9.7	39.3	51.0
10	Liquid + Cu_4Y ⇆ $MgCu_2$ + Cu_7Y_2	957.2	U_4	10.6	25.4	64.1
11	Liquid + Cu_4Y⇆ Cu_6Y + $MgCu_2$	961.4	U_5	6.0	15.7	78.3
12	Liquid + β-Y⇆ hcp-Y + γ	1038	U_6	54.8	32.1	13.1
13	Liquid + γ ⇆ δ + Y_2Cu_2Mg	900.2	U_7	26.6	60.7	12.7
14	Liquid ⇆ ε + $CuMg_2$	710.54	m_1	8.7	77.5	13.8
15	Liquid ⇆ $CuMg_2$ + Y_2Cu_2Mg	766.1	m_2	9.6	55.5	34.9
16	Liquid⇆ $MgCu_2$ + Cu_4Y	995.5	m_3	8.0	19.9	72.1
17	Liquid⇆ Cu_2Y + Y_2Cu_2Mg	1062.4	m_4	35.5	6.4	58.1
18	Liquid⇆ CuY + Y_2Cu_2Mg	1136.3	m_5	46.6	6.8	46.6
19	Liquid⇆ hcp-Y + Y_2Cu_2Mg	1010.3	m_6	58.9	17.1	24.0
20	Liquid⇆ γ + Y_2Cu_2Mg	1013.4	m_7	45.1	38.2	16.7

The melting temperature of the Y_2Cu_2Mg compound was adjusted to be 1256 K by trial and error method, so that the eutectic composition and temperature lies in the desired range. The compound melts congruently at this temperature which is shown in Figure 4.29.

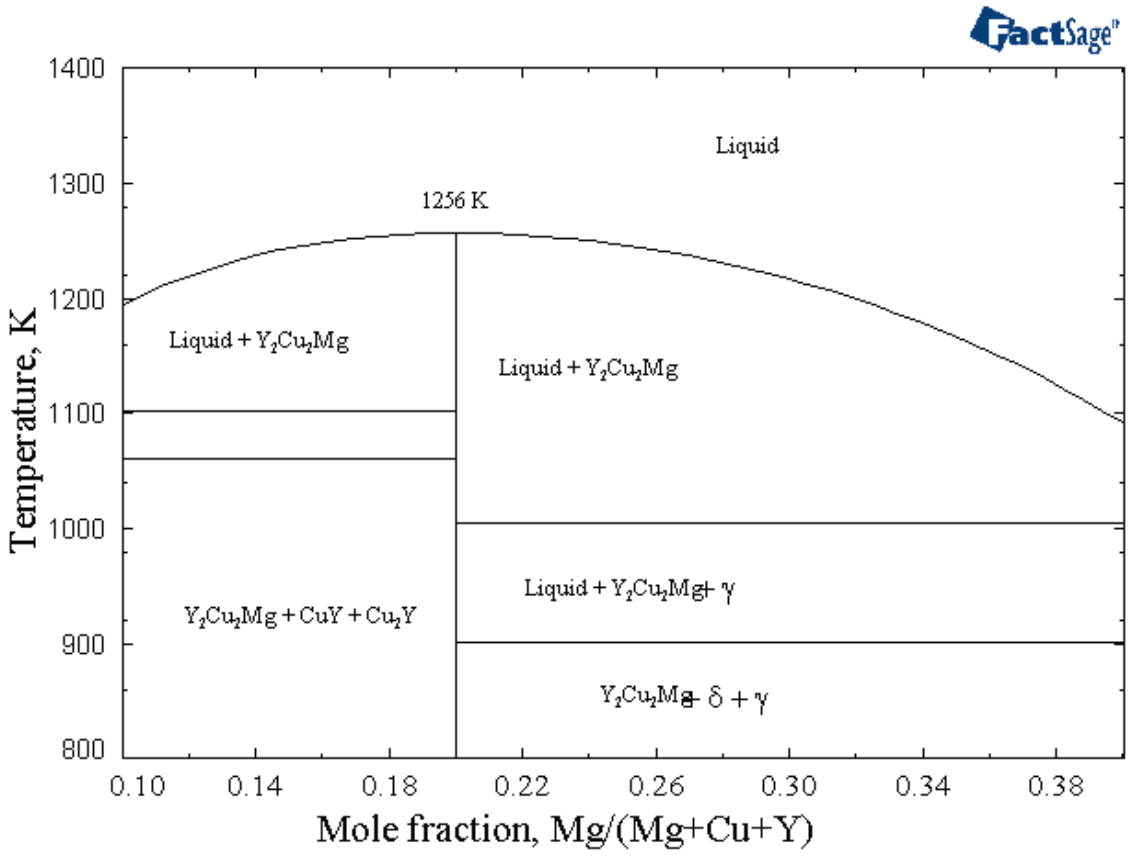

Figure 4.29: Isopleth (constant composition section) of the Mg-Cu-Y system at 40 at.% Y, showing the melting temperature of Y_2Cu_2Mg compound.

The melting temperature of YCu_9Mg_2 should be lower than that of Y_2Cu_2Mg, since the overall Y content is less (8 versus 40 at.% Y). The reported annealing temperature (673 K), which is lower than that of Y_2Cu_2Mg, also supports this assumption. The XRD analysis of Ma *et al.* [66] on the alloy composition $Mg_{58.5}Cu_{30.5}Y_{11}$, shows the existence of Mg_2Cu, $Mg_{24}Y_5$ and one unidentified phase. It

may be assumed that this unidentified phase is Y_2Cu_2Mg. To be consistent with this information the melting temperature of YCu_9Mg_2 was adjusted to be 852 K. A vertical section for 75 at.% Cu in Figure 4.30, shows that at this temperature this compound melts incongruently. The presence of incongruently melting binary (Cu_6Y) compound near YCu_9Mg_2 also justifies its incongruently melting phenomenon.

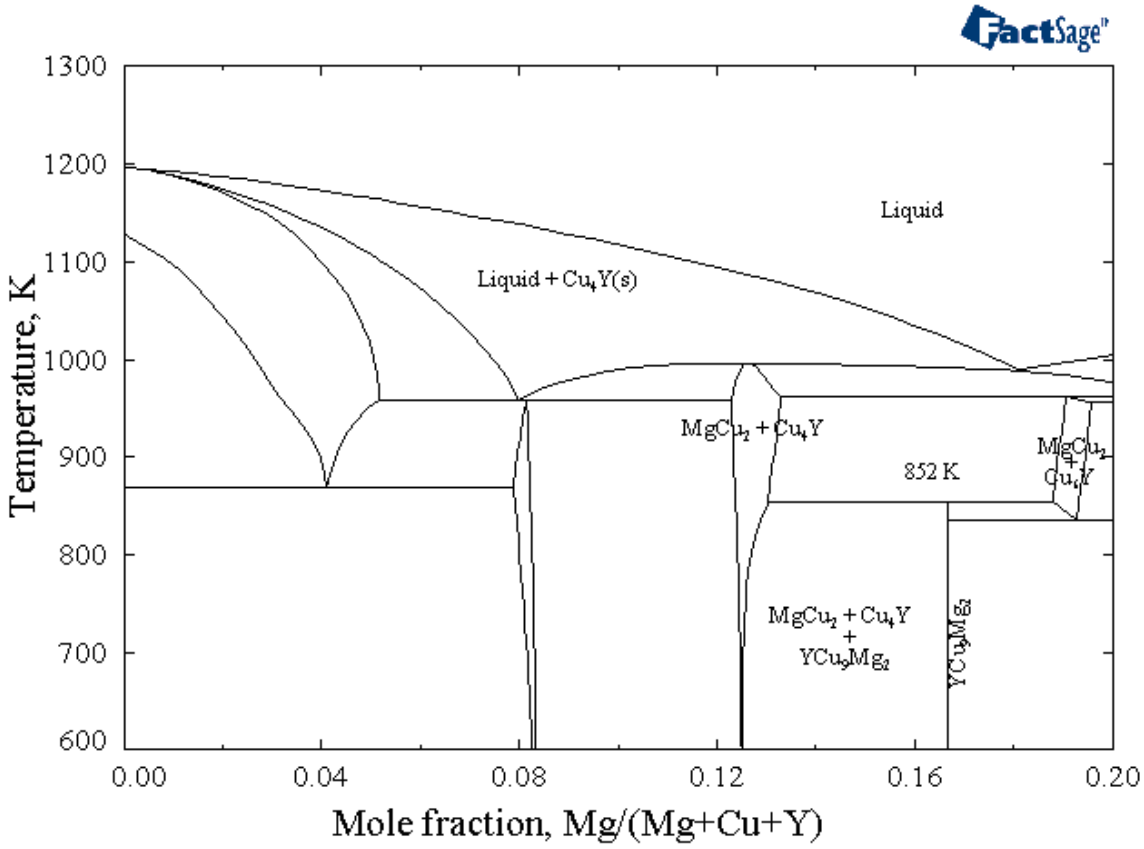

Figure 4.30: Isopleth (constant composition section) of the Mg-Cu-Y system at 75 at.% Cu, showing the melting temperature of YCu_9Mg_2 compound.

The above discussion shows the legitimacy of the current work. The analysis may not be totally accurate but at least it will give closer approximation of the actual equilibrium in the Mg-Cu-Y system. Some key experiments on this system may resolve this uncertainty. This should be attempted during further studies on this system.

CHAPTER 5

Conclusions, Contributions and Suggestions for Future Work

5.1 Conclusion

A comprehensive thermodynamic assesment of the ternary Mg-Cu-Y system was conducted using available experimental data. Based on the assesment, the following conclusions can be drawn:

- Thermodynamic optimization on the Mg-Cu-Y system was done using the well established CALPHAD method.
- A careful investigation was carried out on the three binary systems: Mg-Cu, Cu-Y and Mg-Y. Optimized thermodynamic model parameters for different phases in the binaries were evaluated.
- The Modified Quasichemical model was used to describe the liquid phase in order to account for the short range ordering in the liquid.
- The calculated phase diagrams of Mg-Cu, Cu-Y and Mg-Y system as well as their thermodynamic properties such as activity, enthalpy of mixing and partial Gibbs free energy showed good agreement with the experimental data.
- A self-consistent database for the Mg-Cu-Y system was constructed by combining the optimized parameters of the three constituent binary systems. No ternary interaction parameters were used for the extrapolation.

- The calculated enthalpy of mixing for the liquid Mg-Cu-Y system showed good agreement with the experimental data from the literature.
- The calculated Mg-Cu-Y ternary phase diagram, without the ternary compounds, showed four ternary eutectic points, eight ternary quasi peritectic points and three saddle (max) points.
- The presence of two ternary compounds was included in an alternative approach of optimization by making some reasonable assumptions, since sufficient experimental data was not available, to provide a better understanding of the system. Eight ternary eutectic, eight ternary quasi peritectic and seven saddle (max) points were determined after including the ternary compounds in the system.

5.2 Contributions

Even though the Mg-Cu-Y system is getting considerable attention from the researchers due to their potentiality for metallic glass applications, the entire system is not thermodynamically modeled yet. The present research work, after careful assessment of all the available information, provides a reliable thermodynamic description of the binary constituents of the Mg-Cu-Y system. The presence of short range ordering in the liquid was considered during the optimization process which makes this work more reliable. Also, in an alternative approach two ternary compounds were included in the optimization by making some reasonable assumptions. By successfully constructing a self-consistent thermodynamic database this work opens a field of opportunity, for the researchers, to conduct more experimental work on this system which will eventually

supports the development of metallic glass research. More promising alloy compositions could be easily identifiable through the proper utilization of the calculated phase diagrams of this work.

5.3 Suggestions for Future Work

- More experimental investigation is required to obtain detailed information regarding the two ternary compounds (Y_2Cu_2Mg and YCu_9Mg_2). The melting point of these two compounds should be determined experimentally which is very important to establish a more accurate assessment of Mg-Cu-Y system.
- All the predicted invariant points in the Mg-Cu-Y ternary system are to be verified experimentally. The present work can be used to design key experiments for further verification of this system.

References

[1] Kattner, U. R.: "The thermodynamic modeling of multicomponent phase equilibria", Journal of Metals, vol. 49, no. 12, 1997, pp. 14-19.

[2] Tendler, R.H.; Soriano, M.R.; Pepe, M.E.; Kovacs, J.A.; Vicente, E.E.; Alonso, J.A.: "Calculation of metastable free-energy diagrams and glass formation in the Mg-Cu-Y alloy and its boundary binaries using the miedema model", Intermetallics, vol. 14, no. 3, 2006, pp. 297-307.

[3] Ashley, S.: "Metallic glasses bulk up", Mechanical Engineering, http://www.memagazine.org/backissues/membersonly/june98/features/metallic/metallic.html (cited June 16, 2007).

[4] "Processing Technology for Metallic Glasses", New Energy and Industrial Technology Development Organization, http://www.nedo.go.jp/english/activities/portal/gaiyou/p02014/p02014.html (cited June 16, 2007).

[5] Inoue, A.; Kato, A.; Zhang, T.; Kim, S.G.; Masumoto, T.: "Mg-Cu-Y amorphous alloys with high mechanical strengths produced by a metallic mold casting method", Materials Transactions, vol. 32, no. 7, 1991, pp. 609-616.

[6] Palumbo, M.; Satta, M, Cacciamani, G.; Baricco, M.: "Thermodunamic analysis of the undercooled liquid and glass transition in the Cu-Mg-Y system", Materials Transaction, vol. 47, no. 12, 2006, pp. 2950-2955.

[7] Boudouard, O.: "On the alloys of copper and magnesium", Comptes Rendus Hebdomadaires des Seances de l'Academie des Sciences, vol. 135, 1902, pp. 794-796.

[8] Sahmen, R.: "Alloys of copper with cobalt, iron, manganese and magnesium", Zeitschrift für Anorganische und Allgemeine Chemie, vol. 57, 1908, pp. 1-33.

[9] Urasow, G.G.: "Alloys of copper and magnesium", Zhurnal Russkogo Fiziko-Khimicheskogo Obschestva, vol. 39, no. 9, 1907, pp. 1556-1581.

[10] Jones, W.R.D.: "Copper-magnesium alloys-the equilibrium diagram", Japan Institute of Metals, vol. 574, 1931, pp. 395-419.

[11] Stepanov, N. I.: "Electrical conductivity of alloys", Zeitschrift für anorganische und allgemeine Chemie, vol. 78, 1913, pp. 1-32.

[12] Hansen, M.: "Note on the magnesium rich magnesium copper alloys", Japan Institute of Metals, vol. 428, 1927, pp. 93-100.

[13] Jenkin, J.W.: “Discussion on Hansen’s paper [12]”, Japan Institute of Metals, vol. 428, 1927, pp. 100-102.

[14] Ageew, N.: “Correspondence on Jones paper [10]”, Japan Institute of Metals, vol. 574, 1931, pp. 419-420.

[15] Grime, G. and Morris-Jones, W.: “An x-ray investigation of the copper-magnesium alloys”, Philosophical Magazine, vol. 7, 1929, pp. 1113-1134.

[16] Stepanov, N.I.: Kornilov, I.I.: “Solubility of copper in magnesium in the solid state”, Izvestiya Instituta Fiziko-Khimicheskogo Analiza, Akademiya Nauk SSSR, vol. 7, 1935, pp. 89-98.

[17] Bagnoud, P. and Feschotte, P.: “Binary systems of magnesium-copper and magnesium-nickel, especially the nonstoichiometry of the MgCu2 and MgNi2 laves phases”, Zeitschrift für Metallkunde, vol. 69, no. 2, 1978, pp. 114-120.

[18] Sederman, V.G.: “Cu_2Mg phase in the copper-magnesium system”, Philosophical Magazine, vol. 18, 1934, pp. 343-352.

[19] Runquist, A.; Arnfelt, H.; Westgren, A.: “X-ray analysis of the copper-magnesium alloys”, Zeitschrift für Anorganische und Allgemeine Chemie, vol. 175, 1928, pp. 43-48.

[20] Ekwall, G. and Westgren, A.: “Crystal structure of $CuMg_2$”, Arkiv Kemi, Mineral. Geol. vol. 14B, no. 7, 1940, p. 8.

[21] Friauf, J.B.: “The crystal structure of two intermetallic compounds”, Journal of the American Chemical Society, vol. 49, 1927, pp. 3107-3114.

[22] Chatterjee, G.P.; Mukherjee, J. K.; Som, K. C.: “X-ray diffraction studies of a binary alloy containing metals with dissimilar crystal structures, valencies, and ionic radii”, Transactions of the Indian Institute of Metals, vol. 9, 1956, pp. 219-225.

[23] Nayeb-Hashemi, A.A.; Clark, J.B.: “The Cu-Mg (copper-Magnesium) system”, Bulletin of Alloy Phase Diagrams, vol. 5, no. 1, 1984, pp. 36-43.

[24] Coughanowr, C.A.; Ansara, I.; Luoma, R.; Hamalainen, M.; Lukas, H.L.: “Assesment of the copper-magnesium system”, Zeitschrift für Metallkunde, vol. 82, no. 7, 1991, pp. 574-581.

[25] Redlich, O. and Kister, A.T.: “Thermodynamics of nonelectrolyte solutions, X-Y-T relations in a binary system”, Journal of Industrial and Engineering Chemistry Washington D. C., vol. 40, 1948, pp. 341-345.

[26] Wagner, C.; Schottky, W.: “Theory of arranged mixed phases”, The Journal of Physical Chemistry B, vol. 11, 1930, pp. 163-210.

[27] Zuo, Y.; Chang, Y.A.: “Thermodynamic calculation of the Mg-Cu phase diagram”, Zeitschrift für Metallkunde, vol. 84, no. 10, 1993, pp. 662-667.

[28] Dinsdale A. T.: “Thermodynamic data for the elements”, CALPHAD, vol. 15, 1991, pp. 317-425.

[29] Garg, S. P.; Bhatt, Y. J.; Sundaram, C. V.: “Thermodynamic study of liquid copper-magnesium alloys by vapor pressure measurements”, Metallurgical and Materials Transactions, vol. 4, no. 1, 1973, pp. 283-289.

[30] Schmahl, N.G. and Sieben, P.: “Vapor pressures of magnesium in its binary alloys with copper, nickel and lead and their thermodynamic evaluation”, Physical Chemistry of Metallic Solutions and Intermetallic Compounds, vol. 1, 1960, pp. 268-282.

[31] Juneja, J. M.; Iyengar, G.N.K.; Abraham, K.P.: “Thermodynamic properties of liquid (magnesium + copper) alloys by vapor pressure measurements made by a boiling temperature method”, Journal of Chemical Thermodynamics, vol. 18, no. 11, 1986, pp. 1025-1035.

[32] Hino, M.; Nagasaka, T.; Takehama, R.: “Activity measurement of the constituents in liquid Cu-Mg and Cu-Ca alloys with mass spectrometry”, Metallurgical and Materials Transactions – Series B, vol. 31, no. 5, 2000, pp. 927-934.

[33] Sommer, F; Lee, J.J; Predel, B: “Calorimetric investigations of liquid alkaline earth metal alloys”, Berichte der Bunsen-Gesellschaft, vol. 87, no. 9, 1983, pp. 792-797.

[34] Batlin, G.I.; Sudavtsova, V.S.; Mikhailovskaya, M.V.: “Thermodynamic properties of liquid copper-magnesium alloys”, Izvestiya Vysshikh Uchebnykh Zavedenii, vol. 2, 1987, pp. 29-31.

[35] King, R.C.; Kleppa, O.J.: “A thermochemical study of some selected laves phases”, Acta Metallurgica, vol. 12, no. 1, 1964, pp. 87-97.

[36] Eremenko, V.N.; Lukashenko, G.M.; Polotskaya, R.I.: “Thermodynamic properties of magnesium-copper compounds”, Izvestiya Akademii Nauk SSSR, Metally, vol. 1, 1968, pp. 210-212.

[37] Smith, J.F.; Christian, J.L.: “Thermodynamics of formation of copper-magnesium and nickel-magnesium compounds from vapor-pressure measurements”, Acta Metallurgica, vol. 8, 1960, pp. 249-255.

[38] Domagala, R.F.; Rausch, J.J.; Levinson, D.W.: “The systems Y-Fe, Y-Ni and Y-Cu”, Transactions of the American Society for Metals, vol. 53, 1961, pp. 137-155.

[39] Buschow, K.H.J. and Goot, A.S.: "Composition and crystal structure of hexagonal copper rich rare earth-copper compounds", Acta Crystallographica, vol. 27(B), 1971, pp. 1085-1088.

[40] Chakrabarti, D.J.; Laughlin, D.E.: "Phase diagrams of binary copper alloys", American Society for Metals International; 1981, pp. 478-481.

[41] Sudavtsova, V.S.; Vatalin, G.I.; Kalmykov, A.V.; Kuznetsov, F.F: "Heat of mixing of molten binary alloys of copper with yttrium and zirconium", Izvestiya Bysshikh Uchebnykh Zavedenii, Tsvetnaya Metallurgiya, vol. 6, 1983, pp. 107-108.

[42] Guojun, Q.; Itagaki, K.; Yazawa, A.: "High temperature heat content measurements of copper-RE (RE = yttrium, lanthanum, cerium, praseodymium, neodymium) binary systems", Materials Transactions, vol. 30, no. 4, 1989, pp. 273-282.

[43] Itagaki, K.; Guojun, Q.I.; Sabine,A.; Spencer, P. J.; "Evaluation of the phase diagram and thermochemistry of the Cu-Y system", CALPHAD, vol. 14, no. 4, 1990, pp. 377-384.

[44] Massalski, T.B.; Murray, J.L.; Bennett, L.H.; Barker, H.; "Binary alloy phase diagrams", American Society for Metals, Metals park, Ohio, 1986.

[45] Fries, S.G.; Lukas, H.L.; Konetzki, R.; Schmid-Fetzer, R.: "Experimental investigation and thermal optimization of the Y-Cu binary system", Journal of Phase Equilibria, vol. 15, no. 6, 1994, pp. 606-614.

[46] Abend, U. and Schaller, H.J.: "Constitution and thermodynamics of Cu-Y alloys", Journal of Physical Chemistry, vol. 101, no. 4, 1997, pp. 741-748.

[47] Okamoto, H.; "Cu-Y (copper-yttrium)", Journal of Phase Equilibria, vol. 19, no. 4, 1998, pp. 398-399.

[48] Watanabe, S.; Kleppa, O.J.: "Thermochemistry of alloys of transition metals: alloys of copper with scandium, yttrium, lanthanum and lutetium", Metallurgical Transactions B: Process Metallugry, vol. 15B, no. 2, 1984, pp. 573-580.

[49] Sidorov, O.Y.; Valishev, M.G.; Esin, Y. O.; Gel'd, P.V.; Zamyatin, V.M.: "Partial and integral enthalpies of formation of liquid copper-yttrium and copper-zirconium alloys", Izvestiya Akademii Nauk SSSR, Metally, vol. 4, 1990, pp. 188-190.

[50] Berezutskii, V.V.; Lukashenko, G.M.: "Thermodynamic properties of liquid copper-yttrium alloys", Zhurnal Fizicheskoi Khimii, vol. 61, no. 5, 1987, pp. 1422-1424.

[51] Ganesan, V.; Schuller, F.; Feufel, H.; Sommer, F.; Ipser, H.: "Thermodynamic properties of ternary liquid Cu-Mg-Y alloys", Zeitschift für Metallkunde, vol. 88, no. 9, 1997, pp. 701-710.

[52] Fabrichnaya, O.B.; Lukas, H.L.; Effenberg, G.; Aldinger, F.: "Thermodynamic optimization in the Mg-Y system", Intermetallics, vol. 11, 2003, pp. 1183-1188.

[53] Gibson, E.D.; Carlson, O.N.: "The yttrium-magnesium alloy system", Transactions of the American Society for Metals, vol. 52, 1960, pp. 1084-1096.

[54] Sviderskaya, Z.A.; Padezhnova, E.M.:"Phase equilibriums in magnesium-yttrium and magnesium-yttrium-manganese systems", Izvestiya Akademii Nauk SSSR, Metally, vol. 6, 1968, pp. 183-190.

[55] Mizer, D. and Clark, J.B.: "Magnesium- rich region of the magnesium-yttrium phase diagram", T.Am. I. Min. Met. Eng., vol. 221, 1961, pp. 207-208.

[56] Ran, Q.; Lukas, H.L.; Effenberg, G.; Petzow, G.: "Thermodynamic optimization of the Magnesium-Yttrium System", CALPHAD, vol. 12, no. 4, 1988, pp. 375-381.

[57] Massalski, T.B.: "Binary alloy phase diagrams", Second Edition, ASM International, 1990, pp. 1-3.

[58] Smith, J. F.; Bailey, D.M.; Novotny, D.B.; Davison, J.E.: "Thermodynamics of formation of yttrium-magnesium intermediate phases", Acta Materialia, vol. 13, no. 8, 1965, pp. 889-895.

[59] Flandorfer, H.; Giovannini, M.; Saccone, A.; Rogl, P.; Ferro, R.: "The Ce-Mg-Y system", Physical Metallurgy and Materials Science, vol. 28A, no. 2, 1997, pp. 265-276.

[60] Zhang, M.X.; Kelly, P.M.: "Edge-to- edge matching and it's applications PartII. application to Mg-Al, Mg-Y, and Mg-Mn Alloys", Acta Materialia, vol. 53, 2005, pp. 1085-1096.

[61] Shakhshir, S.; Medraj, M.: "Computational thermodynamic model for the Mg-Al-Y system", Journal of Phase Equilibria and Diffusion, vol. 27, no. 3, 2006, pp. 231-244.

[62] Agarwal, R.; Feufel, H.; Sommer, F.: "Calorimetric measurements of liquid La-Mg, Mg-Yb and Mg-Y alloys", Journal of Alloys and Compounds, vol. 217, no. 1, 1995, pp. 59-64.

[63] Ganesan, V.; Ipser, H.: "Thermodynamic properties of liquid magnesium-yttrium alloys", Journal de Chimie Physique, vol. 94, no. 5, 1997, pp. 986-991.

[64] Pyagai, I. N.; Vakhobov, A. V.; Shmidt, N. G.; Zhikhareva, O. V.; Numanov, M. I.: "Heats of formation of magnesium intermetallic compounds with yttrium, lanthanum, and neodymium.", Doklady Akademii Nauk Tadzhikskoi SSR, vol. 32, no. 9, 1989, pp. 605-607.

[65] Busch, R.; Liu, W.; Johnson, L.: "Thermodynamics and kinetics of the $Mg_{65}Cu_{25}Y_{10}$ bulk metallic glass forming liquid", Journal of Applied Physics, vol. 83, no. 8, 1998, pp. 4134-4141.

[66] Ma, H.; Zheng, Q.; Xu, J.; Li, Y.; Ma, E.: "Rapid communications- boubling the critical size for bulk metallic glass formation in the Mg-Cu-Y ternary system", Journal of Materials Research, vol. 20, no. 9, 2005, pp. 2252-2255.

[67] Mishra, R.; Hoffmann, R-D.; Pottgen, R.: "Original communications-new magnesium compounds RE_2Cu_2Mg (RE= Y, La-Nd, Sm, Gd-Tm, Lu) with Mo_2FeB_2 type structure", Journal of Chemical Sciences, vol. 56, no. 3, 2001, pp. 239-244.

[68] Solokha, P.; Pavlyuk, V.; Saccone, A.; Negri, S.D.; Prochwicz, W.; Marciniak, B.; Sokolowska, E.R.: "Rare earth-copper-magnesium compounds $RECu_9Mg_2$ (RE = Y, La-Nd, Sm-Ho, Yb) with ordered $CeNi_3$-type structure", Journal of Solid State Chemistry, vol. 179, 2006, pp. 3073-3081.

[69] Kaufman, L. and Bernstein, H.: "Computer calculation of phase diagrams with special reference to refractory metals", Academic Press, New York, 1970. (cited in [1]).

[70] Kumar, K.C. and Wollants, P.: "Some guidelines for thermodynamic optimization of phase diagrams", Journal of Alloys and Compounds, vol. 320, 2001, pp. 189-198.

[71] "FactSage 5.4.1", Thermfact (Centre for research in computational thermochemistry), Montreal, QC, Canada, 2006.

[72] Pelton, A.D.; Degterov, S.A.; Eriksson, G.; Robelin, C.; Dessureault, Y.: "The modified quasi-chemical model I – binary solutions", Metallurgical and Materials Transactions B, vol. 31, 2000, pp. 651-659.

[73] Chartrand, P. and Pelton, A.D.: "The modified quasi-chemical model: part III, two sublattices", Metallurgical and Materials Transactions A, vol. 32, 2001, pp. 1397-1407.

[74] Pelton, A.D.; Chartrand, P.; Eriksson, G.: "The modified quasi-chemical model: part IV, two-sublattice quadruplet approximation", Metallurgical and Materials Transactions A, vol. 32, 2001, pp. 1409-1416.

[75] Kohler, F.: "Estimation of the thermodynamic data for a ternary system from the corresponding binary systems", Monatshefte fuer Chemie, vol. 91, no. 4, 1960, pp. 738-740.

[76] Muggianu, Y.M.; Gambino, M.; Bross, J.P.: "Enthalpies of formation of liquid alloys bismuth-gallium-tin at 723.deg.K. choice of an analytical representation of integral and partial excess functions of mixing", Journal de Chimie Physique, vol. 72, no.1, 1975, pp. 83-88.

[77] Toop, G.W.: “Predicting ternary activities using binary data”, Transactions of the American Institute of Mining, vol. 233, no. 5, 1965, pp. 850-855.

[78] Chartrand, P.; Pelton, A.D.: “On the choice of geometric thermodynamic models”, Journal of Phase Equilibria, vol. 21 no. 2, 2000, pp. 141-147.

[79] Pelton, A.D.: “A general geometric thermodynamic model for multicomponent solutions”, CALPHAD, vol. 25, no. 2, 2001, pp. 319-328.

[80] Qiao, Z.Y.; Xing, X.; Peng, M.: “Thermodynamic criterion for judging the symmetry of ternary systems and criterion applications”, Journal of Phase Equilibria, vol. 17, no. 6, 1996, pp. 502-507.

[81] Rogelberg I.L. Tr. Gos. Nauchn.-Issled. Proektn. Ist. Obrab. Tsvetnaya Metally, vol. 16, 1957, pp. 82-89 (Cited in 24).

[82] Wyckoff, W.G.: “Crystal structures”, 2nd ed., John Wiley & Sons, New York, vol. 1, 1963, pp. 365-367.

[83] “Powder Cell for windows”, Version 2.3, 1999, W.Kraus & G. Nolze, Federal Institute for Materials Research and Testing, Rudower Chausse 5, 12489 Berlin, Germany.